Ministry of Higher Education
and Scientific Research
University of Diyala
College of Science
Department of Chemistry

# Corrosion prevention of industrially used aluminium and aluminium alloy (AA6063-T5) using cordia myxa leaves extract and ($TiO_2$,$Fe_2O_3$) Nano-oxides

A Thesis Submitted to the Council of the College of Science, University of Diyala in Partial Fulfillment of the Requirements for the Degree of Master of Science in Chemistry

(Physical Chemistry)

by

HIBA BASSIM DEAB

**B.Sc. in Chemistry Science 2009**

**College of Science – University of Diyala**

**Supervised by**

**Prof. Dr. Ahmed Najem Abd** **Prof. Dr. Karim Henikish Hassan**

**2020 AD** **IRAQ** **1442AH**

بِسْمِ الله الرحمن الرَّحِيم

﴿وَلَقَدْ آتَيْنَا دَاوُودَ وَسُلَيْمَانَ عِلْمًا وَقَالَا الْحَمْدُ لِلَّهِ الَّـذِي فَضَّلَنَا عَلَى كَثِيرٍ مِنْ عِبَـادِهِ الْمُؤْمِنِيـنَ﴾

صدق الله العظيم

النمل: ﴿15﴾

# DEDICATION

*All praise to Allah, today. I fold the days of tiredness by this humble work...*

***My Beloved Father***

*It's difficult to repay him for everything he has don  but at least we can be thankful and express about our love and show him more respect, obedience and appreciation because he's actually deserves that...*

***My Beloved Mother***

*The mother is the flower of life, her satisfaction determines destiny, no rest in the world without her smile, and no paradise in the afterlife when she is angry, learning  how to value her. She is the make  of generations...*

***My Beloved husband***

***I thank my husband( Ahmed Farhan) who has helped me every step of my studies…***

***HIBA…***

# ACKNOWLEDGEMENT

First of all, I thank Allah for inspiring me with strength, patience and willingness to perform this work, I would like to express my sincere gratitude to my supervisor, **Prof. Dr. Ahmed Najem Abd** and **Prof. Dr. Karim Henikish Hassan**, for their inspiration, proper guidance and supervision throughout this project.

Special thanks are extended to the Dean, Chairman, and the staff of the Chemistry Department, College of Science, Diyala University. Thanks also to all postgraduate unit staff, dean assistant for scientific affairs staff.

Many thanks to my husband and my family (Father, Mother, and Sister) who sustained and encouraged me throughout the work and my friend Nawras and all my friends.

HIBA...

# Abstract

The corrosion rates of aluminum and aluminum alloy (AA6063-T5) in (1M $H_3PO_4$) and (at PH of 4) in the presence and absence of (CML) Cordia myxa leaves extract and nanomaterials inhibitors were examined at various temperatures (303,313, 323and 333K). Using the method of weight loss, the plant material, Cordia myxa leaves (CML) extract at concentration of (2-10 mg/L) for ($Fe_2O_3$ and $TiO_2$) nanomaterials, at concentrations (1and 2.5) wt%. The corrosion rate increases with increase of temperature and decreases with increase the concentrations of the inhibitors. Noted that the highest inhibitor efficiency was (90.95%) for aluminum and (87.60%) for aluminum alloy (AA6063-T5) for (CML) extract and (71.43%) for aluminum and (68.78%) for aluminum alloy (AA6063-T5) for ($Fe_2O_3$) nanomaterial. and (67.02%) for aluminum and (60.01%) for aluminum alloy (AA6063-T5) for ($TiO_2$) nanomaterial at a temperature of (333K) and even at the upper concentration limit. Three models have been used to describe the corrosion inhibitor adsorption mechanism on the surface of the metal and it has been found that the inhibition obey the description of the Langmuir adsorption isotherm in their model of action more than the Freundlich adsorption isotherm and more even than the Temkin adsorption isotherm, meaning that the materials that inhibit corrosion operate on the surface of the metal with monolayer formation according to the adsorption. An equation was used (Arrhenius Equation) and the transition state equation, (Activation Energy, Ea), Enthalpy of Activation, ($\Delta H°$) and Entropy of Activation, ($\Delta S°$) values with the presence and absence of inhibitory compounds. To determine the active groups in the (CML) extract before immersion in the corrosion solution and after the immersion process, an infrared spectrum (FTIR) technique was used to determine the active groups in the extract, as there was a difference between the results and the displacement of the FTIR peaks due to the adsorption on the metal surface aggregates .

X ray diffraction(XRD) technique was used to study coated metal surface after corrosion with the presence and absence of nanomaterials inhibitors ($Fe_2O_3$ and $TiO_2$). Atomic Force microscopy (AFM) technique was also to study the metal surface before were used to calculate and after corrosion in the presence and absence of (CML) extract .

coated metal surface after corrosion in the presence and absence of ($Fe_2O_3$ and $TiO_2$) nanomaterials inhibitors. Scanning electron microscopy (SEM) was also used to study coated the metal surface morphology after corrosion with the presence and absence of nanomaterials inhibitors ($Fe_2O_3$ and $TiO_2$).(XRD and SEM) show that in presence nanomaterials ($Fe_2O_3$ and$TiO_2$) reduced the degree of corrosion . Finally from (AFM) in the presence of (CML) extract ($Fe_2O_3$and $TiO_2$) nanomaterials surface became smooth because of the formation of inhibition film over metal surface.

# *Contents*

# List of Tables

# List of Figures

# List of Abbreviation

| Meaning | Abbreviation |
|---|---|
| Aluminum | Al |
| Phosphoric Acid | $H_3PO_4$ |
| Aluminum Alloy | AA6063 – T5 |
| Aluminum –Magnesium-silicon | Al – Mg – si |
| Silicon | si |
| Magnesium | Mg |
| Cordia myxa Leaves | CML |
| Scanning Electron Microscopy | SEM |
| Iron oxide | $Fe_2O_3$ |
| Fourier Transform Infrared Spectroscopy | FTIR |
| Benzene | $C_6H_6$ |
| Acetone | $C_3H_6O$ |
| Optical Emission Spectroscopy | OES |
| Titanium oxide | $TiO_2$ |
| X-ray diffraction | Xrd |
| Sodium Hydroxide | NaoH |
| Atomic force microscope | AFM |

# List of Symbols

| Symbol | Meaning | Units |
|---|---|---|
| CR | corrosion rate | mmpy |
| θ | Surface coverage | – |
| IE | Inhibition Efficiency | – |
| $K_L$ | Langmuir adsorption constant | mg/g |
| $C_i$ | Inhibitor concentration | mg/L |
| $\Delta G^{\circ}_{ads}$ | standard adsorption free energy | kJ $mol^{-1}$ |
| $K_F$ | Freundlich adsorption constant | mg/g |
| n" | Slope | – |
| a | Molecular interaction parameter | – |
| $K_T$ | Temkin adsorption constant | L/gm |
| A | Frequency factor | – |
| $E_a$ | Activation energy | kJ $mol^{-1}$ |
| R | Gas constant | $J.mol^{-1}.K^{-1}$ |
| T | Absolute temperature | K |
| N | Avogadro's number | molecule $mo1^{-1}$ |
| h | Planck's constant | J.s |
| $\Delta S^*$ | Entropy of activation | $kJmol^{-1}K^{-1}$ |
| $\Delta H^*$ | Enthalpy of activation | $kJmol^{-1}$ |
| D | Density of specimen | $g/cm^3$ |
| t | Exposure time | h |
| A | Surface area | square inch ($in^2$) |
| $CR_{uninh}$ | Weight loss without inhibitor | mmpy |
| $CR_{inh}$ | Weight loss with inhibitor | mmpy |
| $R^2$ | Correlation coefficient | – |

# *Chapter one*
# *Introduction & Literature Survey*

## 1.1. Introduction

Corrosion can be characterized as material failure through the chemical process[1]. The three principal explanations for the relevance of corrosion Economics, stability and environmental degradation are preventative. Corrosion engineers with the intention of reducing the economic effects of corrosion. Help for corrosion scientists in order to reduce the loss of material. as well as the associated economic losses arising from piping, tank corrosion metal parts of machinery, ships, bridges, marine structures, etc [2].

Corrosion loss of metal is a waste not only of the metal, but also of the energy and human activities used to manufacture and produce .For much of the current study, the economic aspect is a very powerful incentive. Around corrosion Losses incurred annually by industry and by governments amount to several billions of dollars. Corrosion has a significant impact on the environment, associated breakdown of oil pipelines or gas pipelines or oil tankers in form of water and air pollution. These may have a very negative effect on the environment, contributing to the demise of life at the aquatic level. Industries are strongly reliant upon the use of metals and alloys. One of the protecting metals from corrosion is the most challenging and complicated activities for industry. Corrosion is a universal problem which continues to be of great importance for a wide range of industrial and product applications [2]. Metal corrosion is costing more than billion$300 a year for global industries. The inhibitors by forming a thin adsorbed film on metal reduce the rate of corrosion. Much attention has been fixed in recent decades on the need to improving and designing new materials evolving for protection, against corrosion (nanomaterial's, biomaterials, corrosion inhibitors, sol-gel coatings, self-healing and intelligent materials) as an example. Out of these,

an emerging and wide area is self-healing coating and corrosion inhibitors [3].

Corrosion is usually consist of a set of processes such as reduction ,oxidation reactions, which are electrochemical in nature. Thus, the metal is oxidized to corrosion products at anodic sites and some species, are reduced at cathodic sites. Thermodynamic consideration determines whether or not a reaction can occur. However, in spite of this limitation, thermodynamic is very important to an understanding of the electrochemistry of the corrosion [4].

Due to two primary reasons, it is an inevitable process: The working and environmental, conditions external and internal corrosion are divided into two types. Internal corrosion is the type of corrosion that typically takes place within tanks, pipelines, boilers, etc .It is concerned with the transport and storage of fluids and hydrocarbons within tanks and pressure vessels. There are those motors of internal corrosion. Corrosion component that is found in hydrocarbons and fluids. External corrosion is the type of corrosion that associated with any form can affect the surface exposed to the outside world, including: sea-water, temperature, humidity, rain, microorganisms, and external stresses [5].

## 1.2. Literature survey

Because of their aluminum and aluminum alloy (AA6063-T5), several studies have been submitted. Included high value of technology and a broad range of industrial applications.

**Bataineh et al. (2013),** Using the technique of weight loss, the inhibition efficiency of *Plumb ago european* extract on aluminum corrosion in (1 M NaOH) was tested. The presence of european plumb, extract inhibited the corrosion of aluminum, in the test solution. The inhibition efficiency increased with increasing of plant extract concentration, and increased at increasing temperature and reaches the maximum value of ( % 96.8 ), at the highest extract concentration (20 PPM at 50°C). The experimental data to Langmuir, Temkin and the recently formulated thermodynamic kinetic model of adsorption isotherms. The obtained value and indication of the normal free energy of adsorption is compatible with physical isotherms of adsorption [6].

**(Yaro et al. 2013),** The corrosion inhibition of mild steel in 1 M $H_3PO_4$ solution was tested by using apricot juice at different temperatures the weight loss technique. The inhibitor adsorbed on the metal surface was manifested by activation adsorption and numerical investigation in this search. Langmuir isotherm Corresponds from the adsorption heat value of (-14.93 kJ / mol) the inhibition of mild steel corrosion occurred by physical adsorption, the inhibition efficiency was also reached 75 % at $30^{o}$C where the extract concentration was 40 g / L [7].

**(Al-Ajaj et. al. 2013),** They studied the addition of ($TiO_2$) to the epoxy coating in micro and nanoparticles, where ($TiO_2$) was applied (50 μm and 50 nm) to the coating in volumes (1, 2, 3, 4, 5 , 7, 10, 15 , 20 % vol) to the epoxy coating, improving mechanical properties [8].

**(Panaite and Mușat. 2014),** An addition (about 50 nm) of zinc nanoparticle oxide to the epoxy material was found we used the electrical and weight approaches. Dipping way was used in iron samples. It was found that the addition of nanomaterial strengthened the properties of the surface and decreased the roughness [9].

**(Kumar. 2015),** Coating method is one of the most important means of controlling metal corrosion, especially in the presence of nanomaterials that enhance the coating. The rationale for the increased efficacy has been clarified .The dissemination of nanomaterials in paint has led to an increase in density, which has increased corrosion resistance and chemical resistance [10].

**(Vasudha et.al 2015) ,** The adsorption and inhibition efficacy of the mild steel extract of *Millingtonia hortensis* leaves in 1 M HCl and 1 M $H_2SO_4$ at a temperature range of (303 to 343 K) were examined by mass loss measurements. With the growth of inhibitor concentration, the importance of inhibition effectiveness increased and decreased at 333 K. The value of inhibition efficiency in $H_2SO_4$ was 97.10 % at 323 K and the value of inhibition efficiency in HCl was (97.41 %) at (333 K). The adsorption value of $\Delta G_{ads}$ 12-24 KJ/ mol indicates the mechanism of physisorption. Inhibitor adsorption on the metal was found to follow

Langmuir and Temkin isotherm on the surface. Values of energy activation ($\Delta E_a$), Adsorptive enthalpy ($\Delta H^{\circ}$) and Adsorption entropy ($\Delta S$) were calculated [11].

**(Noor et al. 2016),** Has examinet, Red onion seeds inhibitory function extracts and peels (ROSE, ROPE) and contrast of 0.75 M steel corrosion ($H_3PO_4$) Chemical measurements (evolution of hydrogen and mass loss) and the SEM method were used. The effect of temperature on 0.75 M $H_3PO_4$ steel corrosion in the temperature range of 303-333 K, each extract was studied without and with out some concentration. With increasing concentration, the inhibition efficiency of both extracts increases and gives the Langmuir adsorption isotherm a good suit. With the strongest affinity for ROSE adsorption. Chemisorption and physical adsorption actions for ROSE and ROPE respectively on the steel surface were revealed by the values of $E_a$ without and with inhibitor [12].

**(Khorram, et. al. 2016),** The addition of titanium nano oxide and microwave iron oxide to the epoxy coating through mechanical mixing has been studied. The existence of nanoparticles and very, exact microscopic examinations show the presence of Painted loudly. Electrical methods were used to quantify corrosion rates, which revealed that nanomaterials were introduced to improve corrosion resistance. The highest degree of safety for the metal was the addition of (3%) iron oxide to the coating and the addition of 4% titanium. Coating oxide with its nanostructures [13].

**Kwolek et al .(2016**), Studied aluminum corrosion rates in phosphoric acid solutions were determined gravimetrically, in a presence of sodium moly date which acts, as an inhibitor. Inhibition efficiencies have been measured. The most efficient corrosion inhibition was observed for 0.5 M $H_3PO_4$ and 100 mm of $Na_2MoO_4$. As insoluble corrosion products advanced to specimens and affected the defined corrosion rates, we conducted an examination of the morphology of the specimens using a scanning electron microscope [14].

**Ajeel (2017),** Mild steel corrosion inhibition studied by *Rosmarinus officinal* leaves extract by weight loss and potentiostatic methods in 1 M $H_2SO_4$ solution. Increasing acid concentration contributes to an increase in the electrode corrosion rate. (100 to 1000 ppm at 25 $^0$C) in this study, variable conditions were used. Extract of *Rosmarinus Officinal* is leaves for mild steel. As a convincing consumption inhibitor for gentle steel in acidic medium, it has been found that the concentrates. The process of hindrance is attributed to an adsorbed growth. On the metal surface, the inhibitor film fortifies the metal against corrosion. With growing inhibitor concentration up to 92 % for 1000 ppm at 25 C°, the inhibition efficiency was observed to increase. The findings show that the rate of corrosion without inhibitor 5.6 mpy was 0.43 mpy with inhibitor, which means that the rate of corrosion It has risen more than 90 %. Increased corrosion resistance has also been enhanced by the effects of immersion time (2h) at 25 C° on corrosion inhibition. The results obtained indicate that the extract of Rosmarinus Officinal is Leaves may be an excellent friendly (green corrosion inhibitor) [15].

**Chaubey et al. (2017),** The effects of three trees' stem bark extracts, namely *Moringa oleifera* (MO), were examined. *Terminalia arjuna* and, on the corrosion behavior of aluminum alloy in (1 M NaOH), *Mangifera indica* (MI). Inhibition efficiency was examined using gravimetric, electrochemical and potentiodynamic polarization. impedance spectroscopy (EIS) measurements. The exhibition of these extracts (MO) wa**s** Maximum and benig (85.3% at 0.6 g / L at 303 K). Polarization calculation showed that all of the extracts tested were mixed-type inhibitors, and the best match was found to be Langmuir 's adsorption isotherm [16].

**Xhanari et al. (2017),** is work was conducted over the last two decades on the use of natural compounds as corrosion inhibitors (aluminum and aluminum alloys) in various solutions. Gums, medications, and oils have been regarded as green corrosion inhibitors for plant extracts here. The advantages and drawbacks of the approaches used to obtain green corrosion inhibitors are described. Additionally, the inhibition effect, of these corrosion inhibitors, including the techniques used to test them and the respective inhibition mechanisms, was discussed [17].

**Awad et al.(2018),** Aluminum corrosion inhibition tested in (1 M $H_3PO_4$) was investigated corrosion inhibitor in the absence and presence of *Cydonia Vulgaris leaves* (CVL) extracts. The effect of temperature and the inhibitor concentration at immersion time (3h) was investigated, using the method of weight loss. The findings obtained showed that the extracts of *Cydonia vulgaris* leaves (CVL) inhibited aluminum in ($H_3PO_4$). The corrosion rate was reduced and decreased. The inhibitor's efficiency was improved by increasing the concentration and temperature. Higher inhibition efficiency for aluminum corrosion (95.51 %) was obtained at a higher concentration and temperature level of the inhibitor. The adsorption of extracts of *Cydonia vulgaris leaves* (CVL) was found to comply with

the model of (Langmuir adsorption isotherm). The concepts of free adsorption energy was greater than (-20 kJ / mol), suggesting a mixed of physical and chemical adsorption mode. Enthalpy of activation ($\Delta H^*$) and activation entropy ($\Delta S^*$ ) of aluminum, corrosion was found to be (43.7254) kJ/mol$^{-1}$ , −0.1804 kJ mol 1K $^{-1}$ and (20.2732 kJ mol $^{-1}$, −0.1921 kJ mol -1$K$ $^{-1}$ ) in the absence and presence of an extract, respectively [18].

**Khadom et al.(2018),** In the absence and presence of potassium iodide ( KI) as a corrosion inhibitor, corrosion inhibition of mild steel in 1 M HCl was tested. Using the weight loss technique, the effects of temperature and inhibitor concentration were examined. The obtained outcome shows that (KI) functions as an inhibitor of HCl mild steel and decreases . The efficiency of the inhibition was found to increase with an increase in the concentration of the inhibitor and temperature. At a higher level of inhibitor concentration and temperature, the highest inhibition efficiency was (94 %). The free energy values for adsorption on Ween-20and-40 kJ / mol, which is an example of mixed physical and chemical adsorption modes. To compare the corrosion rate data with independent variables, mathematical models were also suggested [19].

**(Desai. 2018),** In the presence and absence of *Calotropis gigantean* (Aankado) leaves arks, corrosion in (0.4 to 0.6) M hydrochloric acid solution was studied using gravimetric and electrochemical techniques. The findings showed that the *C. gigantic* barks might serve as an effective inhibitor for the corrosion, of aluminum in (HCl) solutions. Inhibition was shown to increasing. The adsorption analysis supports that the Freundlich isotherm better suits the interaction of the metal

surface with the *C. gigantic* leaves arks at presentation. Time at all concentrations for adsorption on the metal surface [20].

**(BinYehme et al. 2018),** Green coffee bean extract was tested as a green corrosion inhibitor for aluminum in artificial acid rain at various temperatures. The rate of corrosion, the degree of surface coverage and the efficiency of inhibition. Using electrochemical analysis calculated (Tafel polarization). The findings showed that in the tested medium, the green coffee bean extract was strong inhibitor for reducing the corrosion attack of aluminum. In addition , the maximum degree of inhibition efficiency was achieved with (8.0 g / L) of 84.4 %, 97.4 % and 98.% at 300,313 and 323 K, respectively. The results proved that the best model for adsorption was the Langmuir isotherm on the checked metal. The variance analysis (ANOVA) test showed that the concentration of green coffee extract played an important role in the inhibition of aluminum corrosion, although there were no major variations in temperature changes [21].

**(Wisdom et al. 2018),** The green inhibitor *Terminalia ivorensis* has been studied to inhibit aluminum alloy (AA8011A) corrosion in the (0.5 M HCl) environment. The adsorption isotherm is analyzed using the gravimetric method. The findings obtained showed that *Terminalia ivorensis* prevents corrosion aluminum alloy (AA8011A) with a maximum inhibition efficiency of (% 89.56 at 0.5 g / L) concentration of the extract. With increasing concentration, the efficacy grew. Adsorption experiments found that there was a mixed adsorption isotherms involving that both the chemical adsorption and physical adsorption reactions took place [22].

**(Coelho et al. 2018),** The inhibitory effect of benzotriazole ((BTA) and cerium chloride ($CeCl_3$) on aluminum alloy (AA2024-T3) was measured individually and combined by electrochemical impedance in (0.05 M NaCl) electrolytes spectroscopy from the study of impedance equipped parameters a synergistic effect tends to occur between both inhibitors until 14 days of immersion. In order to better understand the observed inhibitive behavior, a Al, Cu galvanic pairing model was applied. In addition, secondary ion mass spectrometry (ToF-SIMS) flight time was used to test the in-depth distribution of species linked to the interface of the inhibitive film alloy [23].

## 1.3. Aim of study

**1-** Studying the influence of (1 M $H_3PO_4$) on the corrosion of the pure aluminum (Al) and aluminum alloy (AA6063-T5) at different temperatures.

**2-** Atomic Force Microscope (AFM) study of surface morphology.

**3-** Fourier transform infrared spectroscopy ( FTIR) analysis of the active group in the (CML) inhibitor .

**4-** Studying the surface morphology by scanning electron microscope (SEM).

**5-** Studying the surface morphology of the inhibitor by X-ray diffraction technique.

**6-** Analysis the model of adsorption of aluminum and aluminum alloy (AA6063-T5) surface corrosion inhibitors.

**7-** Studying the regulation of corrosion rates (using the immersion process by commercially available types of coatings (Black coating), Tainted with proportions of nanomaterials ($Fe_2O_3$and $TiO_2$).

# *Chapter Two*

# *Theoretical part*

## 2.1. Mechanism of Corrosion

The suggested suitable process of corrosion of aluminum and aluminum alloy (AA6063-T5), in accordance with experimental the corrosion of metal involves an electrochemical mechanism resulting from dissolution of aluminum and aluminum alloy (AA6063-T5) metal in the acid .The anodic and cathodic processes that are described by equations (2.1) and (2.2) can express this method.

$Al_{(s)} \leftrightarrow Al^{+3} + 3e^{-}$ Oxidation reaction (2.1)

$2H^{+} + 2e \leftrightarrow H_{2(g)}$ reduction reaction (2.2)

The overall electrochemical process can be written as follows:

$2Al_{(S)} + 6H^{+} \leftrightarrow 2Al^{+3} + 3H_{2(g)}$ (2.3)

The cathodic reaction occurs ($H_{chemisorbed}$) by picking up an electron that releases in the anodic reaction ($H+e=H_{chemisorbed}$) in aluminum and aluminum alloy (AA6063-T5) corrosion in (1M $H_3PO_4$). In such, acidic solutions, the ($H_{chemisorbed}$ ) on the metal surface reacts by combining with other adsorbent ($H_{chemisorbed)}$ form $H_2$ gas molecule. That bubbles from the metal surface. A very small amount of uncombined ones ($H_{chemisorbed}$) will remain; however, this amount does not influence the entire process. Therefore, the rates of combination and absorption of ($H_{chemisorbed)}$ are nearly the same [24].

## 2.2. Types of Corrosion

**Corrosion can be categorized in many ways, such as**

### 2.2.1. Temperature of corrosion

Temperature increases the rate of chemical reactions, which leads to increase in corrosion rate . The inhibitor efficiency increases with the increase the temperature. Like most chemical reactions the rate of corrosion of metals in aqueous acid solutions increases with increasing temperature [25].

### 2.2.2. Reaction of corrosion:

#### 2.2.2.1. Electrochemical corrosion

Corrosion can be divided into two or more partial reactions. These partial reactions are divided into two classes: oxidation and reduction [26]. These two separated reactions are taking place at different areas on the metal surface. One of the reactions (oxidation and reduction) being the anodic reaction ,consists of an oxidation type chemical change in which the metal Changes from the metallic state to the ionic state: i.e. by giving off electrons, the valance of the metal is increased

metal transitions from the metallic state to an ionic state: i.e. the valance of metal is increased by giving off electrons.

$$M \rightarrow M^{++} + 2e^{-} \qquad \ldots\ldots\ldots\ldots\ldots\ldots (2.4)$$

At different positions from the anodic one. Cathodic reactions may occur. There are various Cathodic reactions which are frequently encountered in metallic corrosion Cathodic reactions are the most widespread:

1. Hydrogen formation:

$2H^{+}_{(aq)} + 2e^{-} \rightarrow H_{2\,(g)\uparrow}$ $E^{o} = 0.0$ v …… (2.5)

2. Oxygen reduction (acid solution):

$O_{2\,(g)\uparrow} + 4H_{(aq)} + 4e\text{-} \rightarrow 2H_2O_{(L)}$ $E^{o} = 1.23$ v …… (2.6)

3. Oxygen reduction (neutral or basic solutions):

$O_{2(g)} + 2H_2O_{(L)} \rightarrow 4e^{-} + 4OH^{-}_{(aq)}$ $E^{o} = 0.40$ v…….. . (2.7)

4. Metal ion reduction:

$M^{+3} + e^{-} \rightarrow M^{+2}$ …… (2.8)

5. Metal deposition:

$M^{+} + e^{-} \rightarrow M$ …… (2.9)

### 2.2.2.2 Chemical corrosion

An attack resulting from a direct contact to a bare metal is a direct chemical attack, or pure chemical corrosion. Surface to caustic. Gaseous or liquid agents. Unlike an anodic and electrochemical attack. A measurable distance apart, the changes in direct chemical attack are occurring simultaneously at the same point Cathodic changes can take place.

### 2.2.3. Medium of corrosion

In corrosion there are two major classes of metallic materials:

**2.2.3.1-Dry corrosion**: It is a dry gas and it is often repeatedly referred to as corrosion; chemical corrosion is a high temperature corrosion and the best known example [27].

**2.2.3.2-Wet corrosion**: For example, when the corrosion environment is water with dissolved organisms. The liquid is an electrolyte and the process is usually

electrochemical in nature , for example, fused salts and molten metals, corrosion may also occur in other fluids [27].

Therefore, various types of wet corrosion (uniform, pitting, crevice, erosion, intergranular, selective leaching and stress corrosion cracking) have been described and graded, as shown below [28].

**a. General (uniform)**

Corrosion it's an even metal loss rate. Over the corrosion-characterized exposed soil attack occurring uniformly over. The whole area of the surface or a significant proportion of the total area . Uniform corrosion is the simplest type of corrosion, one of the most corrosion types that cause catastrophic failures are easily calculated and fairly predicted. In terms of cost or protection, it is therefore not always the most relevant. But if surface corrosion is allowed to continue the surface can become rough and surface corrosion can lead to more severe kinds of corrosion [28,29].

**b. Pitting corrosion**

Pitting corrosion is characterized by heavily localized metal loss. It looks like a deep, tiny metal hole. With time, but not to the extent, the width of the pit may increase. to which the depth increases. Most often; the opening of the pit remains covered by the corrosion product making it difficult to detect during inspection [28,29]. Pitting can happen in most metal with protective film Initiating a pit is also synonymous with the breakdown of the protective layer on the surface of the metal. In various environments, many metals and their alloys are subject to pitting, such as alloys (carbon steels, stainless steels, titanium, nickel , copper and aluminum) [29].

**c. Crevice corrosion (CC)**

Crevice in which the distance is too wide for liquid to reach the crevice and too narrow for stagnation of the liquid in the crevice. Various metals, e.g. (Al, Fe, Cr and Ni), can suffer from crevice corrosion that is influenced by a variety of factors. Environmental, metallurgical, electrochemical, Physical surface and, last but not least, geometrical nature.; Under lip gaskets, CC occurs in overlap joints between nail and screw heads and paint coating edges. In heat exchangers, etc., tubes and tube plates; The same type of corrosion occurs under deposits of, e.g. corrosion materials, gravel, sand; leaves and marine organisms; in such cases, It is also called corrosion of the deposit. comprises processes, modeling, research methods and outcomes realistic knowledge security measures and tracking. A review of the CC mechanisms has been made available recently, [29].

**d. Galvanic Corrosion**

This happens when a metal or alloy is electrically connected to a different electrode metal potential in the same electrolyte the greater the difference between the potential of the electrode, the greater the will. The level of galvanic corrosion [30].

**e. Erosion-Corrosion**

The term erosion corrosion refers to erosion due to mechanical force oxidation. Erosion corrosion is typically, induced. By a liquid that is gaseous or corrosion flowing over the metal (Velocity, instability, impingement, presence of suspended solids and temperature) are affected. Turbulence phenomena can kill protective films and result in very high material corrosion rates [29].

### f. Intergranular Corrosion

Intergranular corrosion is a localized assault with negligible corrosion to other areas of the surface on or at grain boundaries. The attacks extend through the material. This is a dangerous type of corrosion because of the cohesive forces between the grains may be too weak to withstand tensile stresses; at a relatively early stage, the durability of the material is significantly reduced; and fracture [29].

### g. Selective corrosion

Basically, this kind of corrosion is found in alloys. During selective leaching more active metal of an alloy, is extracted selectively leaving behind a porous deposition of the more noble metal [28].

### h. Stress-corrosion cracking

Stress corrosion cracking (SCC) is a mechanism involving the initiation and propagation of cracks probably up to total part failure,' due to the combined action of mechanical tensile loading and a medium of corrosion. This stress may either be applied external load or can be residual stress in the metal (e.g. due to manufacturing process or heat treatment) [28].

## 2.3. Parameters affect the wet corrosion

### 2.3.1. Effect of temperature

Temperature increases the rate of almost all chemical reactions leading to an increase in the rate of corrosion and an increase in inhibition performance as well. Like other chemical reactions, the rate of corrosion of aluminum ‘and aluminum alloy (AA6063-T5) in aqueous acid solutions increases’ with growing temperature [31]. This effect can be expressed by

Arrhenius equation in which the rate of corrosion reaction is correlated with temperature as in:

$$CR = A \exp\left[-\frac{E_a}{RT}\right] \qquad (2.10)$$

Where (A) is Frequency factor Ea is Activation energy ($kJ\,mol^{-1}$), R is Gas constant ($8.314\,J.mol^{-1}.K^{-1}$), T is Absolute temperature (K). From Arrhenius Equation activation energy and frequency factor can be calculated by taking the natural (logarithm) of the previous equation:

$$\ln(CR) = \ln A - \frac{E_a}{RT} \qquad (2.11)$$

So $\ln(CR)$ can be plotted against $(1/T)$ with a slope of $(-E_a/R)$ and intercept of ln (A) changes in temperature have the greatest effect when the activation process is the rate-determining step. Therefore, it is not surprising that the activation energy of inhibited high coverage reactions may be either greater or smaller than that of uninhibited reactions.

The relationship $\ln CR = f\,(1/T)$ is quite frequently although not always linear in the presence of inhibitor.

Equation of transition state can be used to calculate enthalpy and entropy of activation as [32].

$$CR = \frac{RT}{Nh}\exp\left[\frac{\Delta S^*}{R}\right]\exp\left[-\frac{\Delta H^*}{RT}\right] \qquad (2.12)$$

$$\frac{CR}{T} = \frac{R}{Nh}\exp\left[\frac{\Delta S^*}{R}\right]\exp\left[-\frac{\Delta H^*}{RT}\right] \qquad (2.13)$$

$$\ln\left[\frac{CR}{T}\right] = \ln\left[\frac{R}{Nh}\ \exp\left(\frac{\Delta S^*}{R}\right)\exp\left(-\frac{\Delta H^*}{RT}\right)\right] \quad (2.14)$$

$$\ln\left[\frac{CR}{T}\right] = \ln\left[\frac{R}{Nh}\right] + \left[\frac{\Delta S^*}{R}\right] + \left[-\frac{\Delta H^*}{RT}\right] \quad (2.15)$$

$$\ln\left[\frac{CR}{T}\right] = \ln\frac{R}{Nh} + \left[\frac{\Delta S^*}{R}\right] - \left[\frac{\Delta H^*}{RT}\right] \quad (2.16)$$

Where; $h$ is the Planck's constant, $(j.s)$ N is the Avogadro's number $(\text{molecule mol}^{-1})$ $\Delta S^*$ is the apparent entropy of activation $(\text{kJmol}^{-1}\text{K}^{-1})$ $\Delta H^*$ is the enthalpy of activation $(\text{kJmol}^{-1})$.From equation (2.16) we can plot $\ln(CR/T)$ against $(1/T)$ and the slope of the straight line show a value $(-\Delta H^*/R)$ and intercept show a value of $(\frac{\Delta S^*}{R} + \ln R/Nh)$ from which $(\Delta H^*)$ and $(\Delta S^*)$ can be calculated.

### 2.3.2. Effect of inhibitor concentration

It is well known that the first step in inhibiting the corrosion of metals is the adsorption into the metal of organic inhibitor molecules. The coverage of the surface depends on the efficiency of inhibition and concentration of (CML). The fraction of the surface protected by the adsorbed molecule increases with increased concentration of the inhibitor [33].

## 2.4.Thermodynamics of corrosion

Thermodynamics suggest which reactions are possible, and whether there will be a specific reaction possible. This assists in, understanding of corrosion phenomena and is important to the study of corrosion cells. Chemical

thermodynamics studies, discuss the role of entropy in chemical reactions and explains equilibrium as a function of the elements and compounds present and the environmental conditions e.g, (pressure, temperature, and chemical composition). It is used to decide whether corrosion can occur and to predict the formation of stable corrosion products. The most secure is the rule of nature, which postulates for a collection state. The condition that has the lowest free energy is that of reactants.' Metal surfaces in contact with a solution therefore tend toward the lowest possible free energy condition. There is no further change when the system enters this state. Finally, special lowest energy state is the state of equilibrium. When the system is stable, there are no driving forces available from that state for any change [34].

## 2.5. Methods for corrosion prevention

### 2.5.1. Suitable Material Selection

The use of materials for the medium is extremely resistant to corrosion. That the choice of these materials for the reason penetrated them, of the parameters is based on the tables and the basic errors that are used to corrosion from the choice of the necessary materials. This approach is based on the preference of the appropriate material for the medium in it. That is selecting the material that is suitable. to resist the corrosion that occurs, as a result of the contact of the metal with the medium. The properties of the materials used depend for example, on a variety of factors: engineering requirements, industrialization process, surface conditions of the medium surrounding it [35].

### 2.5.2. Cathode Protection

Definition of the protection of the cathode for the purpose, of service to monitor the corrosion and the protection of structures and metal parameters for the inclined hours. The basic concept of this process is that it is based on the infiltration of the Tiller interstitial variation on the plasticity that is covered, and that in turn the cellophor of the advertised GHLLER is used and the solution will be dulled by using a crystal of other minerals, so it will serve as a cathode. The form of Cathodic protection is well-used in the protection of iron alloy. There are two kinds of Cathodic protection [36].

**1-** Cathode acidity with the anode sacrificed. This approach relies on linking the substance or structure to be protected with another electrode that is more. Efficient for the annealing of the annealed, with a third referring to the Impressed flame.

**2-** By present shedding, Cathodic protection This method relies on the extraction of an external, Tyler on the surface of the material or structure to be covered for deformation , of the resulting consumption of the annealed electronic and for this method, it is considered the most economical inductance for the first method since it does not consume anode electrodes [37].

## 2.5.3. Inhibitor of corrosion

Corrosion Inhibitors (Chemicals, Wearing) with minimal quantities to lower wear rates. No anticorrosive contraceptives are appropriate for all circles and for all advertisers, so it is important to first test all anticonvulsants in the laboratory. These products must be non-toxic and healthy and do not alter the medium requirements and be economical in it . There are several theories that describe the mechanism of action and the adsorption theory which we have concluded that these materials adsorb on the surface of the Adsorption Theory, is the most important of them. The metal is a single or multiple layer that isolates the marketers, in public There are several of the corrosion' inhibitors that can be identified as follows:

**1-** Materials that are mostly organic materials that are adsorbed on are adsorption inhibitors aluminum alloy (AA6063- T5). The entire surface of the metal that forms an insulating drum cover; the anode and cathode positions on the surface of the metal [38].

**2-** Film forming inhibitors that interfere with the metal surface are products, producing new layers and a new chemical structure that can typically be categorized into (anodic inhibitors) used in the Anodic Film Inhibitor and base and (cathodic inhibitors) that function [39].

**3-** The corrosion inhibitors types can be chemicals synthetic natural. The inhibitors can be classified depending to on inhibitory factors such as the chemical kind of the inhibitors , the mechanism of activity , Oxidants or do not oxidants generally the inhibitors interact with the rust corrosion product initially formed resulting in a consistent and insoluble layer on the metal surface [40].

### 2.5.4.Coatings

Coatings are one of the most important materials that are commonly used in our lives, where the metal is coated with various forms of coatings to protect the metals from corrosion. So it is used to protect people from devices and machinery from the corrosion pest that affects the machinery or parts of it and according to the medium in which it works. The adduct of the advertised surface is publicly identified by its surroundings the manner in which it is covered by suitable coatings which prevent oxygen , water or other pollutants from affecting it, and the choice of the type of coating depends on important factors, namely the medium surrounding the metal, the method of application of the coating and the type of metal to be coated. The coatings are used in addition to shielding the metal from corrosion, all for the purpose of giving the equipment the appearance of elegance. It is used for coating as a buffer that isolates the advertiser from the desired current so that it can be used to harden the corrosion process or minimize the reaction time so that the annealed color is the medium that induces corrosion, such as Spraying, Dipping , Brushing , Electroplating and Thermal Coating [41].

There are many types of coating which can be categorized, as: metallic coatings, inorganic coatings, organic coating:

**1**-Metallic Coating

It is a cover that varies over the original metal to be coated, and it can be applied publicly by covering the original metal with a thin layer and with a different thickness, and the mixing of the medium used in it is made of it. The metal coating does not act as a sacrificial anode [41].

**2**-Inorganic coatings

It is a general declaration of inorganic substances that are used for the coating of metallic materials and for example, the advertisers with a layer of porcelain or glass The method of covering the metal with ceramic is used for the ceramic materials used in the household appliances, and in some food factories. Filling the glaze with glaze is a substance that is filled with the salt of the layer, the lowering of the silica gel on the metal surfaces [42].

**3**- Organic Coating

Organic chemicals used to shield metals from corrosion in many applications, since these additives are applied to the metal surface to separate it from the medium in it and avoid the contact between the medium and the metals surface. [43].

## 2.6. Aluminum

Aluminum is one of the most commonly used metals. In competition with steel and in the fields of architecture, transport, and public works, increasingly used [44]. Al is a soft, durable, lightweight, pliable metal, depending on the surface roughness and is non-sparkling [45].

Aluminum is specifically used to decrease weight relative to steel and is alloyed to improve silicon. The solidity of the material. It is well known that silicon solidifies into the (load-bearing surface) in a separate hard point. [46]. Aluminum relies on the production in different environments of a compact adherent passive oxide film for its corrosion immunity. This surface film, however, is amphoteric and dissolves significantly when it is exposed to high (acid or base concentrations).

Phosphoric acid ($H_3$ $PO_4$) is commonly used for aluminum acid cleaning and electro polishing [46].

In fact, aluminum is a very active metal ,meaning that its oxidizing behavior is very fast, while a weakness of this quality for most metals is actually the secret to its ability to resist corrosion. The combination of these properties makes it a favored option for many industrial applications such as vehicles, transportation, aerospace, food handling, containers, electronic devices, buildings, etc [47].

## 2.7. Aluminum Alloy (AA 6063-T5) and elements of impact

Aluminum and aluminum alloys are desirable materials due to cost-effective recyclability, excellent physical and mechanical properties, and excellent materials for a variety of industrial applications. (Low density, high thermal conductivity, strong walkability, high strength-to - weight ratio). In particular, the 6xxx-series (Al–Mg–Si) alloys are widely used in (aerospace, automotive, marine, and construction industries) due to their relatively, good corrosion resistance formability, and low cost as compared to the 2xxx (Al–Cu) and 7xxx (Al–Zn) alloys [48]. The major reason for alloying aluminum is intended to improve the strength of hardness and resistance to fatigue, relaxation of tension, wear or creep. Aluminum and its alloys have valuable industrial and economic properties. Because of its light weight, strong thermal and electrical conductivity and low cost, the value. aluminum most valuable property is its ability to withstand atmospheric effectively; and many aqueous solutions due to the rapid formation of thin film protective oxide that adheres tenaciously to the surface, which acts as a buffer between the corrosive atmosphere and the metal atmosphere. [49]. The elements that are most frequently used in commercial aluminum alloys to provide better

strength especially, when related to strain hardening cold working or heat treatment, or both are; zinc, copper, silicon, magnesium and manganese as shown in figure (2.1). All these elements have high solid solubility in aluminum, and usually, the solubility increases as temperature increases [50].

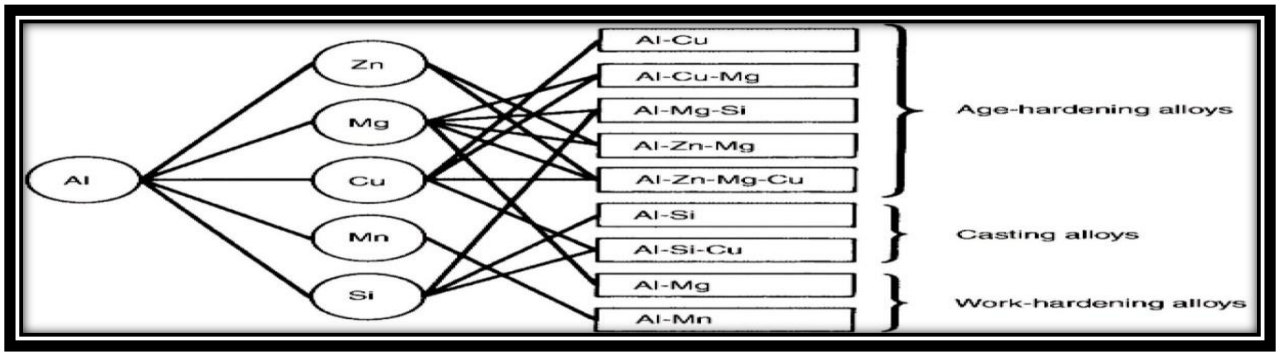


Figure (2.1) The principal aluminum alloys [50].

## 2.8.Studies of green inhibitors

Corrosion, aluminum and aluminum alloy (AA6063-T5) inhibition analysis. In phosphoric acid medium technique, aluminum alloy was used (weight loss method) and the processes of corrosion and inhibition were measured and discussed in detail. Because of its environmental and economic benefits, the use of green corrosion inhibitors is significant [51]. One of the best choices for shielding metals and alloys from corrosion is to use inhibitors.

Many inhibitors in use are either synthesized from inexpensive raw material or selected from 'hetero compounds; atoms in their aromatic or long-chain carbon framework. Most of these, however, are environmentally toxic, containing inhibitors metallic heavy metals [52].

Organic materials, adsorption corrosion inhibitors, inhibitors with the ability to adsorb on the metal can impede the surface the dissolution or corrosion reaction of such metal in the corrosion medium [53]. Corrosion inhibitors are chemicals that are proven to efficiently eliminate unwanted, damaging effects of violent media and avoid metal and alloy dissolution [54].

## 2.9. General features of green inhibitors

Corrosion inhibitors are substances considered to efficiently extract the unnecessary damaging effects of aggressive media and prevent metals and alloys from dissolving [54]. In terms of low cost and secure environment plant extracts are the primary benefit of using due to all the economic and environmental benefits, plant extracts are corrosion inhibitors. Up until now many plant extracts have been used as effective metal corrosion inhibitors.

Performance inhibition of plant extracts typically occurs in the composition of the species because of their presence. Complex organics (tannins, alkaloids and nitrogen bases, proteins and carbohydrates), as well as. Items linked to degradation [55,56]. Typically containing polar organic compounds with (atoms of nitrogen , sulphur or oxygen), as well as those with double, triple or conjugate aromatic rings in the molecular structures, which are the major adsorption centers [57,58]. Inhibitor adsorption at the interface of the metal solution is caused by: (a) the existence and surface charge of the metal, (b) the form of aggressive electrolyte, and (c) the chemical composition of the inhibitor [59].

The successful use of naturally occurring substances to inhibit the corrosion of metals in acidic and alkaline environments has been reported by some research groups [55].

Green inhibitors have features which are equivalent to (non-green) inhibitors. Most of the green inhibitors on the metal surface are adsorbed at room temperature by means of both physical and chemical adsorption. Inhibition occurs at elevated temperatures, mainly by through Chemisorption. On extended corrosion exposure of the green inhibitor environment, inhibitor gains, or loses its effectiveness during the corrosion inhibition process. Evaluation of the effect of additional time on the efficiency of the inhibition. Provides details on the time scale on the stability of the green inhibitors inhibitive actions. In most cases, the efficacy of the as time increases the inhibitor decreases, meaning that the adsorption of the inhibitor molecules on the metal surface occurs mainly through physical interactions [60].

## 2.10. Classes of green inhibitors

**According to their mechanism, inhibitors are divided into:-**

### 2.10.1. Anodic inhibitors

It is a substance that slows down or cancels positive electrode reactions of the anode reactions over a metal, surface and in general. Combined with products of corrosion and above are soluble .salt. The optimistic surface Interactions with electrodes and inhibits. The additional value must, in order to promote anodic reactions, be greater than the stated critical value. Materials chromates, nitrates, hydroxides, alkaline metal carbonates [61].

### 2.10.2 . Cathodic inhibitors

They are a chemicals that neutralize or suppress cathodic reactions and are supplied with combined positive ions. The cathodic basis for the formation of insoluble materials on the cathode cluster. Cathodic inhibitors are safer when used than anodic inhibitors since there is no essential value, a low degree of safety is obtained for their concentrations and even low concentrations are used zinc, magnesium, nickel and sulfates are examples of cathodic corrosion inhibitors used [61].

### 2.10.3. Mixed inhibitors

These are inhibitors that slow down both the reactions and cause corrosion on the foot (anodic and cathodic) Forms (polyphosphate, silicate) are part of the inhibitor [62].

### 2.10.4.Inorganic green inhibition

Inorganic elements or metals, when they are in trace quantities, play a vital role in living organisms. Increased concentrations of certain metals cause toxicity to all life forms. It is also true for metal derivatives. Chromium compounds, for instance, are primarily chromates. Widely used in aqueous substances as possible corrosion inhibitors. Excellent adhesive properties on surfaces made of metal. In the type of both pre-coatings, a large variety of polymers have been tested for their anti-corrosion properties [63,64]. In a number of corrosion fluids, both on the metal and an inhibitor [65].

### 2.10.5.The organic green inhibitor

Flavonoids, alkaloids and other natural products derived from natural sources, such as plants, are inhibitors. Synthetic compounds with negligible toxicity are also included. The figure (2.2) shows Classification of corrosion inhibitors. Some of the notable developments in organic green inhibitors are discussed here, especially plant extracts [66].

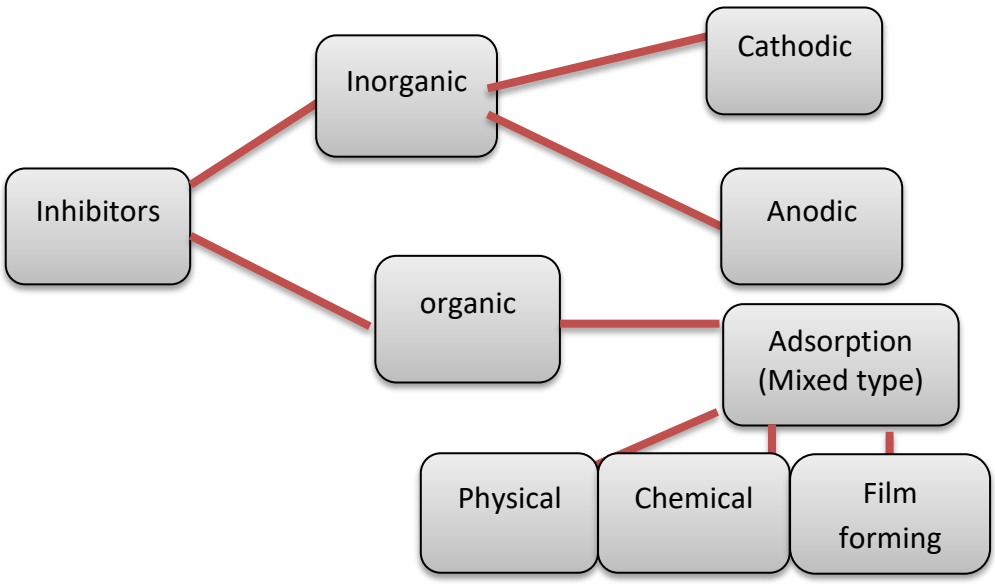


Figure (2.2): Shows classification of corrosion inhibitors .

## 2.11. Properties of effective inhibitor

To prevent or mitigate corrosion, metallic inhibitors of the materials in question must be able to comply with the following measures [67].

**1-** It has to be successful at a very high level of corrosion safety. The inhibitor is low in concentrations.

**2-** It has to the device that are exposed to corrosion attack must be protected.

**3-** It must preserve its performance , high velocity and temperature in extreme operating conditions.

**4-** During submission. The incidence of corrosion must not significantly increase under the dosage of the inhibitor.

**5-** No deposit can be produced on the inhibitor or inhibitor materials. Specifically surface metal in regions of heat transfer.

**6-** It must reduce corrosion, both localized and uniform. The efficiency range has to be long.

**7-** It must not present a health threat or possible emissions [67].

## 2.12. Mechanism of inhibitor action

Inhibitors influence the kinetics of inhibitors. On the metal surface, electrochemical reactions that constitute the corrosion mechanism adsorb corrosion inhibitors and thus modify the structure double-layer electricity. Organic compounds containing (oxygen, sulfur, nitrogen atoms) that contribute to the adsorption of compounds on the metal surface are the majority of effective inhibitors used in industry. [68]. Green or safe corrosion inhibitors do not contain heavy metals or other harmful substances and are biodegradable. In general,

corrosion inhibitors control corrosion by shaping different kinds of films. Inhibitors form films in many ways by adsorption, bulky precipitate formation and forming, a passive coating on the surface of the metal. The majority of organic inhibitors retard corrosion by corrosion by adsorption to shape just a few molecules thick to form a thin, invisible film [69]. Existing data indicate that most organic inhibitors are adsorbed on the metal, surface on the surface by displacing water molecules and creating a compact, protective barrier. Facilitating the availability of no bonded (lone pair) and electrons in inhibitor molecules Transference of electrons from the inhibitor to the metal. A co-ordinate covalent bond can be formed involving the transfer of electrons from the inhibitor to the metal surface.

## 2.13. Plants used in preparation of extracts (Cordia myxa leaves)

In certain Asian and African regions, the Assyrian plum is a common tree that bears *Cordia myxa* tree leaves and fruit have major applications in various cultures and the fruit is known for its medicinal uses The leaf shape is variable with a blade that can be broadly ovate or orbicular with a base that can be round cord ate with an apex that can be either rounded or acuminate and margins, that vary from entire to toothed figure (2.3). There are approximately 300 different species of trees and shrubs in the Boraginaceous family of the *Cordia* genus. Its extravagant, fragrant flowers, hairy leaves, and edible fruits characterize The name *Cordia* derives from the surname of the German botanist Valerius Cordus of the sixteenth century and the name of the genus, myxa, comes from the Greek word for mucus. Common *Cordia myxa* fruit names include Assyrian plum and sebesten. The tree is often referred to as the nest tree of the bird(*Cordia myxa L*). It is possibly native to a region ranging from tropical africa to the middle east.

It is part of a genus that belongs to the Boraginaceous (Hound's-Tongue) family, of around 320 tropical species [70].

Figure (2.3) Cordia myxa plant leaves

## 2.14. Adsorption isotherm

The surface of the metal is still covered with adsorbed water molecules in aqueous solutions. Adsorption of inhibitor molecules from an aqueous solution is therefore a quasi-substituted process [71].

The descriptive mechanism is given by adsorption isothermal studies. How the organic inhibitors adsorb to the surface of the metal [72]. (Langmuir, Freundlich, Temkin), are the most commonly used isotherms. The degree of surface coverage (Ɵ) for different concentrations of the inhibitor must be determined to obtain the adsorption isotherm and the different models must be determined. To demonstrate

the consistency of the model with data via equations, tests must be carried out follows:

$$\Theta = \frac{IE}{100} \qquad (2.17)$$

Where; (Θ) is the surface coverage, (IE) is the effectiveness of the inhibitor.

## - Langmuir adsorption isotherm

There is a set of uniform adsorption sites in the Langmuir isotherm model and several instances of heavy adsorption do not match this isotherm. This isotherm is, mathematically, given as [73].

$$\theta = \frac{K_L C_i}{1 + K_L C_i} \qquad (2.18)$$

Where; $K_L$ is the equilibrium constant (mg/g) representing the degree of adsorption for the (Langmuir adsorption isotherm) (i.e. , the higher the $K_L$ value indicates that the inhibitor is strongly adsorbed on the metal surface ($C_i$) is the concentration of the inhibitor (mg / L), and the surface coverage is (Θ) Equation Rearrangement (2.18) will give:

$$\frac{C_i}{\theta} = \frac{1}{K_i} + C_i \qquad (2.19)$$

It equation (2.19) as ($C_i/\theta$ ) against ($C_i$) The values $K_L$ can be determined from the intercept. another useful equation also is :

$$K_L = \frac{1}{55.5} \exp \frac{\Delta G^\circ}{RT} \qquad (2.20)$$

Where; $\Delta G^o$ ads is standard adsorption free energy (kJ $mol^{-1}$ ), The value of (55.5) is the water concentration in solution expressed in M.

- **Freundlich adsorption isotherm**

This isotherm can be represented by the equation .

$$\theta = K_F C_i^{n''} \qquad (2.21)$$

Where, for a given system at a given temperature, $K_F$ ((Freundlich constant) and n " are constants [74]. This isotherm can be written as:

$$\ln\theta = \ln\left(K_F C_i^{n''}\right) \qquad (2.22)$$

$$\ln\theta = \ln K_F + n'' \ln C_i \qquad (2.23)$$

Equation (2.23) can be plotted as $(\ln\theta)$ against $(\ln C_i)$, where the slope and intercept yield the values of n" and $K_F$ respectively.

- **Temkin adsorption isotherm**

Temkin isothermal adsorption, as defined in equation (2.25), was used to describe the adsorption of aluminum metal and aluminum alloy (AA6063-T5) surface adsorption inhibitors.

$$\exp(-2a\theta) = K_T C_i \qquad (2.24)$$

$$\theta = \frac{1}{-2a}\ln K_T - \frac{1}{2a}\ln C_i \qquad (2.25)$$

Where; and is the molecular parameter of interaction, $K_T$ is the equilibrium, (Temkin adsorption isotherm) constant, (L / gm) equation (2.25) can be plotted as surface coverage (Ɵ) versus (lnCi), where slope and intercept yield a and $K_T$ values , respectively [75].

## 2.15. The Adsorption mechanism

The mechanism of adsorption of the organic compound depends on the charge and the existence of the metal surface, the electronic characteristics of the metal surface, the temperature of the corrosion reaction the adsorption of the solvent and other ionic organisms, and the electrochemical ability of the metal interface. Two forms of potential contact with the metal surface include adsorption of the inhibitor:

**1**-The first one due to electrostatic attraction between inhibiting organic ions, weak undirected interaction is or dipoles and, electrically, the metal's charged surface. This relationship is known as actual, adsorption or physisorption.

**2**-The second if there is an interaction between the adsorbate and the adsorbent, there is some sort of interaction. This kind of contact includes the exchange of charges or the transfer of charges. To form a coordinate style bond, the interaction is called chemical, adsorption or chemisorption from adsorb ate to the atoms of the metal surface. It identifies About the adsorptive Organic inhibitors' action. It mainly depends, on the nature and charge of the metal surface adsorption of solvent. Electronic properties and other ionic species of metal corrosion reaction surface temperature at the solution interface [76,77].

## 2.16. Nanomaterials

Nanomaterials are classified as those having standardized components less than (1-100) nm (1nm=$9^{-10}$ m) [78]. with at least one dimension.

Manufactured nanoparticles or nano crystals, The mechanical, electrical, magnetic optical, chemical and other properties of metal semiconductors or oxides are of particular interest [79,80]. They have been used as quantum nanoparticles. Dots and, for example, nanomaterial-based catalysts as chemical catalysts. Recently, a

variety of nanoparticles for biomedical applications have been thoroughly investigated. Tissue engineering, delivery of medicines, biosensors, etc [81,82].

## 2.16.1 Nanomaterials in applications

Nanomaterials are used in a number of items used in production processes. Paints, filters, insulation and lubricant additives, as well as health care. Nanoezymes are nanomaterials in healthcare with enzyme-like properties [83]. They are an evolving type of artificial enzyme used for wide-ranging applications such as bio sensing, bio imaging, tumor diagnosis, [84]. These filters are capable of removing particles as small as a virus as seen in a water filter provided by Technologies and can be generated using nanostructures of high quality. Nano technology has been used in the field of air purification to tackle the spread of (MERS) in hospitals in Saudi Arabia (2012). As an additive to lubricants. In moving parts, nano materials have the ability to decrease friction. Worn and corroded sections with self-assembling anisotropic nanoparticles called Tribo (TEX) can also be fixed [85].

## 2.16.2 Synthesis of nanomaterials

The purpose of any synthetic process for nanomaterials is to create a material that exhibits properties that are a function of the nanometer range (1-100 nm) of their characteristic length scale. The synthetic method should therefore show size regulation in this range so that one, property or other can be achieved. The methods are also divided into two primary categories (bottom up and top) [86].

### 2.16.2.1 Bottom up methods

The assembly of atoms or molecules is involved towards nanostructured arrays. In these raw material approaches, origins may be in the form of liquid or solid gases. The latter involves some kind of disassembly before they are inserted into a

nanostructure. Methods (bottom up) normally fall into two categories (chaotic and controlled). In order to make the state unstable, chaotic processes include raising the constituent atoms or molecules to a chaotic state and then instantly altering the conditions. (Through clever handling. Items shape primarily as a result of insurance kinetics of any number of parameters. Collapse) can be difficult or impossible to control from the chaotic state and so ensemble statistics also rule. The resultant distribution of measurements and the average height. Nanoparticle formation is therefore regulated by modulation of the end state of the materials. Laser ablation, for example, of chaotic processes [86].

### 2.16.2.2 Top down methods

Methods take some force (e. g. mechanical force-laser) to break down bulk materials into nanoparticles, top down. A common method involves the mechanical breakdown of bulk materials into ball milling nanomaterials. In addition, laser ablation may also be made of nanoparticles that apply short pulse lasers (e. g. femtosecond laser) to ablate a target (solid) [86].

\

# *Chapter Three*
# *Experimental part*

## 3.1. Experimental

For the purpose of achieving the aim of the research, it is to study the change of corrosion rates by using (CML) leaves extract and ($Fe_2O_3$ and $TiO_2$) nanomaterials inhibitors of pure aluminum and aluminum alloy (AA 6063 - T5) in different temperatures. An integrated laboratory program was used for this purpose and details of this system. All devices and materials will be mention. The method of laboratory experiments ($1MH_3PO_4$) and ($1MH_3PO_4$ at PH of 4) different concentrations (2, 4, 6, 8 ,10 mg/L) of (CML) extract and ($Fe_2O_3$ and $TiO_2$) with different weight of oxides (1,1.5,2,2.5wt%) in addition to using different temperature.

## 3.2. Chemicals and Materials

### 3.2.1. Chemicals

#### 3.2.1.1- Phosphoric acid

Phosphoric acid was used as a corrosion solution after dilution to (1 M) and produced in Italy Properties of phosphoric acid. With the chemical formula ($H_3PO_4$), phosphoric acid is a weak acid. Ortho phosphoric acid rises to phosphoric acid, which is the term for this material (IUOAC ID). The (%85) solution is a (colorless , odorless, and non-volatile) solution is acidic enough to be corrosion also phosphoric acid has purity 99.89% molecular weight 97.944g / mol and density is 1.685g / ml , From (1M $H_3PO_4$) a solution with pH of 4 was prepared by the addition of few drops of (NaOH solution).

**3.2.1.2 -Acetone** : Acetone is a chemical with the formula ($C_3H_6O$) and (99.9%) purity and molecular weight (58.08g / mol). It was used to dry the mineral coupons before and after each test, designed by (ROMIL) company and manufactured in Europe.

**3.2.1.3- Benzene $C_6H_6$:** Produced in Europe, 99.7% purity. The substance was used for cleaning and extracting samples. The adherent fatty substances on the metals surface. .It was prepared by the laboratories of the Chemistry Department / College of Science / University of Diyala.

**3.2.1.4- Distilled water:** was used to prepare and clean the lead water samples and was obtained from the laboratories of the Department of Chemistry / College of Science / University of Diyala.

**3.2.1.5- Coating:** The black paint, manufactured by the Iraqi Keynes Company, was used with lead and mercury free requirements, and a thinner (1:5) ratio was diluted.

**3.2.1.6- Thinner:** used to dilute the paint made in Iraq, Nanomaterial.

**3.2.1.7- Iron oxide :** Size:20-30 nm; Alpha with specifications

Purity: 99.9% A Chinese facility produced by Nanjing Nano Technology, a company.

**3.2.1.8- Titanium oxide :** Size:20-50 nm. With specifications

Purity :99.9%. Produced by a company Hongwu International group Ltd –china .

## 3.2.2. Materials

basic materials are The listed as in table (3.1).

Table (3.1) the mineral materials used in this study.

| Material | | Formula | Manufacturer | Purity |
|---|---|---|---|---|
| 1 | Aluminum | Al | Iraqi | % 99.69 |
| 2 | Aluminum Alloy (AA6063 – T5) | AA | China | %98.45 |

The proportions of pure aluminum and aluminum alloys (AA6063-T5) are shown in the following table. An analysis was made in the Central Organization for Standardization and Quality Control.

The optical emission spectrum (OES) shown in table (3.2).

Table (3.2): Composition of aluminum and aluminum alloy (AA6063 – T5)

| composition (% Wt) | | | | | |
|---|---|---|---|---|---|
| Pure aluminum | | | | aluminum alloy (AA6063 – T5) | |
| Element | (%)Weight | Element | (%)Weight | Element | (%)Weight |
| Si | % 0.0666 | Na | % 0.0005 | Si | % 0.478 |
| Fe | % 0.139 | Bi | % 0.0020 | Fe | % 0.177 |
| Cu | % 0.0039 | Zr | % 0.0005 | Cu | % 0.0266 |
| Mn | % 0.0017 | B | % 0.0028 | Mn | % 0.0044 |
| Mg | % 0.0001 | Ga | % 0.0078 | Mg | % 0.0734 |
| Zn | % 0.0070 | Cd | % 0.0003 | Cr | % 0.0001 |
| Cr | % 0.0001 | Co | % 0.0002 | Ni | ---------- |
| Ni | % 0.0008 | Ag | % 0.0011 | Zn | % 0.0097 |
| Ti | % 0.0002 | Hg | % 0.0005 | Ti | % 0.0002 |
| Be | % 0.0001 | In | % 0.0005 | Ga | ---------- |
| Ca | % 0.0001 | P | % 0.0020 | V | ---------- |
| Li | % 0.0001 | As | % 0.0030 | Other | 0.0454 |
| Pb | % 0.0009 | Ce | % 0.0010 | | 0.0707 |
| Sn | % 0.0597 | La | % 0.0002 | Al | %98.45 |
| Sr | % 0.0001 | Sb | % 0.0050 | | |
| V | % 0.0028 | Al | %99.69 | | |

### 3.3. Instruments

The instruments, used in this study are listed in the table (3.3) with their model, Origin in College of Science, Diyala University .

Table (3.3): The instruments used in this study.

| No. | Instruments | Model | Origin |
|---|---|---|---|
| 1 | Electronic Balance | KERN & Shone GmbH, Type ACS 120-4, NO. WB12AE0308,CAPACITY 120g, READABILITY 0.1mg. | Germany |
| 2 | Thermostatic Water Bath | THERMOSTAT Water Bath HH-2 | China |
| 3 | Distillation Device | LUZ DE AVISO AGUA INSUFICICENTE | Germany |
| 4 | Laboratory Thermal Oven | BINDER, Hotline International | Germany |
| 5 | pH – meter | PH/Ion Bench top WTW in Lab PH Meters 7110 Bench top Meters | Germany |
| 6 | Hot Plat Magnetic Stirrer | AREC | Germany |

### 3.4.Devices used in characterization

The devices used are shown in table (3.4). with their model, and location.

Table (3.4): Devices used in the Characterization.

| No | Devices Names | Model | Location |
|---|---|---|---|
| 1 | Optical Emission spectrometer(OES) | Foundry Master X pert, Oxford-Instruments | Chemistry Laboratory, Department of Engineering, Industries, Central Organization for Standardization and Quality Control, Iraq |
| 2 | Fourier Transform Infrared Spectroscopy(FTIR) | Perkin Elmer Spectrum 65,type (400-4000$cm^{-y}$, | Laboratories of Chemistry Department, College of Science, University of Diyala, Iraq |
| 3 | Atomic Force Microscope (AFM) | Scanning Probe Microscope, AA 3000 SPM 220 V- Angstrom Advanced Inc., AFM contact | The Special Laboratory of Dr. Abdul Kareem M.A. AL-Sammarraie , College of Science, University of Baghdad, Iraq |
| 4 | X-ray Diffraction Spectroscopy (XRD) | X' pert high score pan alytical (021-44862778) | The Special Laboratory, Tehran ,Iran College of Science, University of Tehran |
| 5 | Scanning Electron Microscope (SEM) | TESCAN(Czech Republic) | The Special Laboratory, Tehran ,Iran College of Science, University of Sharif of Technology |

## 3.5. Preparation of corrosion solution

The solution of (1 M $H_3$ $PO_4$) was prepared using distilled water by dilution of (% 85) as shown in figure (3.1). The extract was applied directly to the corrosion solution in the pH range of (1-2) after preparing the solution.

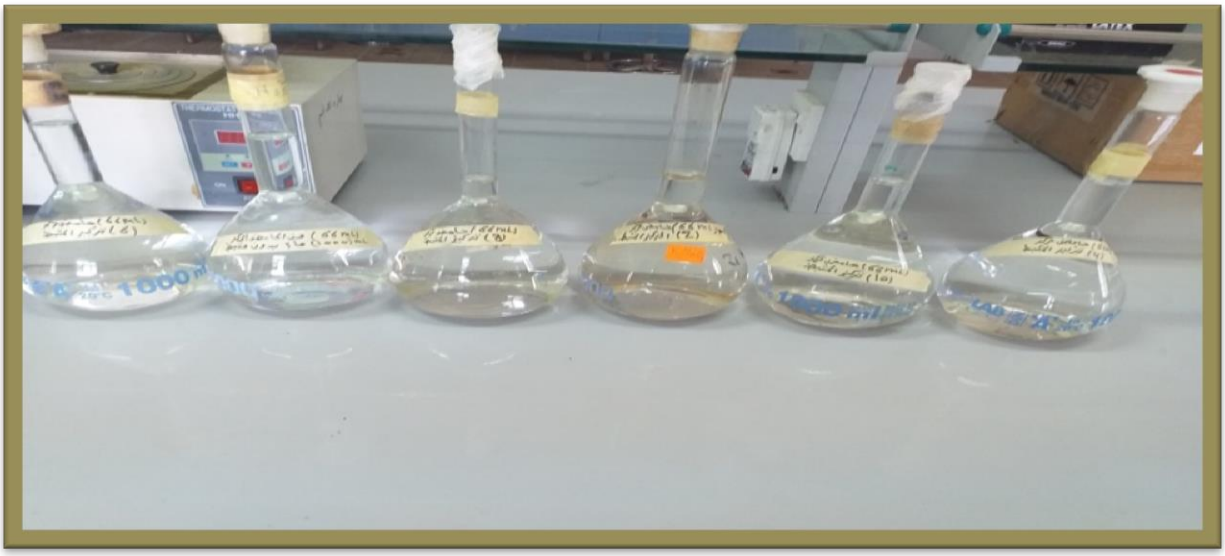

Figure (3.1): The preparation of phosphoric acid ($H_3PO_4$) corrosion solution.

### 3.6. Preparation of Cordia myxa leaves (CML) extract

A small fallen tree with bright leaves and medium-sized yellow flowers is available in Diyala Governorate / Iraq. Leaves collected from the garden were put in a dark place with distilled water grounded and pulverized after cleaning. The extract was prepared by taking 10 g powder of leaves and added to (100 ml) (1 M $H_3PO_4$) acid for 3 h and was left for a whole night. Figure (3.2 A) show Cordia myxa fresh leaves. figure (3.2B) show Cordia myxa leaves dried in the stray. Figure ( 3.2 C) show Cordia myxa powder dry leaves. figure (3.2 D) show Cordia myxa powder with (1 M $H_3PO_4$) acid. figure (3.2 E) show the refluxing extract. Figure (3.2F) show the extract before filtering. figure (3.2G and H) show the extract after filtering [18].

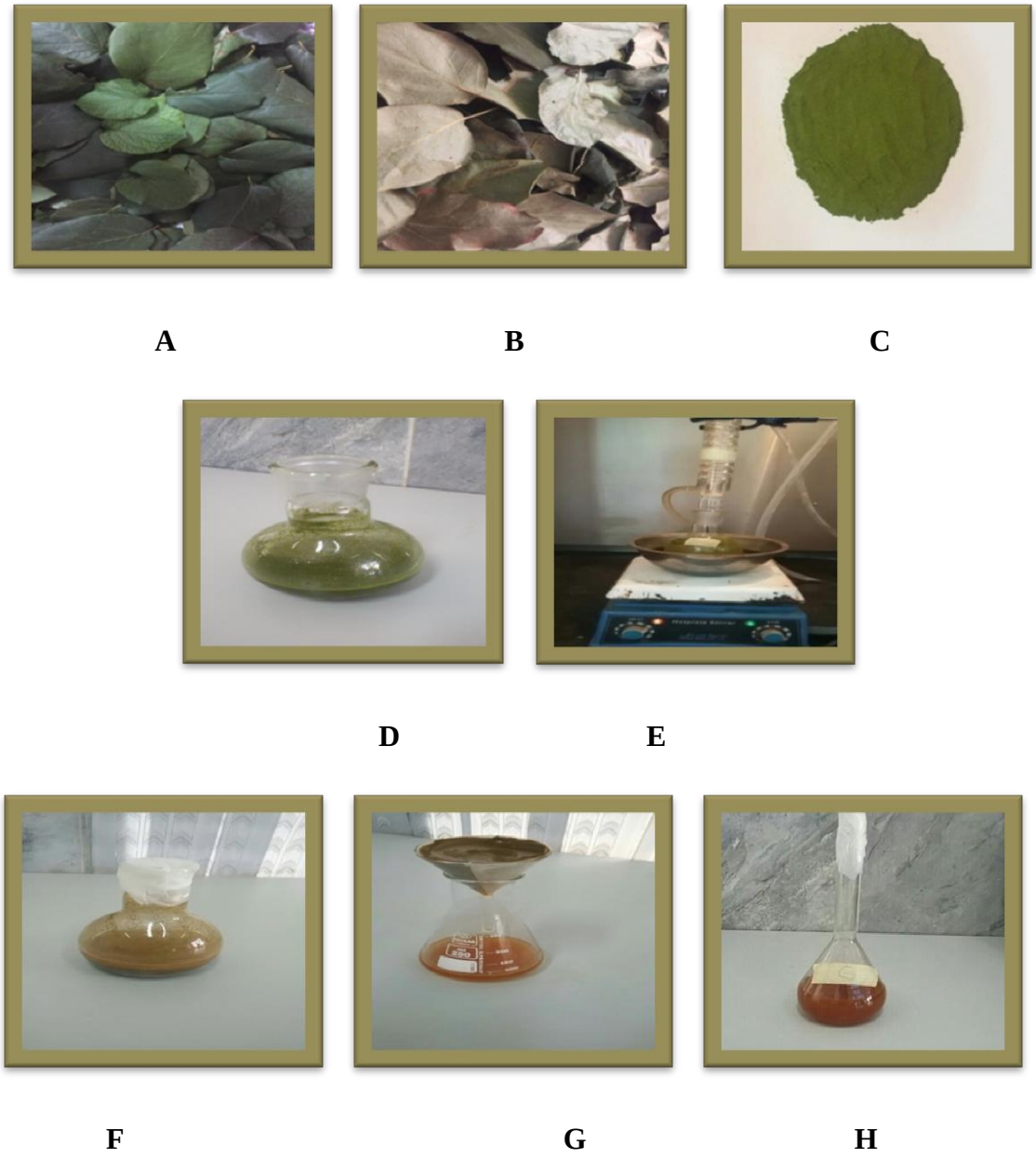


Figure (3.2): The preparation steps of (CML) extract.

## 3.7. Preparation of samples test of aluminum and aluminum alloy (AA6063 – T5)

The thickness samples (1 cm) were cut from pure aluminum and aluminum Alloy (AA6063-T5). Samples from. Dimension (3 cm x 3 cm) with a hole for easy suspension into the corroding solution (drilled on its side), as shown in Figure (3.3A, 3.3B and 3.3C) [87]. The samples were abraded with paper of various grades (220,400,600,800,1000,1500 and 2000),figure (3.3D), Then the samples were rinsed with flow of tap water followed, by distilled water. It is dried and immersed in acetone and hot air figure (3.3E), And then dried again and then packed in a silica gel desiccator over figure (3.3F), The samples were (weighted by the electronic balance of 4 digits) figure (3.3G), and the dimensions were measured by an electronic vernier, as shown in figure (3.3H), They were Completely immersed in the corrosion solution and moved to the water bath as shown in figure (3.3I and J), and after immersion samples as shown in Figure (3.3 K and L).

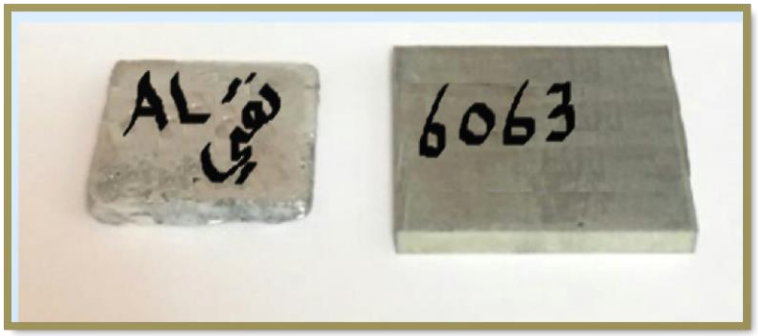


**A**

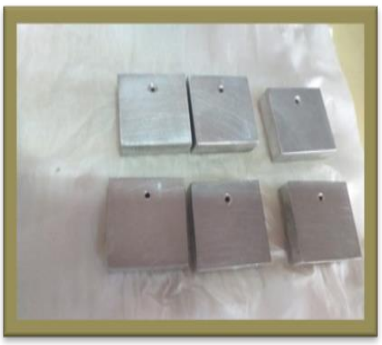

**C** **B**

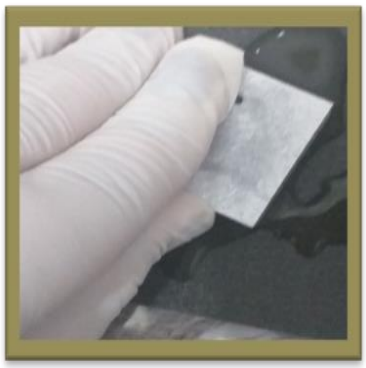

**D** **E**

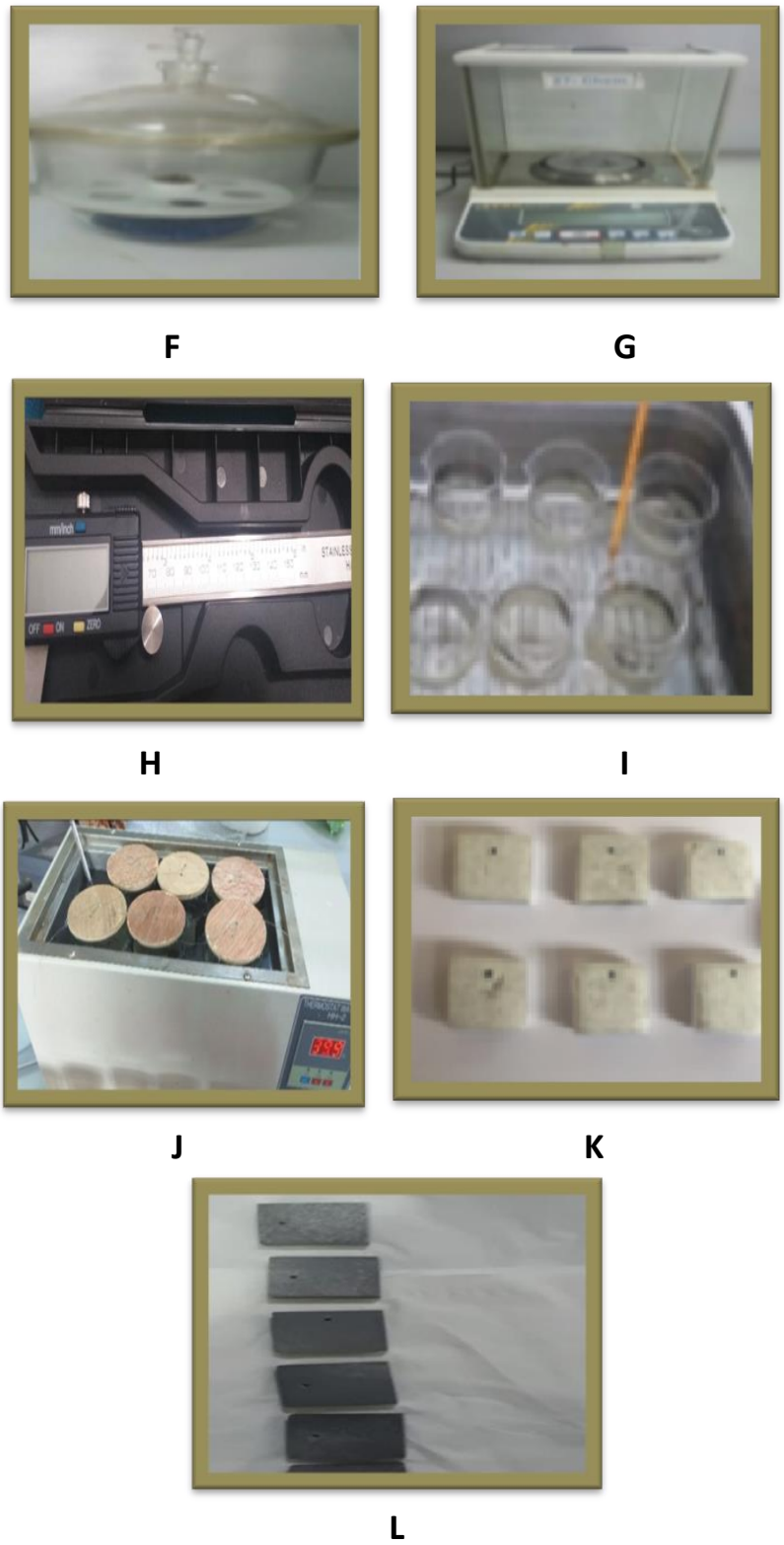


Figure (3.3): The preparation steps of pure aluminum and aluminum alloy (AA6063 – T5).

## 3.8. Nanomaterials experiments steps

Experiments were performed on samples of pure aluminum and aluminum alloy (AA6063-T5) and medium acidity level (1M$H_3PO_4$ at pH of 4) temperature and nanoparticles applied weight proportions to the coat for both ($Fe_2O_3$ and $TiO_2$) (1, 1.5,2,2.5) wt % at different temperatures (303, 313, 323and 333K) All these were done in one aqueous medium (1M$H_3PO_4$ at pH of 4) acid and experiments were done in a time period (3h) for every practical experience.

## 3.9. Preparation of samples test of aluminum and aluminum alloy (AA6063-T5) in nanomaterials

The process of preparing the samples was done in several steps, as follows [88].

**1-** Models of pure aluminum and aluminum alloy (AA6063-T5) were cut into pieces with a surface area close to (3 x 0.1 x 1) (cm). The area of each sample was measured using the electronic ruler inserted and accurately for two orders after the sorter.

**2-** The samples were cleaned and softened, as they were used for this purpose for sanding paper and various gradations from coarse to smoother (220,400,600,1000.1500.2000) to remove all deposits and obtain a smooth satin surface.

**3-** Samples were washed with plain water and then with distilled water and dried with clean pieces of cloth and then immersed in benzene to remove fat and grease layers if found and dried and then immersed in acetone for the purpose of removing moisture and then dried with another clean cloth.

**4-** The samples were then kept in the dryer until they used for their analysis.

**5-** After completing all the previous steps, the weight of the samples was measured with high accuracy before each experiment using the sensitive scale and for four ranks after sorting and recording (W1).

## 3.10 .Nanomaterials process of addition

As two types of nanomaterial have been used, is to increase the consistency of was the coating and protect the metal from corrosion iron oxide ($Fe_2O_3$) and titanium oxide ( $TiO_2$) were used separately, where a ratio of (1,1.5,2,2.5) wt % of each oxide has been applied separately to the coating used., then conducting experiments and calculating the rates of corrosion , and was added in steps as follows:

**1-** The quantity of nano oxide was added using the sensitive electronic balance.

**2-** Carefully, add the weighted amount to (20 ml ) of Thinner and leave it on the magnetic stirrer for 30 min to get a nanomaterial stuck.

**3-** the suspended solution was added to ( 100 ml) of coating and left on the magnetic motor for another half an hour in order to mix well.

**4-** After that, the coating process was done once immersion coating for one minute for each sample then the patterns were left to dry at room temperature for 24 hours.

**5-**Then it was heated in an electric oven for (15 minutes) at a temperature of 80 $^{\circ}$C in order to dry completely.

**6-**Then the sample weight and reading record (w1) were then measured.

**7-**Then the sample was weighed again and recorded (w2).

## 3.11. Weight - Loss Measurement

Samples of aluminum and aluminum alloy (AA6063-T5) were used to measure the weight. The samples that were cleaned and dried completely were immersed in (200 ml) of solution ( $1MH_3PO_4$) with (CML) inhibitor and un inhibitor for (3 h). As for the nanomaterial, the samples were coated and dried. Completely and immersed in ($1MH_3PO_4$ at PH of 4) with ($Fe_2O_3$ and $TiO_2$) inhibitor and un inhibitor for (3h). Weight loss was determined using experiments conducted with different concentrations of plant extracts and nanomaterial, as the concentrations of plant extracts were ( 2, 4 , 6 , 8 , 10) mg / L and the concentrations of ($TiO_2$ and $Fe_2O_3$) nanomaterials for each are (1, 1.5, 2, 2.5) wt% at different temperatures (303,313,323and 333 K) as shown in figure (3.4).

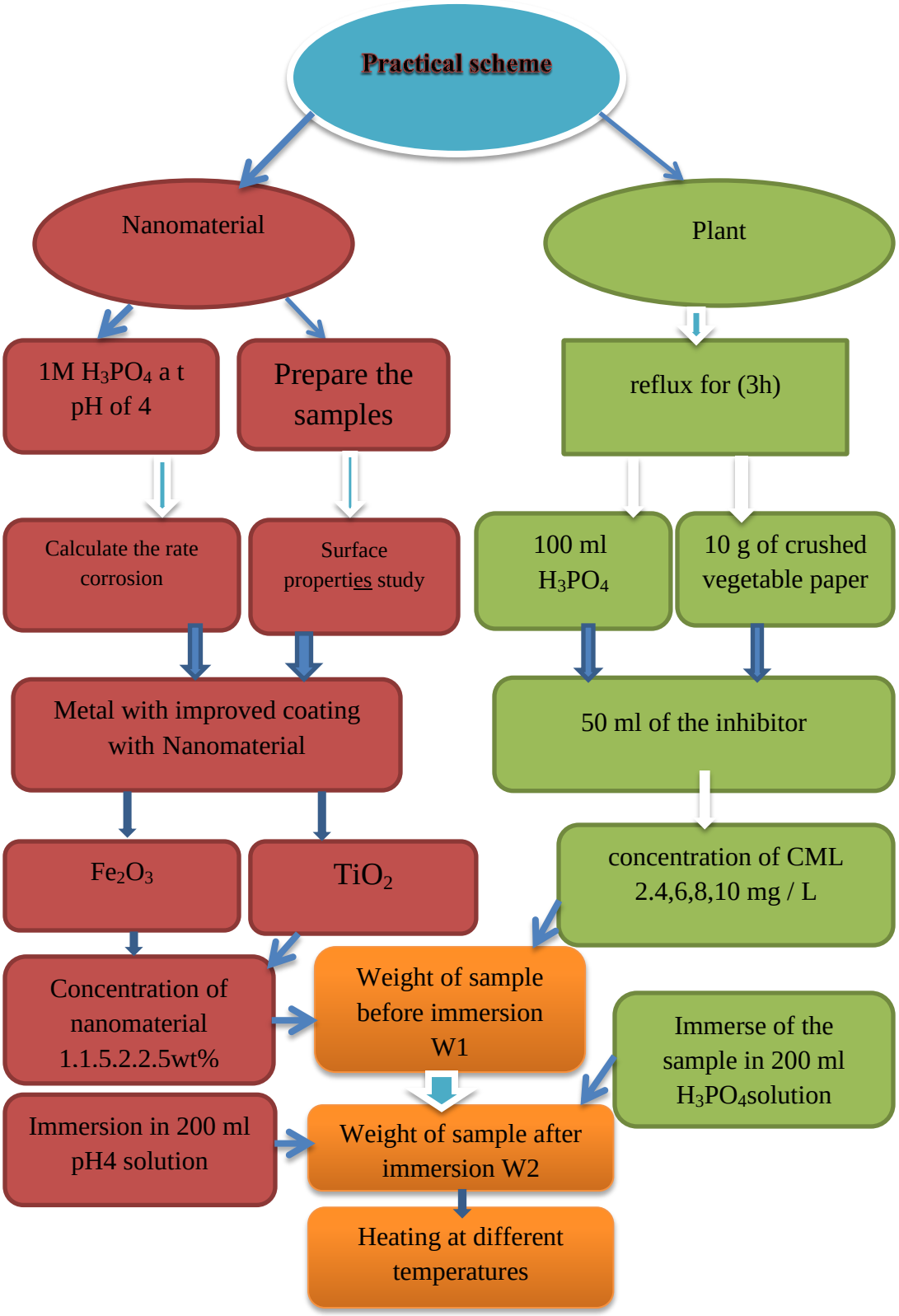


Figure (3.4): The experimental set up of corrosion study

# *Chapter Four*
# *Results*
# *&*
# *Discussion*

## 4.1. Weight - Loss Measurement

From the change in weight of specimens, the corrosion rate ($CR_{corr}$) was calculated by using the following relationship [89].

$$C_{R\,corr}\ (\text{mmpy}) = \frac{87.6w}{D.t.A} \qquad (4.1)$$

Where; W: weight loss in milligram, D: density of specimen ($g/cm^3$), t: the exposure time in hours, A: area of the specimen in square inch

(noting that 1 $in^2$ = 6.5416 $cm^2$).

$$\text{mmpy} = \text{millimeters penetration per year}$$

The inhibition efficiency (% IE) was calculated by using the following formula:

$$\%\ \text{IE} = \frac{CR_{uninh} - CR_{inh}}{CR_{uninh}} X100 \qquad (4.2)$$

Where ; $CR_{uninh}$ = corrosion rate without inhibitor, $CR_{inh}$= corrosion rate with inhibitor [90].

Corrosion rates and inhibitor efficiency was evaluated at different temperatures using inhibitor concentrations and ($1MH_3PO_4$) and ($1MH_3PO_4$ at PH of 4) the results were collected in tables (4.1) to (4.6). It is important that the rate of corrosion increased with temperature while decreased with the inhibitor's increased concentration. The inhibition efficiency increased with increasing inhibitor concentration.

Table (4.1): Effect of temperature on the corrosion rate,inhibition efficiency and surface coverage of aluminum in (1 M $H_3PO_4$) in absence and presence of Cordia myxa leaves (CML) extract as a corrosion inhibitor.

| Time (3h) | | | | | |
|---|---|---|---|---|---|
| Run | $C_{inh}$/(mg/L) | Temperature/(°C) | CR/mmpy | θ (surface coverage) | % IE |
| 1 | Blank | 30 | 5.4 | 0 | 0 |
| 2 | | 40 | 10.8 | 0 | 0 |
| 3 | | 50 | 14.4 | 0 | 0 |
| 4 | | 60 | 22.1 | 0 | 0 |
| 5 | 2 | 30 | 1.9 | 0.6481 | 64.81% |
| 6 | | 40 | 2.7 | 0.75 | 75% |
| 7 | | 50 | 3.2 | 0.7777 | 77.77% |
| 8 | | 60 | 3.4 | 0.8461 | 84.61% |
| 9 | 4 | 30 | 1.5 | 0.7222 | 72.22% |
| 10 | | 40 | 2.2 | 0.7962 | 79.62% |
| 11 | | 50 | 2.7 | 0.8125 | 81.25% |
| 12 | | 60 | 2.9 | 0.8687 | 86.87% |
| 13 | 6 | 30 | 1.3 | 0.7592 | 75.92% |
| 14 | | 40 | 1.7 | 0.8425 | 84.25% |
| 15 | | 50 | 2.1 | 0.8541 | 85.41% |
| 16 | | 60 | 2.7 | 0.8778 | 87.78% |
| 17 | 8 | 30 | 1 | 0.8148 | 81.48% |
| 18 | | 40 | 1.5 | 0.8611 | 86.11% |
| 19 | | 50 | 1.7 | 0.8819 | 88.19% |
| 20 | | 60 | 2.5 | 0.8868 | 88.68% |
| 21 | 10 | 30 | 0.8 | 0.8518 | 85.18% |
| 22 | | 40 | 1.3 | 0.8796 | 87.96% |
| 23 | | 50 | 1.6 | 0.8888 | 88.88% |
| 24 | | 60 | 2 | 0.9095 | 90.95% |

Table (4.2): Effect of temperature on the corrosion rate,inhibition efficiency surface coverage and of aluminum alloy $(AA6063-T5)$ in $(1\ M\ H_3PO_4)$ in absence and presence of Cordia myxa leaves (CML) extract as a corrosion inhibitor.

| Time (3h) | | | | | |
|---|---|---|---|---|---|
| Run | $C_{inh}$/(mg/L) | Temperature/(°C) | CR/ mmpy | θ (surface coverage) | % IE |
| 1 | Blank | 30 | 6.1 | 0 | 0 |
| 2 | | 40 | 12.2 | 0 | 0 |
| 3 | | 50 | 16.8 | 0 | 0 |
| 4 | | 60 | 24.2 | 0 | 0 |
| 5 | 2 | 30 | 2.3 | 0.6229 | 62.29% |
| 6 | | 40 | 3.7 | 0.6967 | 69.67% |
| 7 | | 50 | 4.5 | 0.7321 | 73.21% |
| 8 | | 60 | 5.4 | 0.7768 | 77.68% |
| 9 | 4 | 30 | 1.9 | 0.6885 | 68.85% |
| 10 | | 40 | 3.3 | 0.7295 | 72.95% |
| 11 | | 50 | 3.7 | 0.7797 | 77.97% |
| 12 | | 60 | 4.2 | 0.8264 | 82.64% |
| 13 | 6 | 30 | 1.6 | 0.7377 | 73.77% |
| 14 | | 40 | 2.9 | 0.7623 | 76.23% |
| 15 | | 50 | 3.2 | 0.8095 | 80.95% |
| 16 | | 60 | 3.6 | 0.8512 | 85.12% |
| 17 | 8 | 30 | 1.3 | 0.7868 | 78.68% |
| 18 | | 40 | 2.5 | 0.7951 | 79.51% |
| 19 | | 50 | 2.9 | 0.8273 | 82.73% |
| 20 | | 60 | 3.2 | 0.8677 | 86.77% |
| 21 | 10 | 30 | 1.1 | 0.8196 | 81.96% |
| 22 | | 40 | 2.1 | 0.8278 | 82.78% |
| 23 | | 50 | 2.8 | 0.8333 | 83.33% |
| 24 | | 60 | 3.0 | 0.8760 | 87.60% |

Table (4.3): Effect of temperature on the corrosion rate ,inhibition efficiency and surface coverage of aluminum in ($1MH_3PO_4$ at pH of 4) absence and presence of ($Fe_2O_3$) nanomaterial .

| Time (3h) | | | | | |
|---|---|---|---|---|---|
| Run | Nano $Fe_2O_3$% | Temperature/(°C) | CR/ mmpy | θ (surface coverage) | % IE |
| 1 | Blank | 30 | 7.6 | 0 | 0 |
| 2 | | 40 | 9.2 | 0 | 0 |
| 3 | | 50 | 11.1 | 0 | 0 |
| 4 | | 60 | 16.1 | 0 | 0 |
| 5 | 1 | 30 | 5.2 | 0.3157 | 31.57% |
| 6 | | 40 | 5.9 | 0.3586 | 35.86% |
| 7 | | 50 | 6 | 0.4594 | 45.94% |
| 8 | | 60 | 6.2 | 0.6149 | 61.49% |
| 9 | 1.5 | 30 | 4.6 | 0.3947 | 39.47% |
| 10 | | 40 | 5.1 | 0.4456 | 44.56% |
| 11 | | 50 | 5.3 | 0.5225 | 52.25% |
| 12 | | 60 | 5.4 | 0.6645 | 66.45% |
| 13 | 2 | 30 | 4.4 | 0.4211 | 42.11% |
| 14 | | 40 | 4.8 | 0.4733 | 47.33% |
| 15 | | 50 | 4.9 | 0.5585 | 55.85% |
| 16 | | 60 | 5.1 | 0.6832 | 68.32% |
| 17 | 2.5 | 30 | 3.7 | 0.5131 | 51.31% |
| 18 | | 40 | 4.1 | 0.5543 | 55.43% |
| 19 | | 50 | 4.3 | 0.6126 | 61.26% |
| 20 | | 60 | 4.6 | 0.7143 | 71.43% |

Table (4.4): Effect of temperature on the corrosion rate, inhibition efficiency and surface coverage of aluminum alloy (AA6063-T5) in ($1MH_3PO_4$ at pH of 4) in absence and presence of ($Fe_2O_3$) nanomaterial.

| Time (3h) | | | | | |
|---|---|---|---|---|---|
| Run | Nano $Fe_2O_3$% | Temperature/ (°C) | CR/mmpy | θ (surface coverage) | % IE |
| 1 | Blank | 30 | 8.5 | 0 | 0 |
| 2 | | 40 | 9.8 | 0 | 0 |
| 3 | | 50 | 11.9 | 0 | 0 |
| 4 | | 60 | 17.3 | 0 | 0 |
| 5 | 1 | 30 | 6.1 | 0.2824 | 28.24% |
| 6 | | 40 | 6.5 | 0.3367 | 33.67% |
| 7 | | 50 | 6.9 | 0.4201 | 42.01% |
| 8 | | 60 | 8.2 | 0.5261 | 52.61% |
| 9 | 1.5 | 30 | 5.6 | 0.3412 | 34.12% |
| 10 | | 40 | 5.8 | 0.4081 | 40.81% |
| 11 | | 50 | 6 | 0.5042 | 50.42% |
| 12 | | 60 | 6.9 | 0.6012 | 60.12% |
| 13 | 2 | 30 | 5.2 | 0.3882 | 38.82% |
| 14 | | 40 | 5.3 | 0.4591 | 45.91% |
| 15 | | 50 | 5.6 | 0.5294 | 52.94% |
| 16 | | 60 | 5.9 | 0.6589 | 65.89% |
| 17 | 2.5 | 30 | 4.6 | 0.4588 | 45.88% |
| 18 | | 40 | 4.8 | 0.5102 | 51.02% |
| 19 | | 50 | 5.1 | 0.5714 | 57.14% |
| 20 | | 60 | 5.4 | 0.6878 | 68.78% |

Table (4.5): Effect of temperature on the corrosion rate, inhibition efficiency and surface coverage of aluminum in ($1MH_3PO_4$ at pH of 4) absence and presence of ($TiO_2$) nanomaterial.

| Time (3h) | | | | | |
|---|---|---|---|---|---|
| Run | Nano $TiO_2$% | Temperature/(°C) | CR/mmpy | θ (surface coverage) | % IE |
| 1 | Blank | 30 | 9.3 | 0 | 0 |
| 2 | | 40 | 10.8 | 0 | 0 |
| 3 | | 50 | 12.7 | 0 | 0 |
| 4 | | 60 | 18.8 | 0 | 0 |
| 5 | 1 | 30 | 6.7 | 0.2795 | 27.95% |
| 6 | | 40 | 7.2 | 0.3333 | 33.33% |
| 7 | | 50 | 7.6 | 0.4016 | 40.16% |
| 8 | | 60 | 9.9 | 0.4734 | 47.34% |
| 9 | 1.5 | 30 | 6.3 | 0.3226 | 32.26% |
| 10 | | 40 | 6.5 | 0.3982 | 39.82% |
| 11 | | 50 | 6.6 | 0.4803 | 48.03% |
| 12 | | 60 | 7.8 | 0.5851 | 58.51% |
| 13 | 2 | 30 | 5.5 | 0.3656 | 36.56% |
| 14 | | 40 | 6.1 | 0.4351 | 43.51% |
| 15 | | 50 | 6.2 | 0.5118 | 51.18% |
| 16 | | 60 | 7 | 0.6276 | 62.76% |
| 17 | 2.5 | 30 | 5.3 | 0.4301 | 43.01% |
| 18 | | 40 | 5.5 | 0.4907 | 49.07% |
| 19 | | 50 | 5.7 | 0.5511 | 55.11% |
| 20 | | 60 | 6.2 | 0.6702 | 67.02% |

Table (4.6): Effect of temperature on the corrosion rate, inhibition efficiency and surface coverage of aluminum alloy (AA6063-T5) in ($1MH_3PO_4$ at pH of 4) absence and presence of ($TiO_2$) nanomaterial.

| Time (3h) | | | | | |
|---|---|---|---|---|---|
| Run | Nano $TiO_2$% | Temperature/(°C) | CR/mmpy | θ (surface coverage) | % IE |
| 1 | Blank | 30 | 9.9 | 0 | 0 |
| 2 | | 40 | 11.4 | 0 | 0 |
| 3 | | 50 | 13.7 | 0 | 0 |
| 4 | | 60 | 19.8 | 0 | 0 |
| 5 | 1 | 30 | 7.7 | 0.2222 | 22.22% |
| 6 | | 40 | 8.5 | 0.2543 | 25.43% |
| 7 | | 50 | 8.6 | 0.3723 | 37.23% |
| 8 | | 60 | 11.5 | 0.4191 | 41.91% |
| 9 | 1.5 | 30 | 7.5 | 0.2424 | 24.24% |
| 10 | | 40 | 7.6 | 0.3333 | 33.33% |
| 11 | | 50 | 7.9 | 0.4234 | 42.34% |
| 12 | | 60 | 10.3 | 0.4797 | 47.97% |
| 13 | 2 | 30 | 6.7 | 0.3032 | 30.32% |
| 14 | | 40 | 6.9 | 0.3947 | 39.47% |
| 15 | | 50 | 7.3 | 0.4672 | 46.72% |
| 16 | | 60 | 9.2 | 0.5353 | 53.53% |
| 17 | 2.5 | 30 | 6.1 | 0.3838 | 38.38% |
| 18 | | 40 | 6.5 | 0.4298 | 42.98% |
| 19 | | 50 | 6.8 | 0.5090 | 50.90% |
| 20 | | 60 | 7.9 | 0.6001 | 60.01% |

## 4.2. Effect of different conditions on corrosion rate

### 4.2.1.Effect of temperature on corrosion rates in the absence of CML extract and nanomaterials inhibitors.

Weight loss measurements were used to determine the rates of corrosion in uninhibited acid solutions at different temperatures after (3 h) immersion time for aluminum and aluminum alloy ($AA6063-T5$) in ($1M H_3PO_4$),(1M $H_3PO_4$ at pH of 4) It was found that the corrosion rate increased in case of aluminum (5.4 to 22.1 mmpy) and in aluminum alloy (AA6063-T5) (6.1to 24.2 mmpy) while temperature increased from ($303, 313, 323$ and $333$ K) as shown in figures(4.1) and(4.2). Also it was found that the corrosion rate increased in case of aluminum uncoated ($Fe_2O_3$) from (7.6 to 16.1 mmpy), aluminum alloy (AA6063-T5) from , (8.5 to 17.3 mmpy). The rates of corrosion increased in case of aluminum uncoated ($TiO_2$) from (9.3 to 18.8 mmpy) and for aluminum alloy($AA6063-T5$ from (9.9 to 19.8 mmpy) as temperature increased from ($303, 313, 323$ and $333$ K) as shown in figures (4.3),(4.4),(4.5) and(4.6).

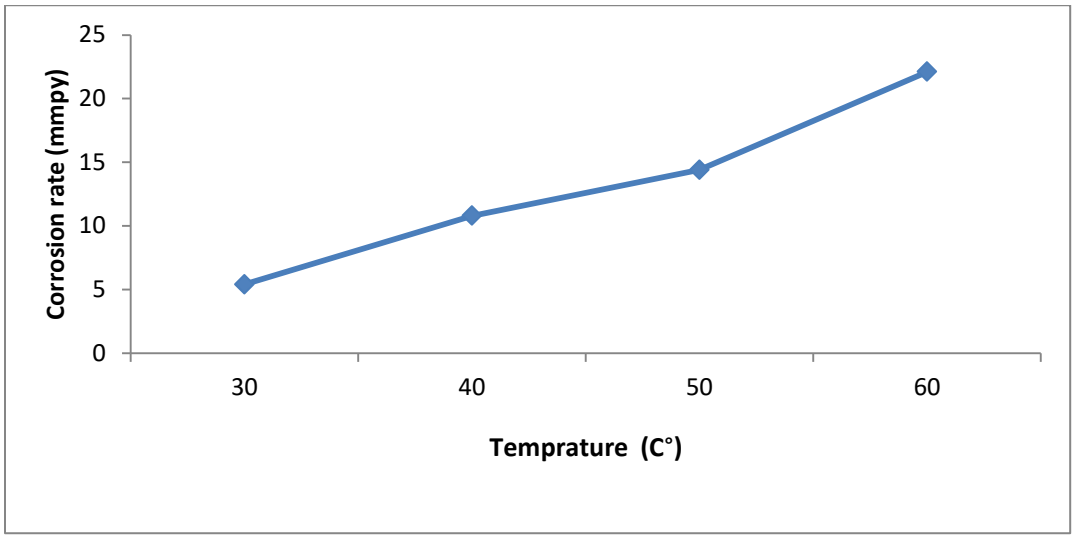


Figure (4.1): Effect of temperature on the corrosion rate of Cordia myxa leaves(CML) extract for aluminum immersed in (1 M $H_3PO_4$) for (3 h).

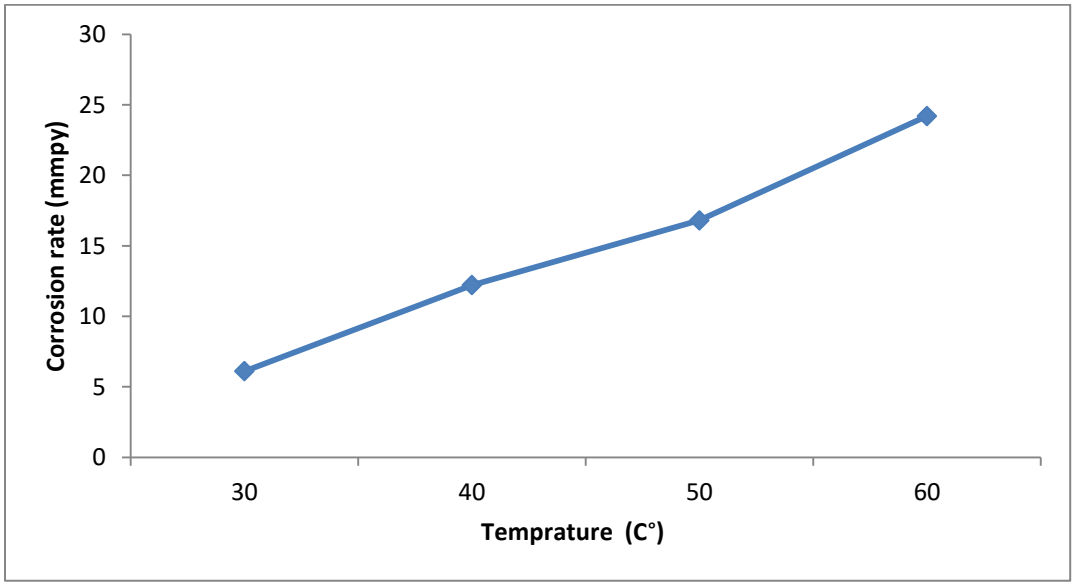


Figure (4.2): Effect of temperature on the corrosion rate of Cordia myxa leaves (CML) extract for aluminum alloy (AA6063 – T5) immersed in (1 M $H_3PO_4$) for (3 h).

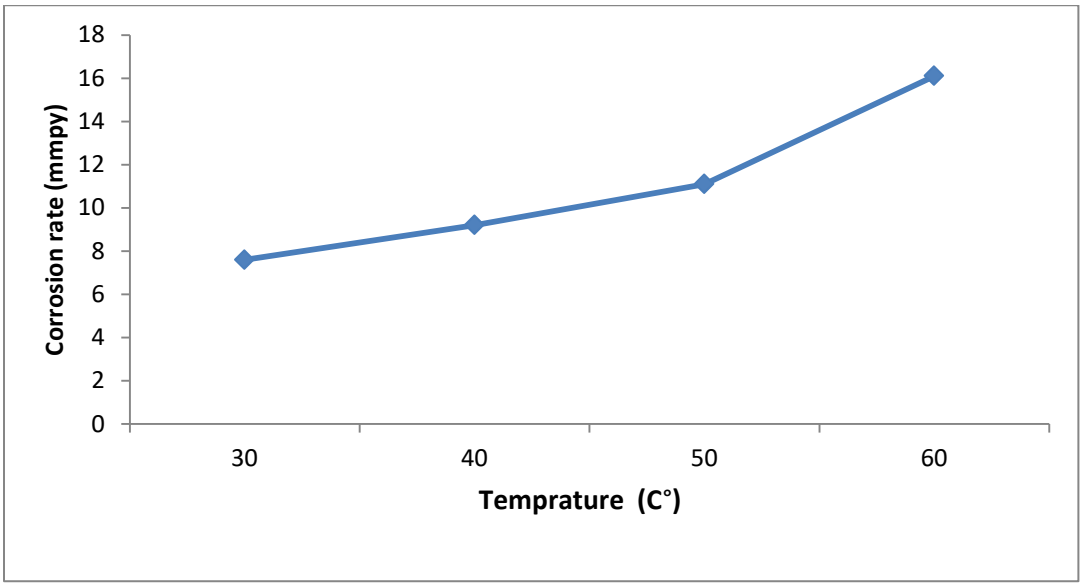


Figure (4.3): Effect of temperature on the corrosion rate of ($Fe_2O_3$) nanomaterial for aluminum immersed in ($1MH_3PO_4$ at pH of 4) for (3 h).

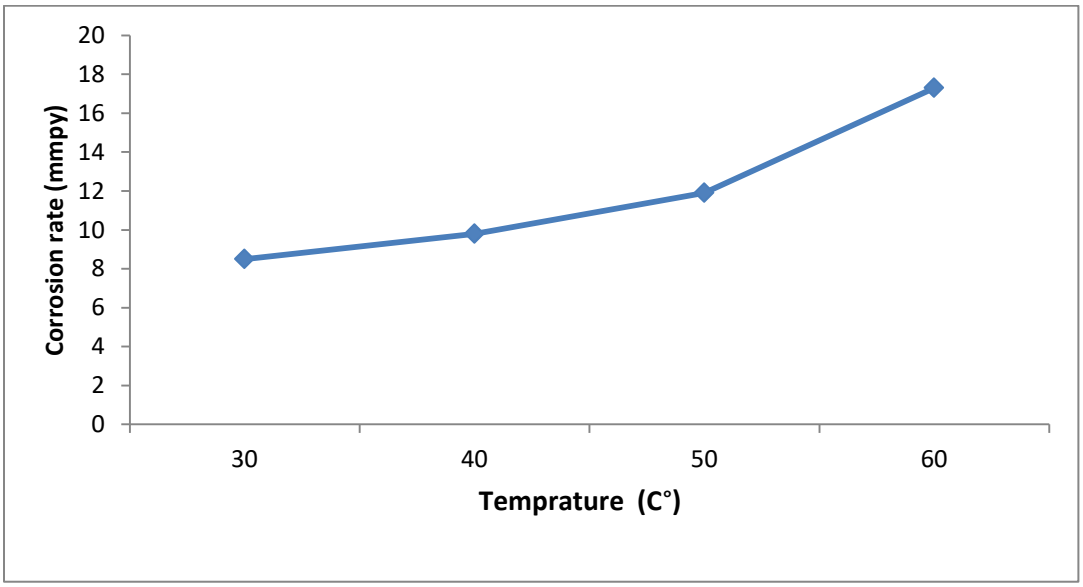


Figure (4.4): Effect of temperature on the corrosion rate of ($Fe_2O_3$) nanomaterial for aluminum alloy (AA6063- T5) immersed in ($1MH_3PO_4$ at pH of 4) for (3 h).

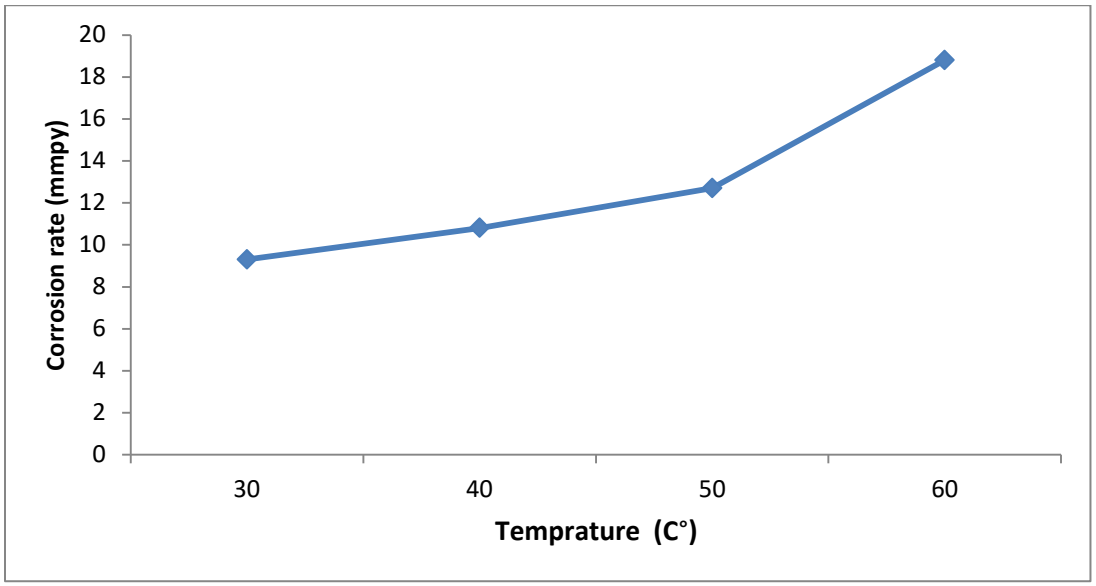


Figure (4.5): Effect of temperature on the corrosion rate of ($TiO_2$) nanomaterial for aluminum immersed in ($1MH_3PO_4$at pH of 4) for (3 h).

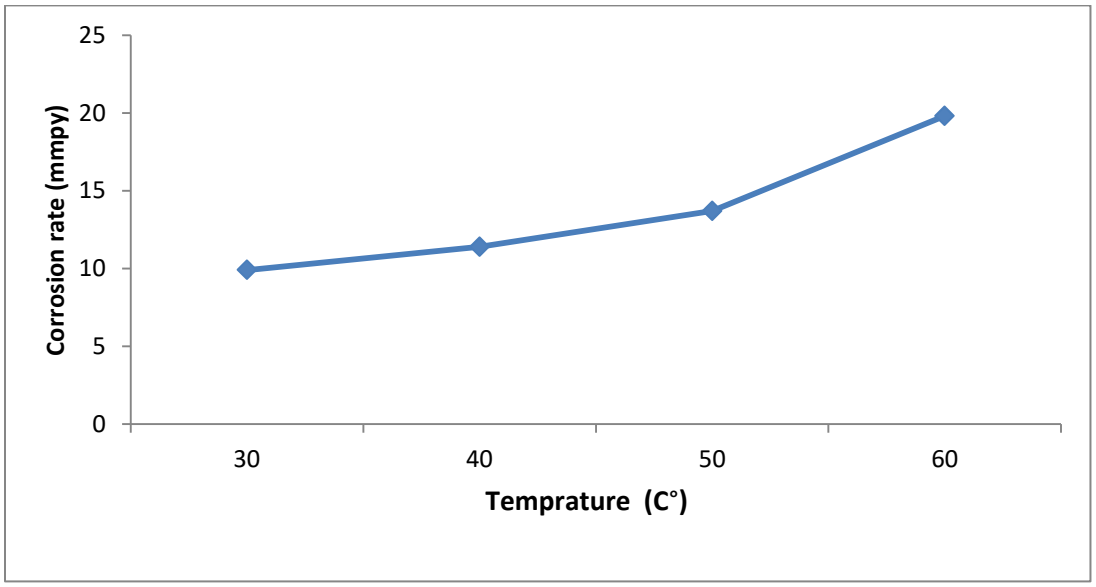


Figure (4.6): Effect of temperature on the corrosion rate of ($TiO_2$) nanomaterial for aluminum alloy (AA6063- T5) immersed in ($1MH_3PO_4$ at pH of 4) for (3 h).

## 4.2.2- Corrosion rates of acid in the presence of CML extract and nanomaterials inhibitors.

It is important that the addition of the extract of Cordia myxa leaves (CML) significantly reduces the rates of corrosion, as in tables (4.1)and (4.2) and the corrosion rate was found to increase with temperatures typically for aluminum and aluminum alloy (AA6063-T5). The higher (CML) concentration added, the lower was corrosion rate in (1 M $H_3PO_4$) Therefore, (CML) decreased the aluminum and aluminum alloy $(AA6063-T5)$ corrosion rate in $(1\ M\ H_3PO_4)$, which indicates that it can be used as a corrosion inhibitor for both as shown in figures (4.7) and (4.8) [91]. Table ( 4.3 to 4.6) shows the rates of corrosion of aluminum and aluminum alloy (AA6063-T5) where we note that the presence of ($Fe_2O_3$ and $TiO_2$) led to a decrease in the rate of corrosion and increase the efficiency of coatings. A lot of literature has proven that coatings are one of the methods widely used to protect metals from the influence of salty and acidic media [92-93] and that the rate of corrosion decreases at ($1MH_3PO_4$at PH of 4). This indicates the use of nanomaterial on the metal and alloys with the results given in figures (4.9 ) to (4.12).

The effect of temperature on corrosion rate at various CML extract inhibitor concentration is describe in figures (4.13) and (4.14). These figures show that the corrosion rate increases with increasing in temperature at all studied inhibitor concentration. At inhibitor concentration of (2 mg/L) the corrosion rate increases significantly when the temperature increased from (303,313,323and333 K).The effect of (4 mg/L) inhibitor concentration is higher than (2 mg/L). While at the inhibitor concentration of (6, 8and 10 mg/L) The temperature marginally, increases the rate of corrosion. This may be due to the partial desorption of the temperature-controlled surface of the aluminum and

aluminum alloy (AA6063-T5) and higher inhibitor concentrations. [94]. Figures (4.15) to (4.18) describe the effect of temperature on the corrosion rate at various nanomaterial concentrations. These data shows that temperature increases the rate of most chemical reactions [95] and that temperature increases have several effects on chemical reactions, because corrosion rates have been found to increase at temperature. of (303,313.323and 333K) [36]. As inhibitor efficiency increase with increasing of inhibitor concentration figures (4.19) to (4.24) show the difference inhibitor efficiency with inhibitor concentration . It was (% 64.81 and % 90.95 ) for (2 and 10 mg/L) of (CML) in (1 M $H_3PO_4$ ) for aluminum respectively, and (% 62.29 and % 87.60 ) for (2 and 10 mg/L) of (CML) in (1 M $H_3PO_4$ ) for aluminum alloy (AA6063 − T5) respectively [96]. also it was (% 31.57 and % 71.43) for (1and 2.5wt %) of ($Fe_2O_3$)in (1M$H_3PO_4$at pH of 4) for aluminum ,respectively it was (% 28.24 and % 68.78 ) for (1 and 2.5 wt% of ($Fe_2O_3$) in (1M$H_3PO_4$at PH of 4) for aluminum alloy (AA6063 − T5) respectively while, it was (% 27.95 and % 67.02) for (1 and 2.5 wt%) of ($TiO_2$) in (1M$H_3PO_4$ at PH of 4) for aluminum respectively, and was (% 22.22 and % 60.01 ) for (1 to 2.5wt %) of ($TiO_2$) in (1M$H_3PO_4$ at PH of 4) for aluminum alloy (AA6063 − T5), respectively. Figures (4.25) − (4.30), show the effect of temperature on inhibitor efficiency.

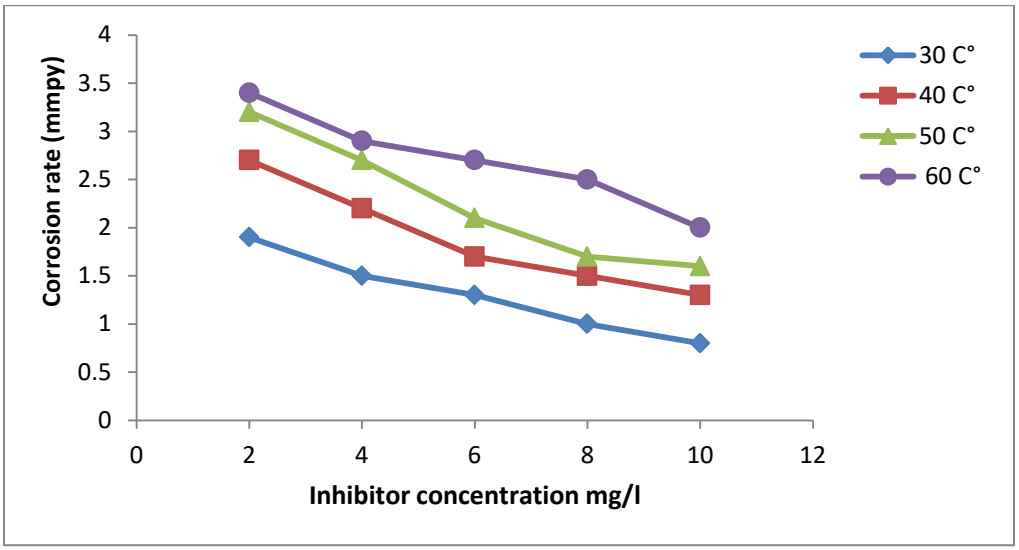


Figure (4.7): Effect of inhibitor concentration (CML extract) on the corrosion rate of aluminum immersed in (1 M $H_3PO_4$) for (3 h).

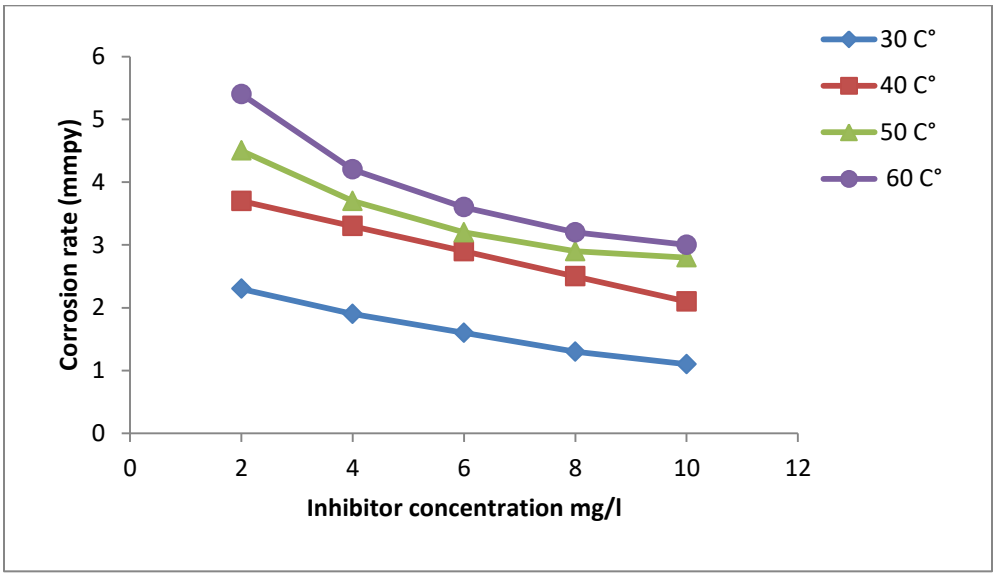


Figure (4.8): Effect of inhibitor concentration (CML extract) on the corrosion rate of aluminum alloy (AA6063 – T5) immersed in (1 M $H_3PO_4$) for (3 h).

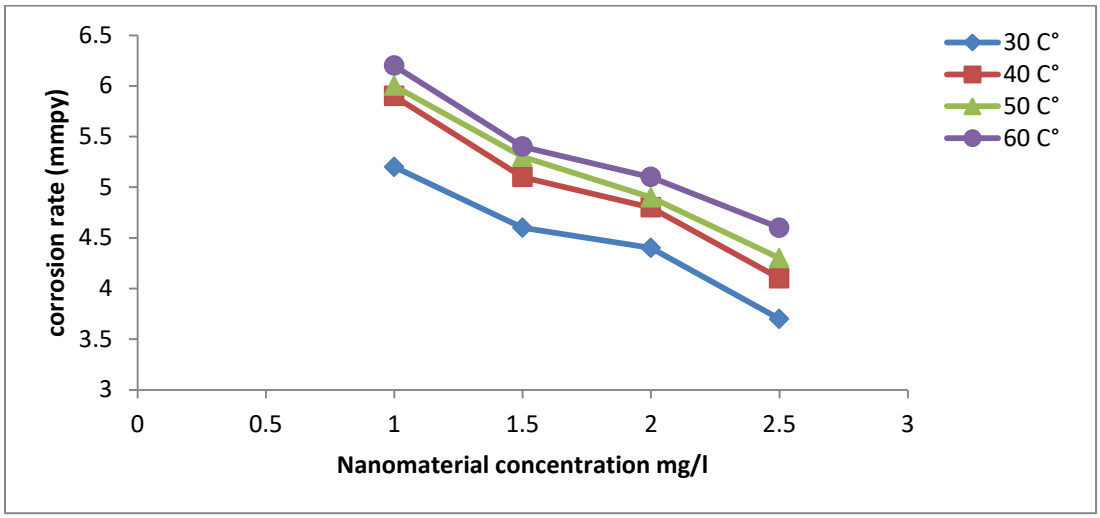


Figure (4.9): Effect of inhibitor concentration on ($Fe_2O_3$) nanomaterial on the corrosion rate of aluminum immersed in (1M$H_3PO_4$ at pH of 4) for (3 h).

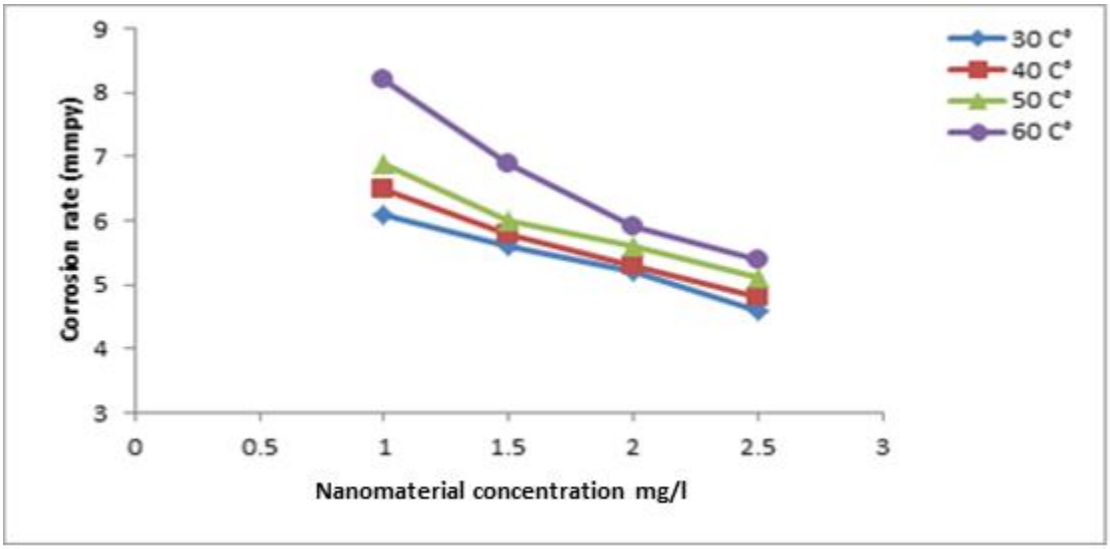


Figure (4.10):Effect of inhibitor concentrate on ($Fe_2O_3$) nanomaterial on the corrosion rate of aluminum alloy (AA6063- T5) immersed in in (1M$H_3PO_4$ at pH of 4)for (3h).

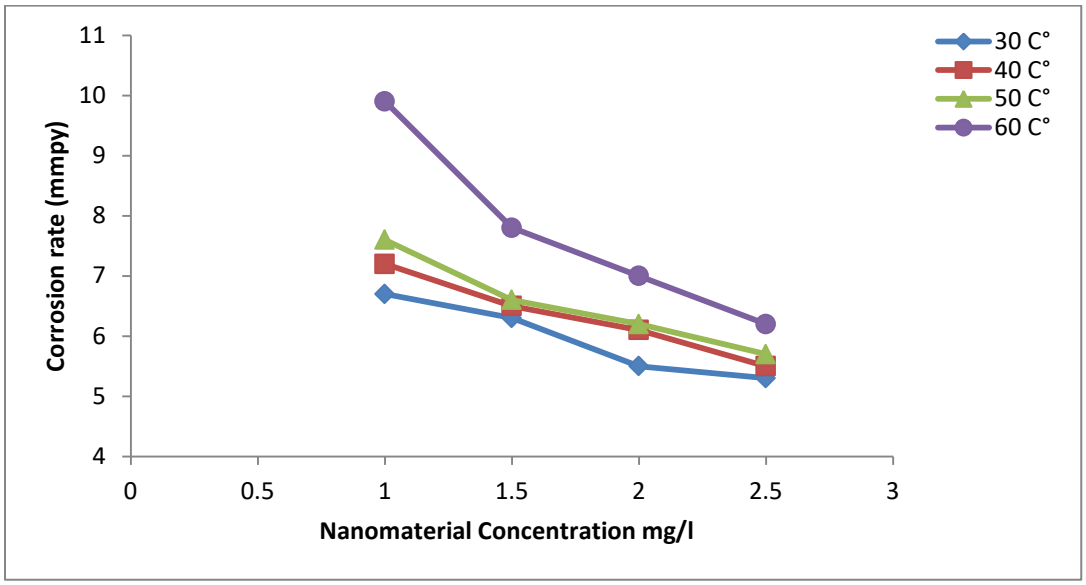


Figure (4.11): Effect of inhibitor concentration ($TiO_2$) nanomaterial on the corrosion rate of aluminum immersed in ($1MH_3PO_4$ at pH of 4) for (3h).

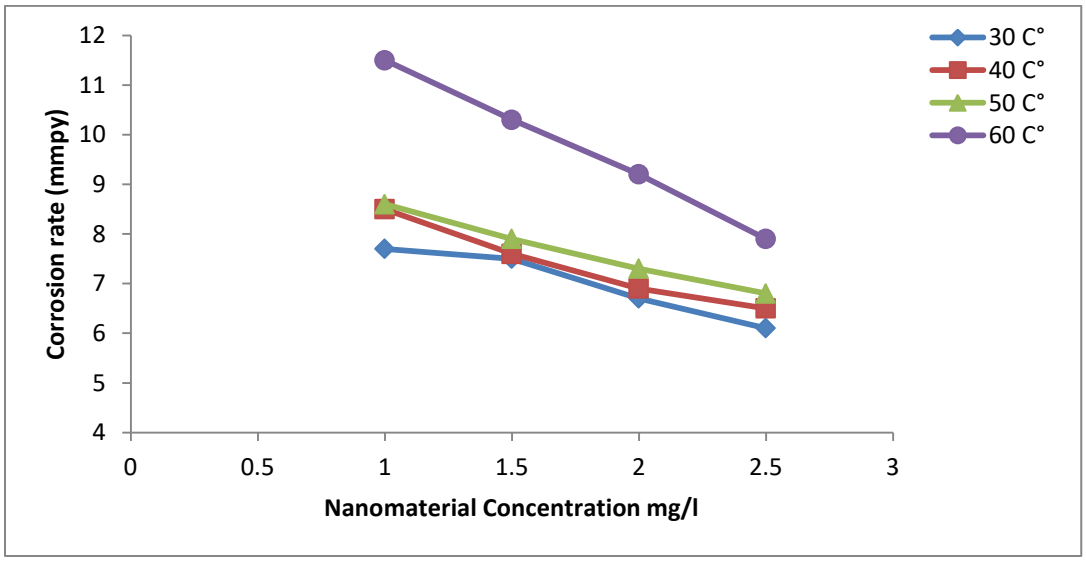


Figure (4.12): Effect of inhibitor concentration ($TiO_2$) nanomaterial on the corrosion rate of aluminum alloy(AA6063-T5) immersed in ($1MH_3PO_4$ at pH of 4) for (3h).

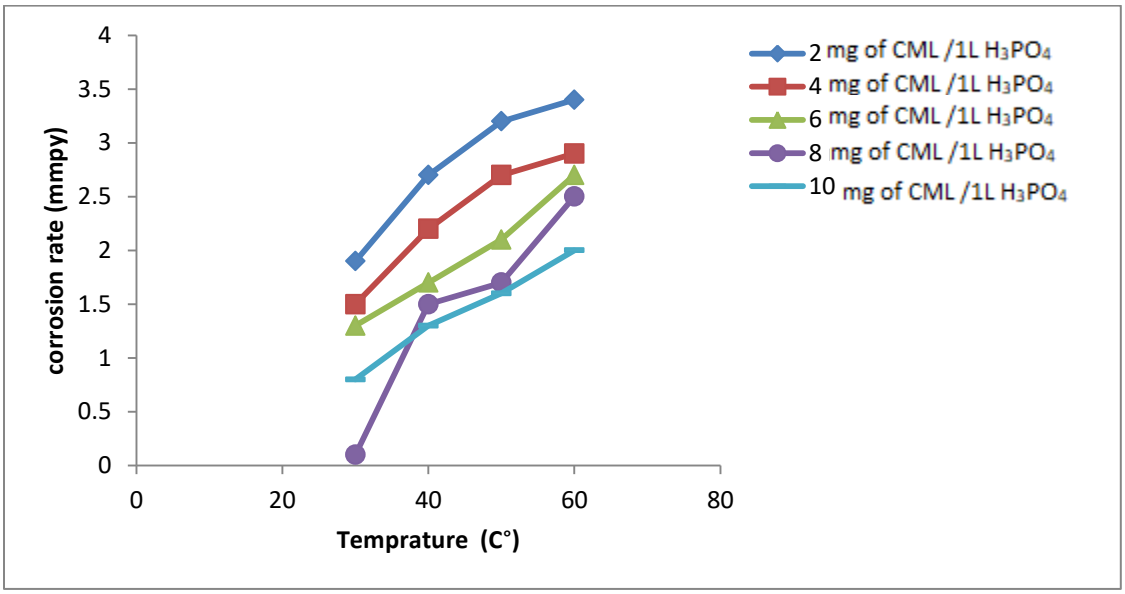


Figure (4.13): Effect of temperature on the corrosion rate of aluminum in $(1\ M\ H_3PO_4)$ at different inhibitor concentration (CML extract).

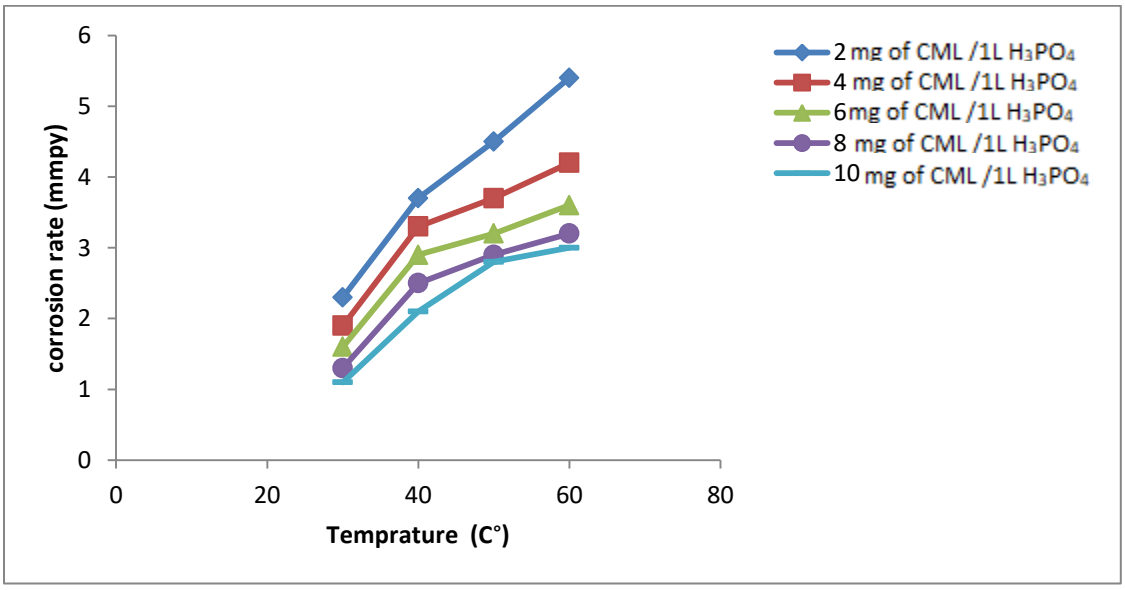


Figure (4.14): Effect of temperature on the corrosion rate of aluminum alloy $(AA6063-T5)$ in $(1\ M\ H_3PO_4)$ at different inhibitor concentration (CML extract).

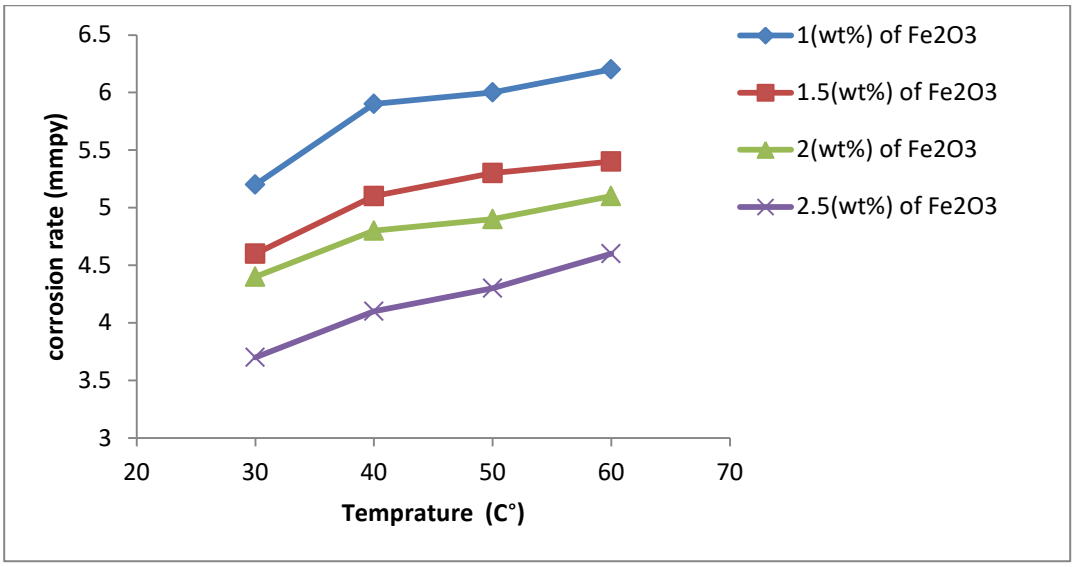


Figure (4.15): Effect of temperature on the corrosion rate of aluminum in ($1MH_3PO_4$ at pH of 4) at different nanomaterial concentration ($Fe_2O_3$).

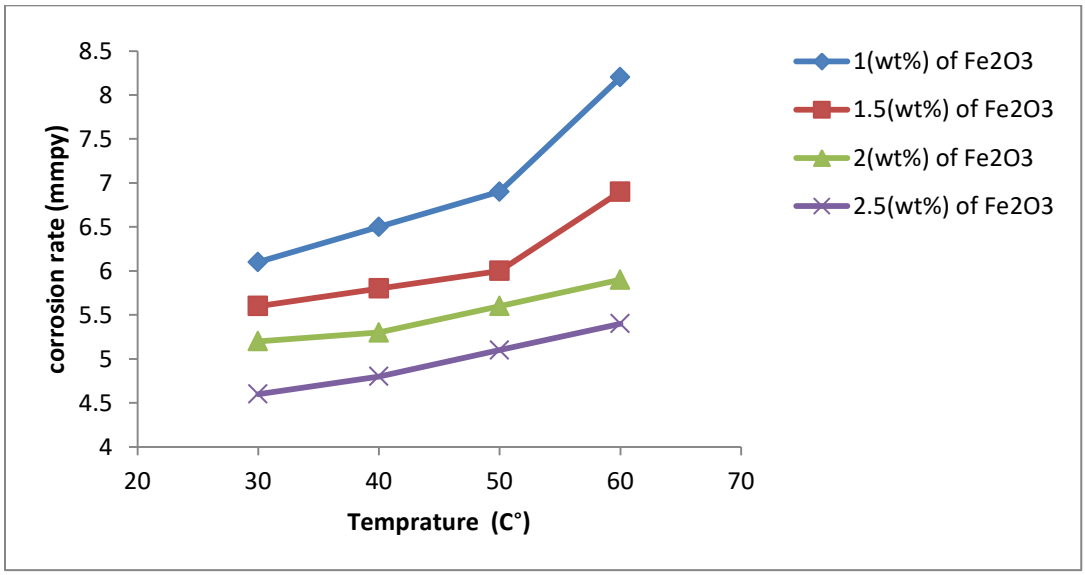


Figure (4.16): Effect of temperature on the corrosion rate of aluminum alloy in ($1MH_3PO_4$ at pH of 4) at different nanomaterial concentration ($Fe_2O_3$).

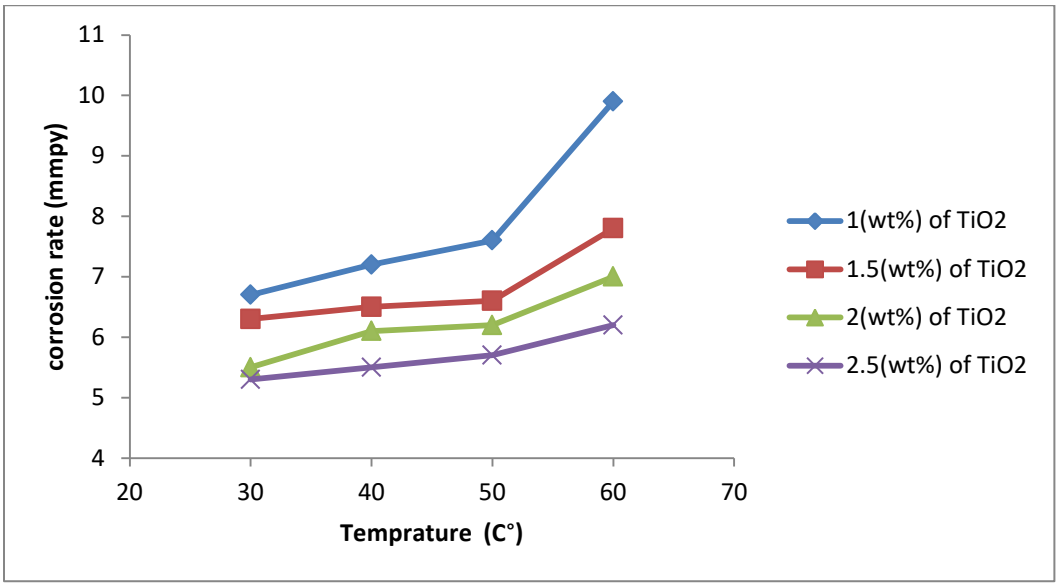


Figure (4.17): Effect of temperature on the corrosion rate of aluminum in ($1MH_3PO_4$at pH of 4) at different nanomaterial concentration ($TiO_2$).

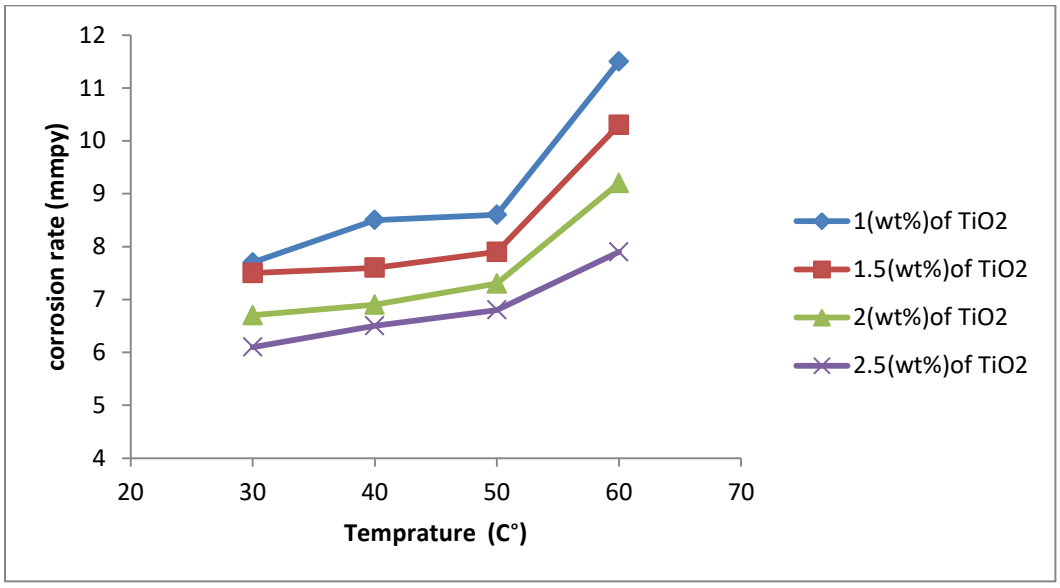


Figure (4.18): Effect of temperature on the corrosion rate of aluminum alloy (AA6063-T5) in(1M $H_3PO_4$ at pH of 4) at different nanomaterial concentration ($TiO_2$).

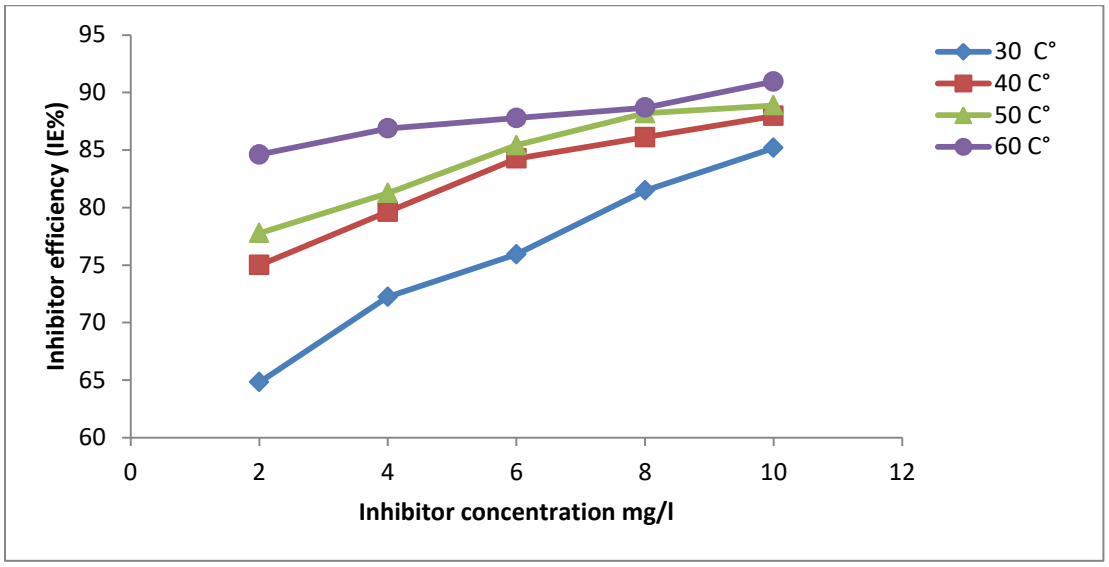


Figure (4.19): Effect of concentration of Cordia myxa plant leaves (CML) extract on inhibitive efficiency of aluminum corrosion in (1 M $H_3PO_4$).

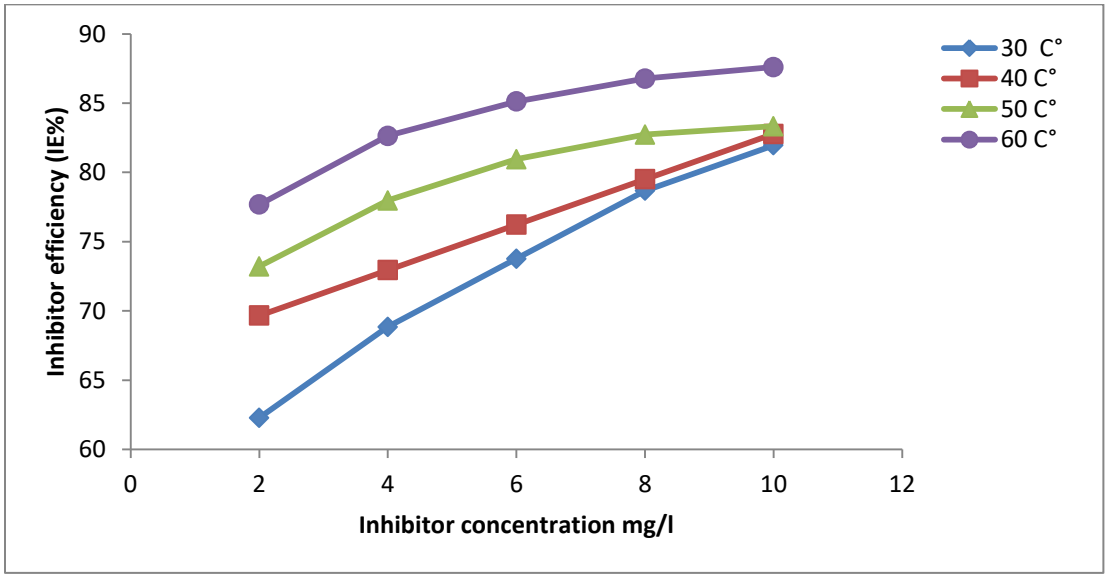


Figure (4.20): Effect of concentration of Cordia myxa plant leaves (CML) extract on inhibition efficiency of aluminum alloy (AA6063-T5) corrosion in (1 M $H_3PO_4$).

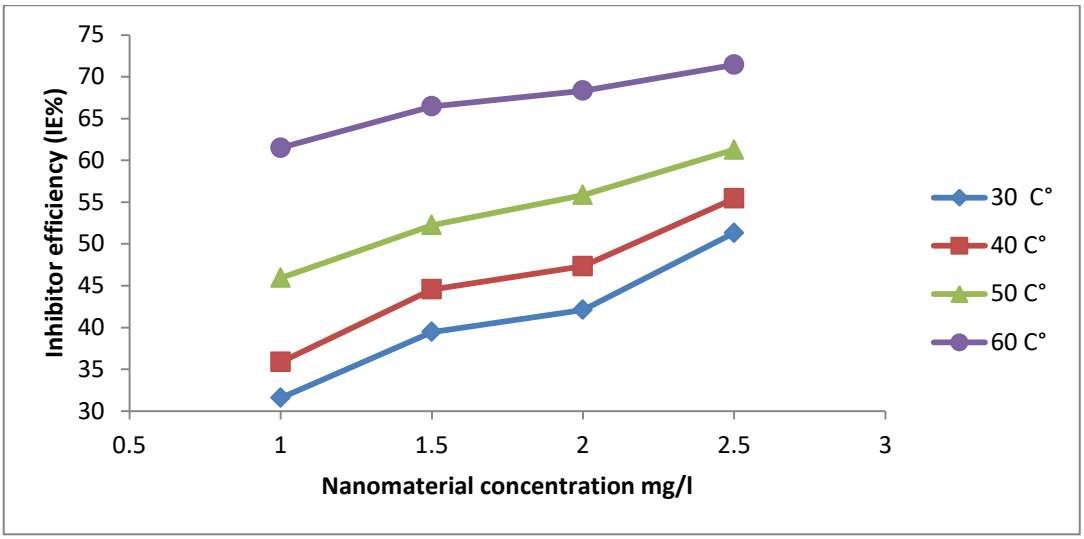


Figure (4.21): Effect of concentration of ($Fe_2O_3$) nanomaterial on inhibition efficiency of aluminum corrosion in (1M$H_3PO_4$ at pH of 4).

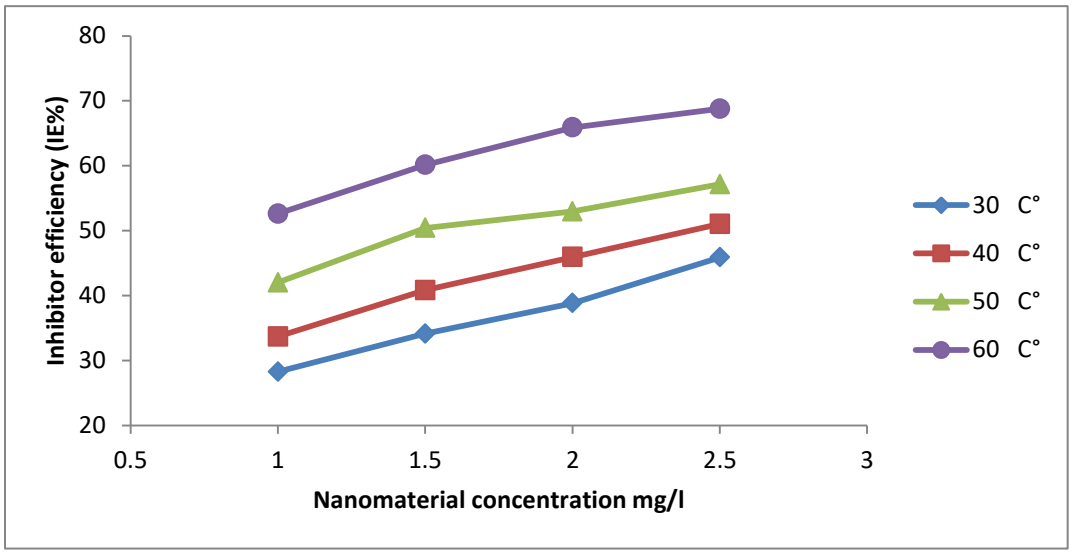


Figure (4.22): Effect of concentration of ($Fe_2O_3$) nanomaterial on inhibition efficiency of aluminum alloy (AA6063- T5) corrosion in (1M$H_3PO_4$ at pH of 4).

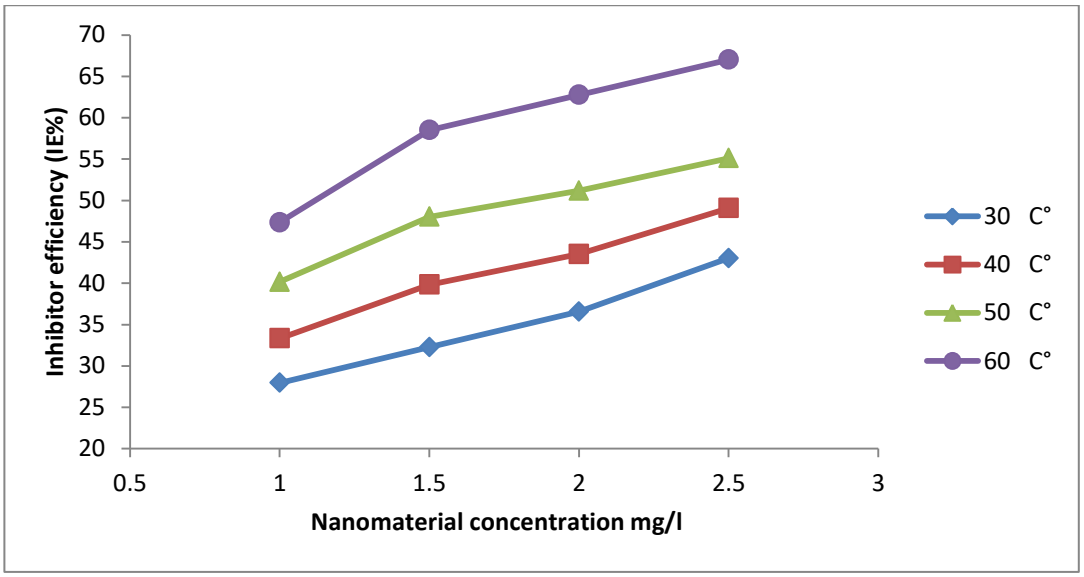


Figure (4.23): Effect of concentration of ($TiO_2$) nanomaterial on inhibition efficiency of aluminum corrosion in ($1MH_3PO_4$ at pH of 4).

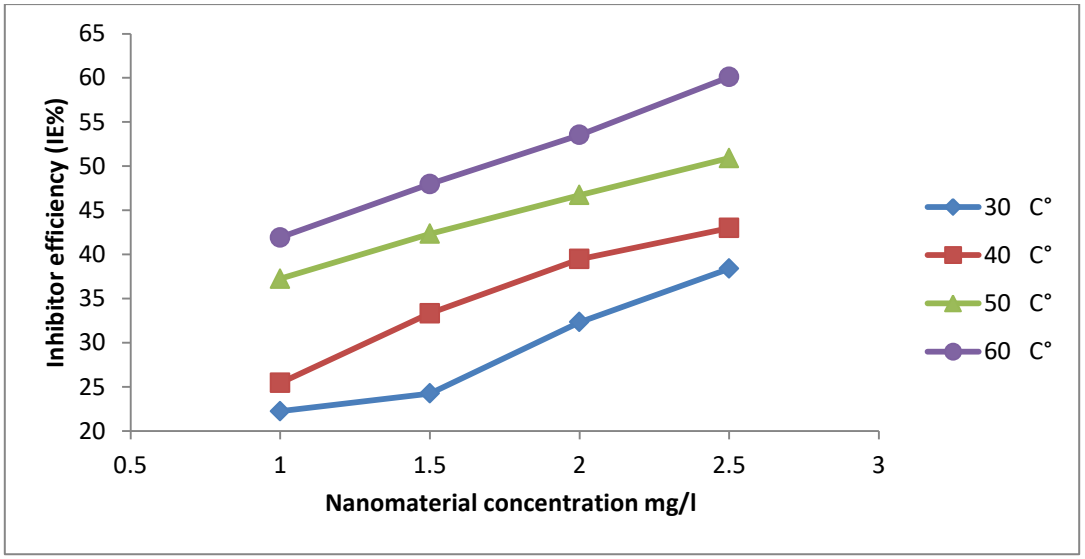


Figure (4.24): Effect of concentration of ($TiO_2$) nanomaterial on inhibition efficiency of aluminum alloy (AA6063-T5) corrosion in ($1MH_3PO_4$ at pH of 4).

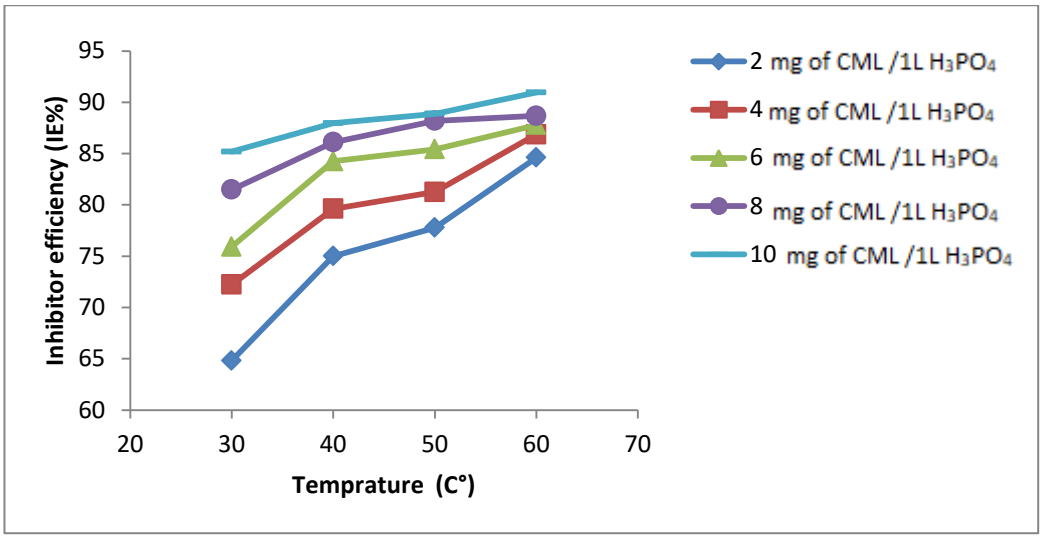


Figure (4.25): Effect of temperature on inhibitive efficiency of Cordia myxa plant leaves (CML) extract for aluminum corrosion in ( 1 M $H_3PO_4$).

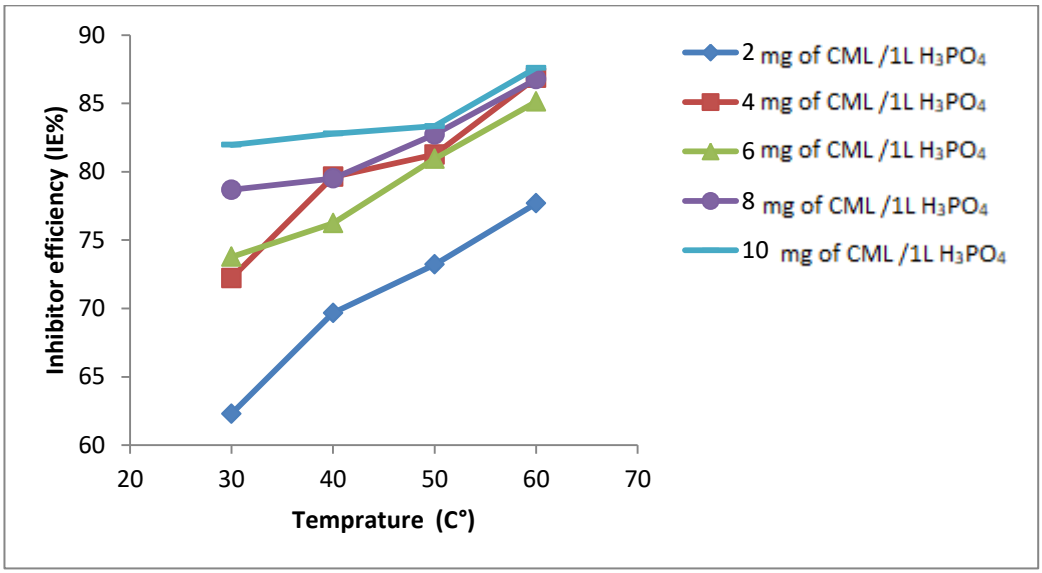


Figure (4.26): Effect of temperature on inhibition efficiency of Cordia myxa plant leaves (CML) extract for aluminum alloy (AA6063-T5) corrosion in (1 M $H_3PO_4$).

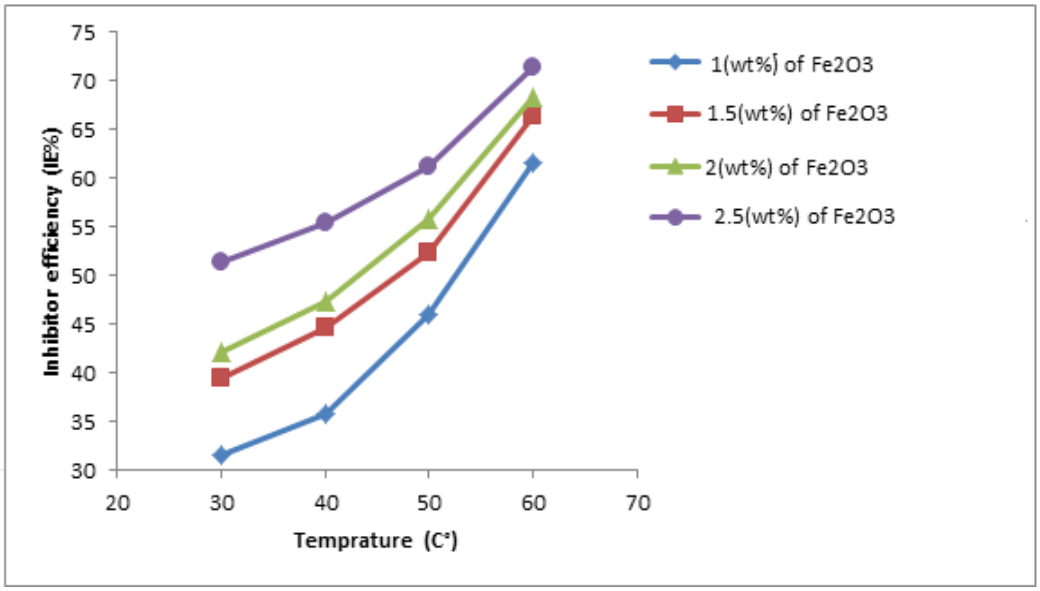


Figure (4.27): Effect of temperature on inhibition efficiency of ($Fe_2O_3$) nanomaterial for aluminum corrosion in (1M $H_3PO_4$ at pH of 4).

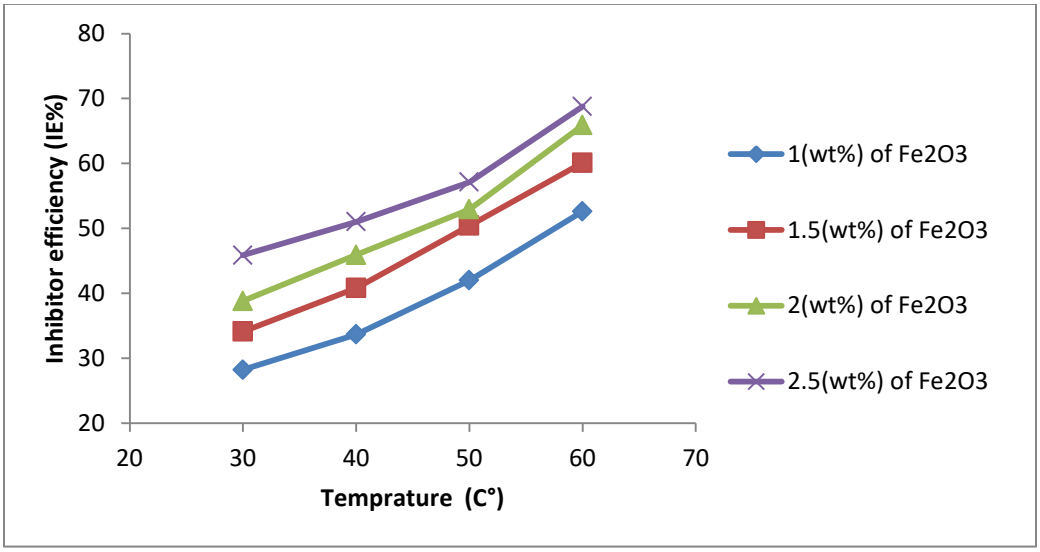


Figure (4.28): Effect of temperature on inhibition efficiency of ($Fe_2O_3$) nanomaterial for aluminum alloy(AA6063-T5) corrosion in (1M$H_3PO_4$ at pH of 4).

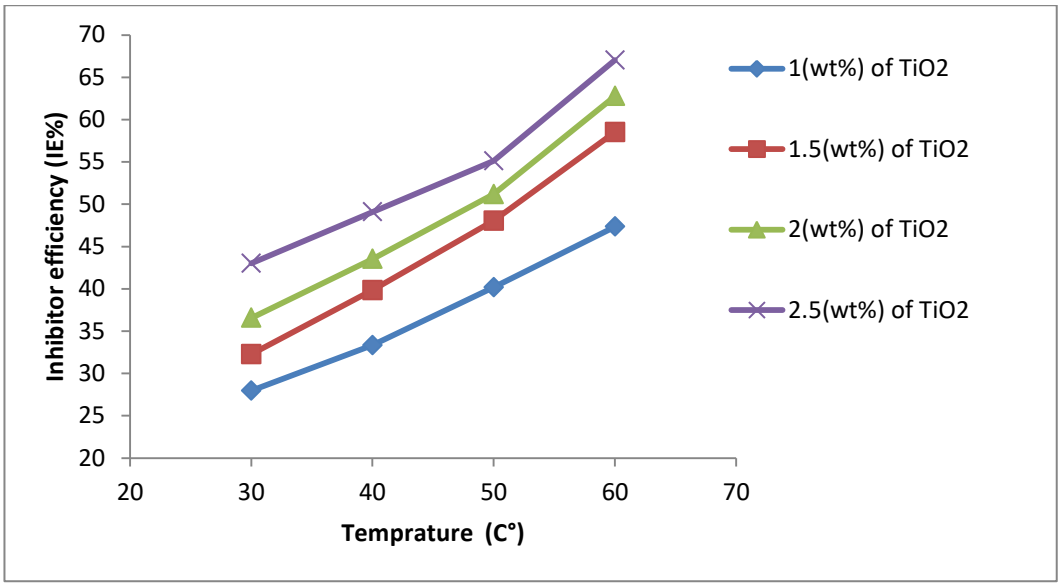


Figure (4.29): Effect of temperature on inhibition efficiency of ($TiO_2$) nanomaterial for aluminum corrosion in ($1MH_3PO_4$ at pH of 4).

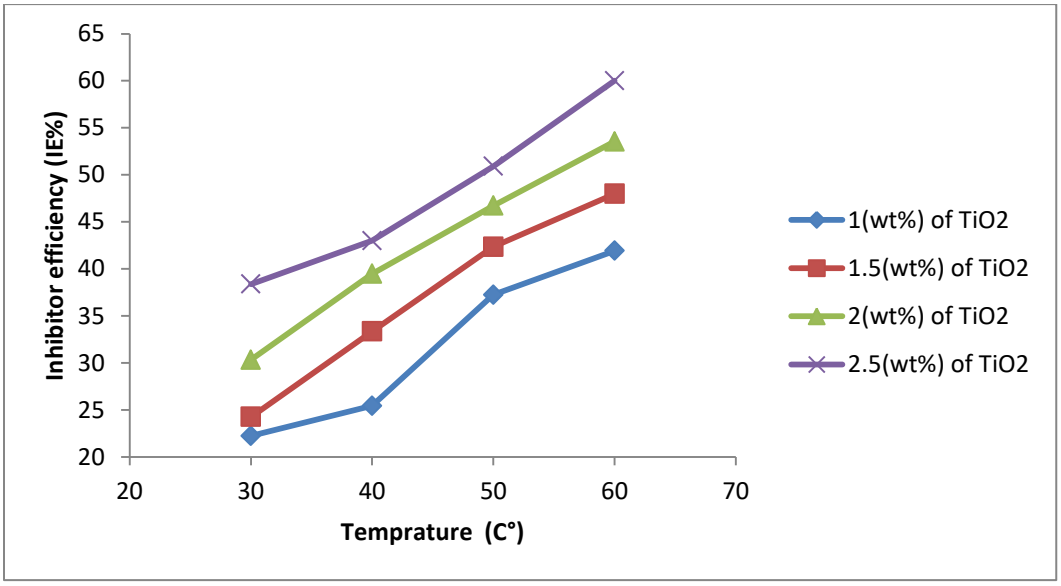


Figure (4.30): Effect of temperature on inhibition efficiency of ($TiO_2$) nanomaterial for aluminum alloy (AA6063- T5) corrosion in($1MH_3PO_4$ at pH of 4).

## 4.3. Performance and adsorption studies of inhibitors

It has been displayed that increasing the CML and nanomaterials inhibitors concentration from (2 to10mg/L)and(1 to 2.5wt%) reduces the rate of corrosion to very low levels. Figures (4.7) to (4.12), . It is clear from these figures that the corrosion rate approaches its minimum value when the inhibitor concentration is (10 mg/L) the nanomaterial is concentration (2.5wt %) . This might be due to that (10mg/L) inhibitor and nanomaterial concentration (2.5wt% ), is enough to cover the metal surface at the temperature range of (303,313,323and 333K) for (8 mg/L) inhibitor concentration and nanomaterial concentration (2wt%) the effect of inhibitor concentration and nanomaterial concentration will be less than in (10 mg/L),(2.5 wt%).The increase in temperature from (303 to 313,323and333 K) the corrosion rate values changed markedly. At inhibitor concentration and nanomaterial concentration of (6 and 2 mg/L), (1.5 to1wt%) shown in figures (4.7) to (4.12) and tables (4.1 – 4.6) the reduction in corrosion rate is small and decreases at higher Temperature The data on surface coverage (Ɵ) is very helpful when explaining the characteristics of adsorption. The inhibitor 's surface coverage at a given concentration was determined using the equation (2.17). In order to analyze the adsorption mechanism .the corrosion rate data can be used [18] .

### 4.3.1- Langmuir adsorption isotherm

It is determined by using equation (2.19). Figures (4.31) to (4.36) show plots of $(C_i/\theta)$ versus ,$(C_i)$ Langmuir adsorption isotherm for (CML), extract inhibitors in ($1MH_3PO_4$ , and ($Fe_2O_3$,$TiO_2$) nanomaterials in ($1MH_3PO_4$ at pH of 4) at(303,313,323and333 K). dependent on the equation (2.19). The results suit straight lines showing that inhibitors are adsorbed according to the adsorption of Langmuir isotherm, the increase in inhibition efficiency can also be explained by increasing the extract concentration as an indicator of the increase in the amount of solvent molecules adsorbing on the aluminum and aluminum alloy surface (AA6063-T5) and blocking active sites from direct acid attacks and then protection of metals from corrosion [97].

The values ($K_L$) can be measured from the intercept of the straight line, which can then be replaced in Equation(2.20) to calculate $\Delta G^{\circ}_{ads}$. Tables (4.7-4.12) show values of $K_L$ and $\Delta G^{\circ}_{ads}$. The equilibrium constant of the inhibitor adsorption $K_L$ values increase with increasing temperature from (303to 333 K). The higher $K_L$values clearly proved the strong adsorption of (CML)extract and (nanomaterials) molecules on aluminum and aluminum alloy (AA6063 – T5) surfaces [98].

It seem that the kind of adsorption is physical because $\Delta G°_{ads}$ value is about 20 kJmol-1 . For free energy of adsorption ($\Delta G_{\circ ads}$) for studied inhibitor and nanomaterial was between (-9.783) and (-14.898) kJ/mol$^{-1}$ in table (4.7), (-9.656) and (- 13.669) kJ mol$^{-1}$ in table (4.8), (-8.345) and (-13.863) kJ mol$^{-1}$ in table (4.9),(-7.948) and (-11.895) kJ mol$^{-1}$ in table (4.10), (-8.101) and (-11.188) kJ mol$^{-1}$ in table (4.11),(-6.794) and (-10.756) ) kJ mol$^{-1}$ in table (4.12). The negative values of $\Delta G°_{ads}$ means that the adsorption of the extract of Cordia myxa leaves on the surface of aluminum and aluminum alloy (AA6063-T5) and ($Fe_2O_3$ and $TiO_2$)

nanomaterials was spontaneous process. the negative values of $\Delta G°_{ads}$ indicated weekly interaction of the inhibitor molecules with the aluminum and aluminum alloy (AA6063-T5) also shows [99].

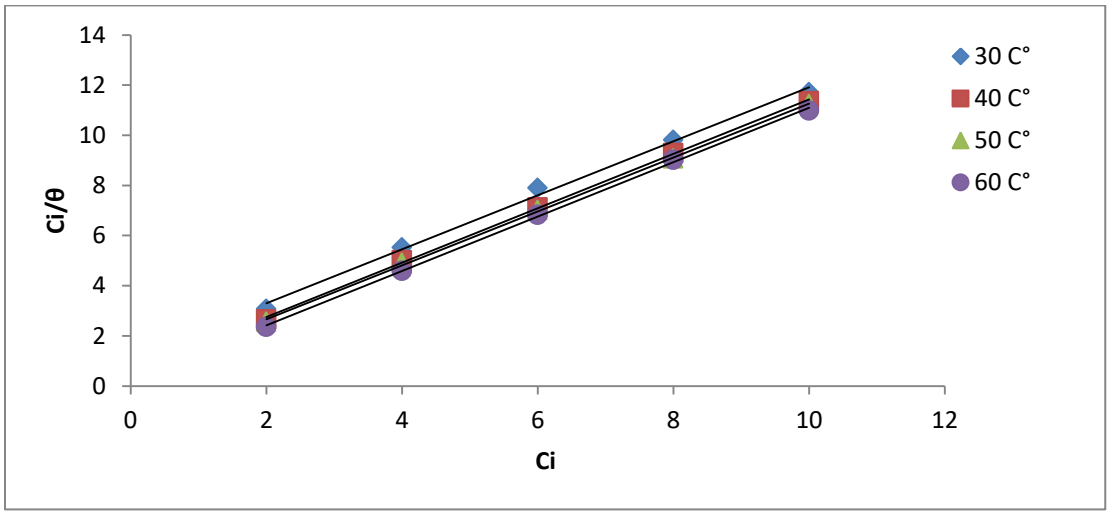


Figure (4.31): Langmuir adsorption isotherm of Cordia myxa plant leaves (CML) extract for aluminum corrosion in (1 M $H_3PO_4$).

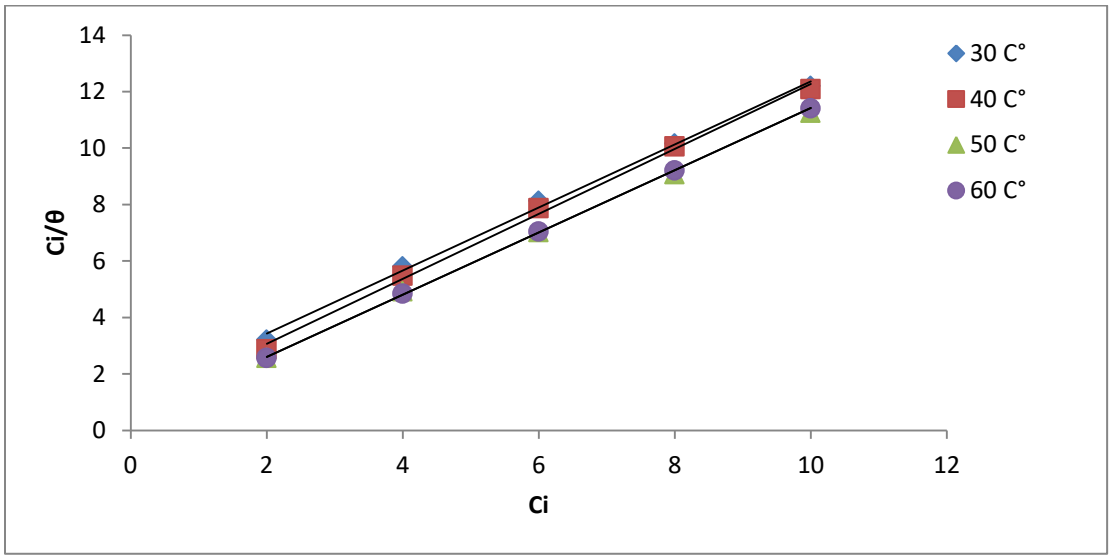


Figure (4.32): Langmuir adsorption isotherm of Cordia myxa plant leaves (CML) extract for aluminum alloy (AA6063-T5) corrosion in (1 M $H_3PO_4$).

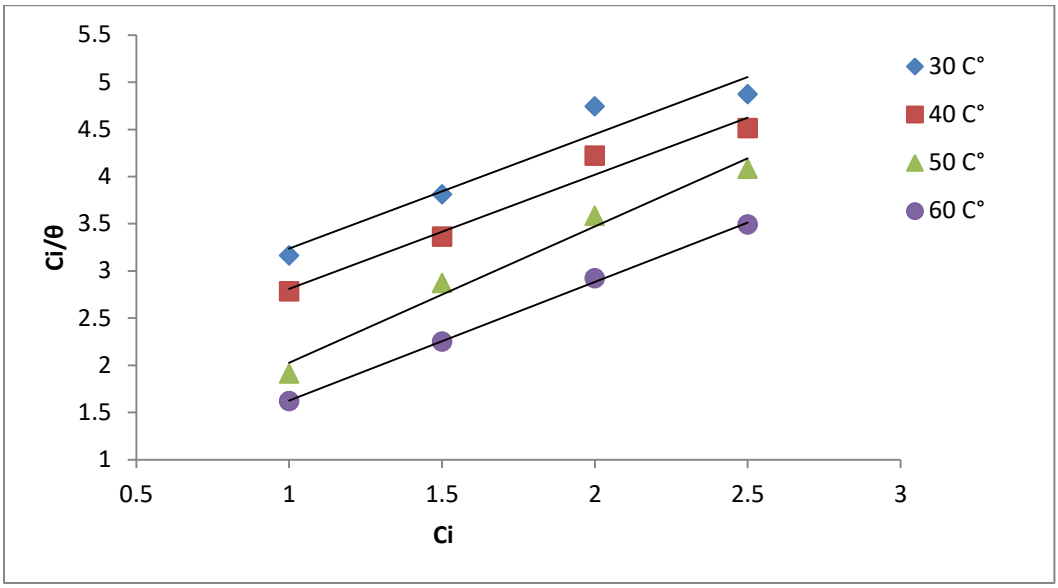


Figure (4.33): Langmuir adsorption isotherm of ($Fe_2O_3$) nanomaterial for aluminum corrosion in ($1MH_3PO_4$ at pH of 4).

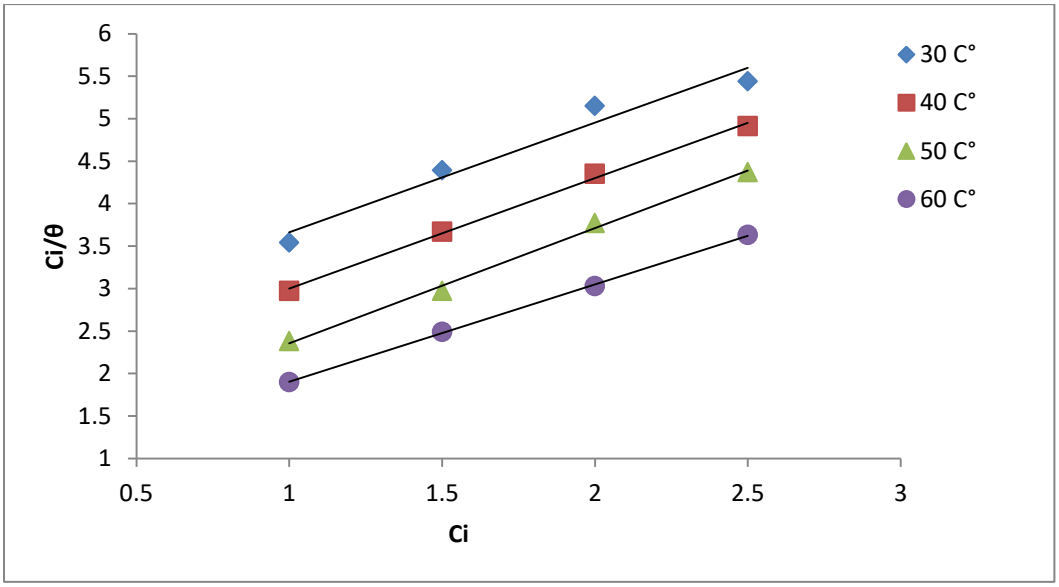


Figure (4.34): Langmuir adsorption isotherm of ($Fe_2O_3$) nanomaterial for aluminum alloy (AA6063-T5) corrosion in ($1MH_3PO_4$ at pH of 4).

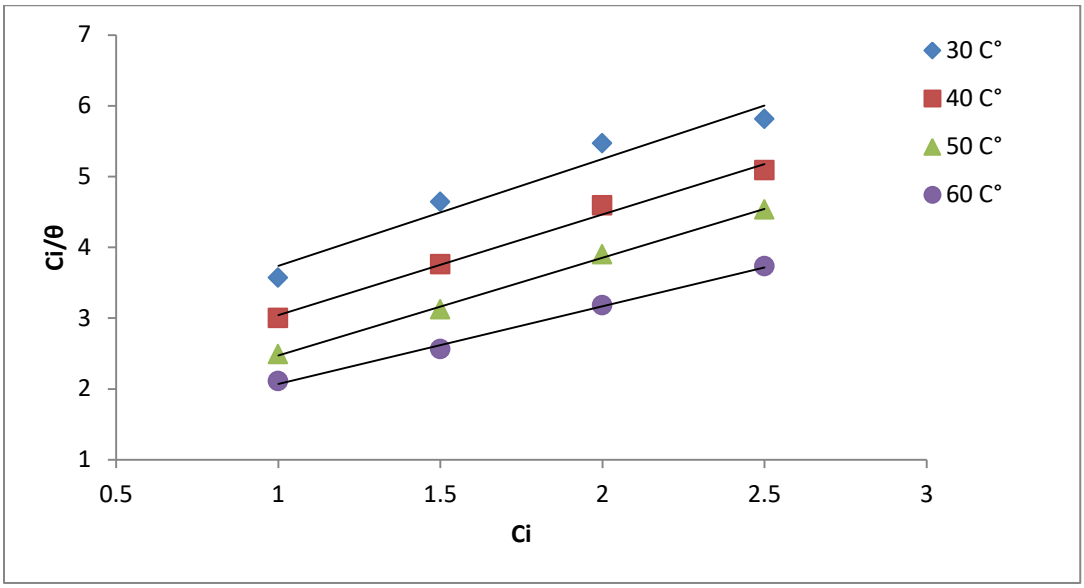


Figure (4.35): Langmuir adsorption isotherm of ($TiO_2$) nanomaterial for aluminum corrosion in ($1MH_3PO_4$ at pH of 4).

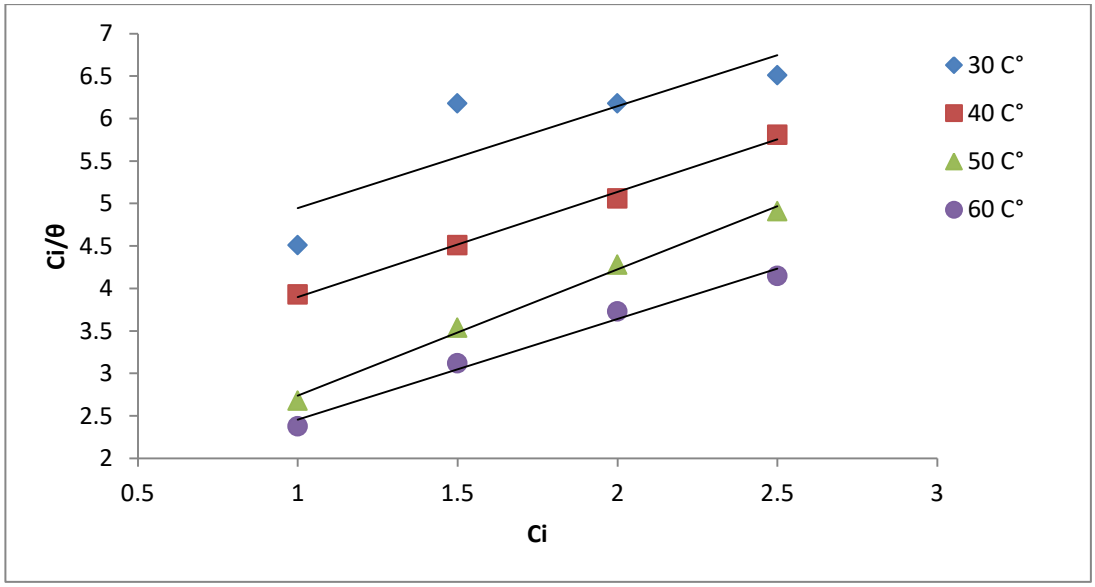


Figure (4.36): Langmuir adsorption isotherm of ($TiO_2$) nanomaterial for aluminum alloy (AA6063-T5) corrosion in ($1MH_3PO_4$ at pH of 4).

Table (4.7): Equilibrium constant ($K_{ads}$), standard adsorption free energy ($\Delta G^{\circ}_{ads}$), and correlation coefficient ($R^2$) for Langmuir type adsorption isotherm of the inhibitor CML extract for aluminum corrosion in($1\ M\ H_3PO_4$) at different temperatures.

| Temperature (K) | $K_L$(mg/g) | $\Delta G^{\circ}_{ads}$ (kJ $mol^{-1}$) | $R^2$ |
|---|---|---|---|
| 303 | 0.8741 | -9.783 | 0.9961 |
| 313 | 1.6977 | -11.834 | 0.9995 |
| 323 | 1.9493 | -12.583 | 0.9993 |
| 333 | 3.9062 | -14.898 | 0.9994 |

Table (4.8): Equilibrium constant ($K_{ads}$), standard adsorption free energy ($\Delta G^{\circ}_{ads}$), and correlation coefficient ($R^2$) for Langmuir type adsorption isotherm of the inhibitor CML extract for aluminum alloy ($AA6063-T5$) corrosion in ($1\ M\ H_3PO_4$) at different temperatures.

| Temperature (K) | $K_L$(mg/g) | $\Delta G^{\circ}_{ads}$ (kJ $mol^{-1}$) | $R^2$ |
|---|---|---|---|
| 303 | 0.8312 | -9.656 | 0.9971 |
| 313 | 1.2953 | -11.130 | 0.9974 |
| 323 | 1.9493 | -12.583 | 0.9995 |
| 333 | 2.5062 | -13.669 | 0.9999 |

Table (4.9): Equilibrium constant ($K_{ads}$), standard adsorption free energy ($\Delta G^{\circ}_{ads}$), and correlation coefficient ($R^2$) for Langmuir type adsorption isotherm of ($Fe_2O_3$) nanomaterial for aluminum corrosion in ($1M H_3PO_4$ at pH of 4)at different temperature. .

| Temperature (K) | $K_L$(mg/g) | $\Delta G^{\circ}_{ads}$ (kJ $mol^{-1}$) | $R^2$ |
|---|---|---|---|
| 303 | 0.4940 | -8.345 | 0.9637 |
| 313 | 0.625 | -9.233 | 0.9797 |
| 323 | 1.7152 | -12.240 | 0.9927 |
| 333 | 2.6881 | -13.863 | 0.9991 |

Table (4.10): Equilibrium constant ($K_{ads}$), standard adsorption free energy ($\Delta G^{\circ}_{ads}$), and correlation coefficient ($R^2$) for Langmuir type adsorption isotherm of ($Fe_2O_3$) nanomaterial for aluminum alloy (AA6063-T5) corrosion in ($1M H_3PO_4$ at pH of 4) at different temperatures.

| Temperature (K) | $K_L$(mg/g) | $\Delta G^{\circ}_{ads}$ (kJ $mol^{-1}$) | $R^2$ |
|---|---|---|---|
| 303 | 0.4221 | -7.948 | 0.9894 |
| 313 | 0.5882 | -9.075 | 0.9975 |
| 323 | 0.9970 | -10.782 | 0.9963 |
| 333 | 1.3210 | -11.895 | 0.9996 |

Table (4.11): Equilibrium constant ($K_{ads}$), standard adsorption free energy ($\Delta G^{\circ}_{ads}$), and correlation coefficient ($R^2$) for Langmuir type adsorption isotherm of ($TiO_2$) nanomaterial for aluminum corrosion in($1MH_3PO_4$ at pH of 4) at different temperatures.

| Temperature (K) | $K_L$(mg/g) | $\Delta G^{\circ}_{ads}$ (kJ $mol^{-1}$) | $R^2$ |
|---|---|---|---|
| 303 | 0.4484 | -8.101 | 0.9645 |
| 313 | 0.6154 | -9.192 | 0.9932 |
| 323 | 0.9132 | -10.546 | 0.9981 |
| 333 | 1.0235 | -11.188 | 0.9964 |

Table (4.12): Equilibrium constant ($K_{ads}$), standard adsorption free energy ($\Delta G^{\circ}_{ads}$), and correlation coefficient ($R^2$) for Langmuir type adsorption isotherm of ($TiO_2$) nanomaterial for aluminum alloy (AA6063-T5)corrosion in ($1MH_3PO_4$ at pH of 4) at different temperatures.

| Temperature (K) | $K_L$(mg/g) | $\Delta G^{\circ}_{ads}$ (kJ $mol^{-1}$) | $R^2$ |
|---|---|---|---|
| 303 | 0.2670 | -6.794 | 0.9350 |
| 313 | 0.3758 | -7.908 | 0.9949 |
| 323 | 0.7987 | -10.186 | 0.9952 |
| 333 | 0.8755 | -10.756 | 0.9855 |

### 4.3.2- Freundlich adsorption isotherm

This isotherm is produced on an equation basis (2.23) figures (4.37) to (4.42) show produced by plotting ($\ln\theta$) against ($\ln C_i$) with slope and intercept yield the values of (n") and ($K_F$) respectively , with the data given in tables (4.13-4.18). Freundlich does not seem to apply well to this method because the values of the correlation coefficient are low, but Langmuir isotherm applies and provides the adsorption isotherm method with more fitness because the values of the correlation coefficient are high [100].

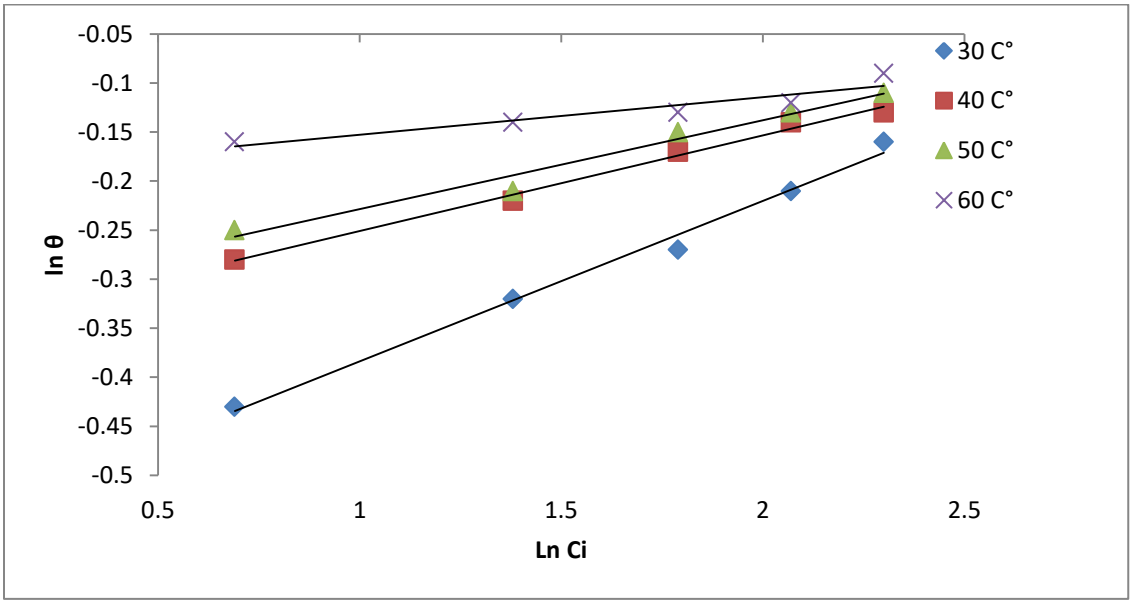


Figure (4.37): Freundlich adsorption isotherm of Cordia myxa plant leaves (CML) extract as corrosion inhibitor for aluminum corrosion in (1 M $H_3PO_4$).

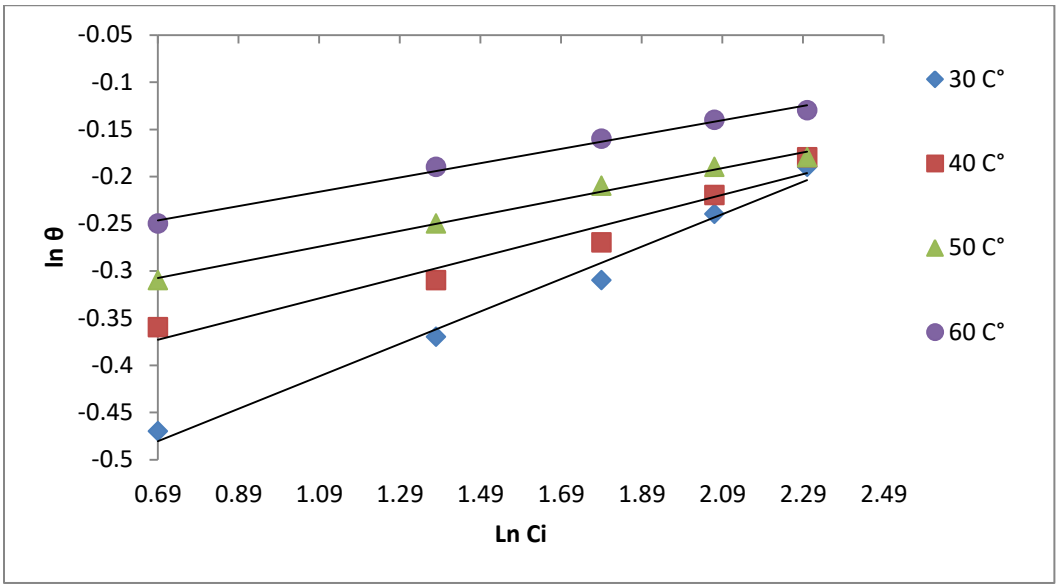


Figure (4.38): Freundlich adsorption isotherm of Cordia myxa plant leaves (CML) extract as corrosion inhibitor for aluminum alloy (AA6063-T5) corrosion in (1 M $H_3PO_4$).

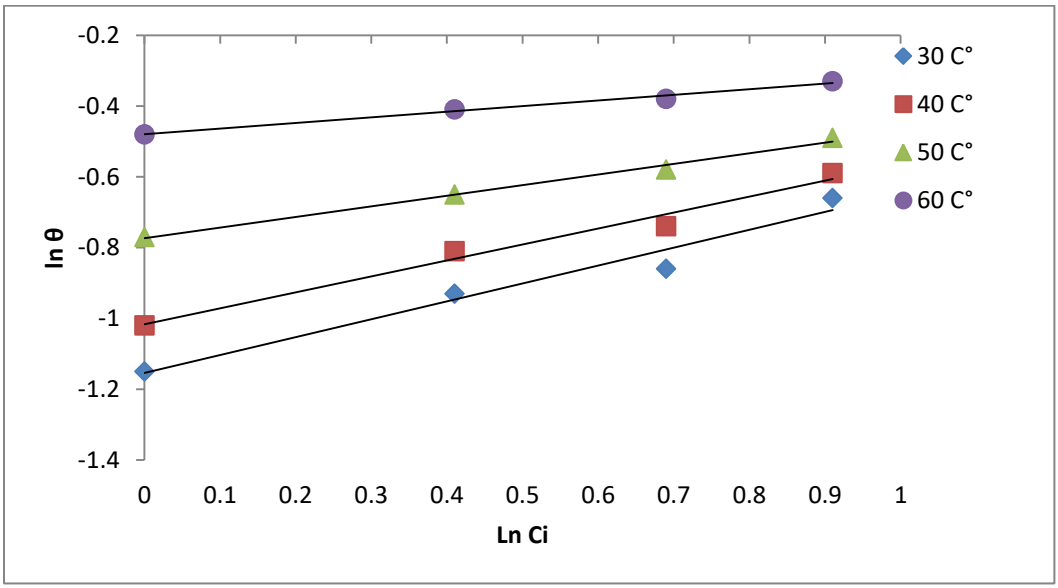


Figure (4.39): Freundlich adsorption isotherm of ($Fe_2O_3$) nanomaterial as corrosion inhibitor for aluminum corrosion in (1M$H_3PO_4$ at pH of 4).

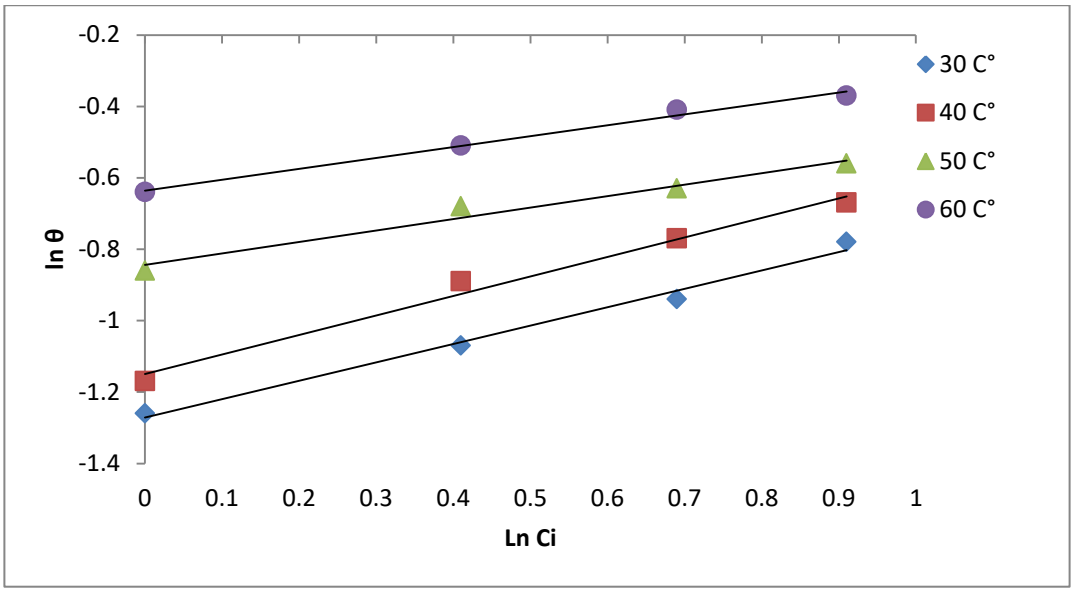


Figure (4.40): Freundlich adsorption isotherm of ($Fe_2O_3$) nanomaterial as corrosion inhibitor for aluminum alloy (AA6063-T5) corrosion in ($1MH_3PO_4$ at pH of 4).

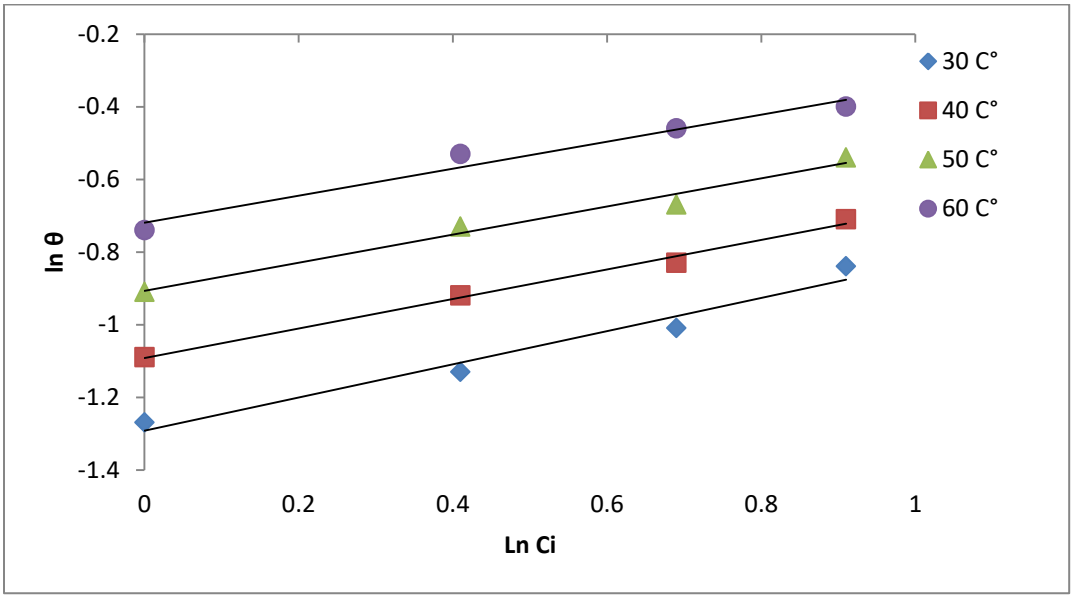


Figure(4.41): Freundlich adsorption isotherm of ($TiO_2$) nanomaterial as corrosion inhibitor for aluminum corrosion in ($1MH_3PO_4$ at pH of 4).

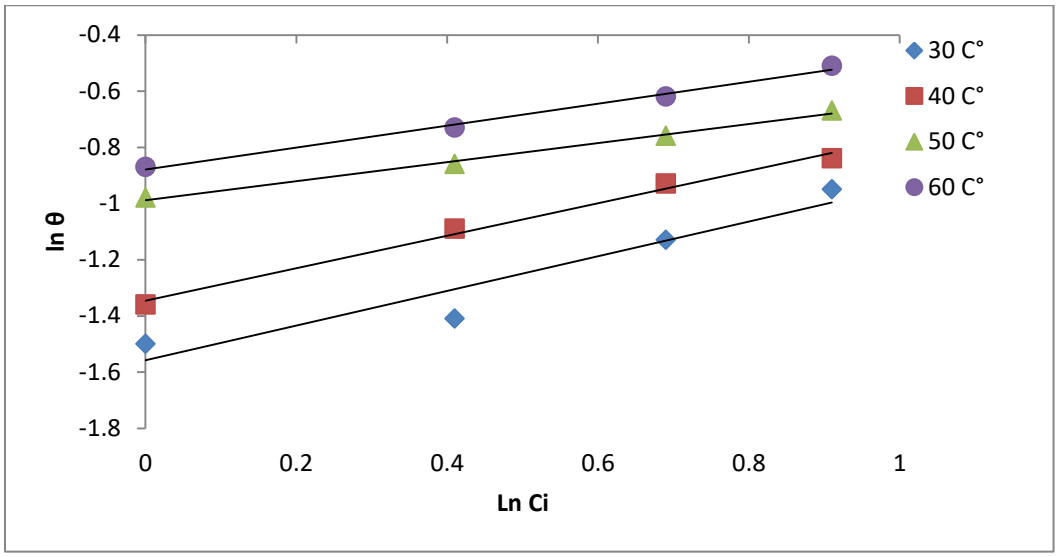


Figure (4.42): Freundlich adsorption isotherm of ($TiO_2$) nanomaterial for aluminum alloy (AA6063-T5) corrosion in ($1MH_3PO_4$ at pH of 4).

Table (4.13): Equilibrium constant ($K_F$), slope (n"), and correlation coefficient ($R^2$) for Freundlich type adsorption isotherm of the (CML) extract inhibitor for aluminum corrosion in (1 M $H_3PO_4$) at different temperatures.

| Temperature (°C) | $K_F$ (mg/g) | n" | $R^2$ |
|---|---|---|---|
| 30 | 1.7281 | 0.1635 | 0.9911 |
| 40 | 1.4171 | 0.0975 | 0.9915 |
| 50 | 1.3761 | 0.0906 | 0.9744 |
| 60 | 1.2104 | 0.0383 | 0.8818 |

Table (4.14): Equilibrium constant ($K_F$), slope (n"), and correlation coefficient ($R^2$) for Freundlich type adsorption isotherm of the (CML) extract inhibitor for aluminum alloy ($AA6063-T5$) corrosion in ($1\ M\ H_3PO_4$) at different temperatures.

| Temperature (℃) | $K_F$ ( mg/g ) | n " | $R^2$ |
|---|---|---|---|
| 30 | 1.8199 | 0.1718 | 0.9851 |
| 40 | 1.5658 | 0.1096 | 0.9951 |
| 50 | 1.4406 | 0.0833 | 0.9919 |
| 60 | 1.3479 | 0.0757 | 0.9921 |

Table (4.15): Equilibrium constant ($K_F$), slope (n"), and correlation coefficient ($R^2$) for Freundlich type adsorption isotherm of the nanomaterial ($Fe_2O_3$) inhibitor for aluminum corrosion in ($1MH_3PO_4$ at pH of 4) at different temperatures.

| Temperature (℃) | $K_F$ ( mg/g ) | n" | $R^2$ |
|---|---|---|---|
| 30 | 3.1711 | 0.5055 | 0.9358 |
| 40 | 2.7632 | 0.4506 | 0.9697 |
| 50 | 2.1666 | 0.2999 | 0.9801 |
| 60 | 1.6157 | 0.1588 | 0.9877 |

Table (4.16): Equilibrium constant ($K_F$), slope (n"), and correlation coefficient ($R^2$) for Freundlich type adsorption isotherm of the nanomaterial ($Fe_2O_3$) inhibitor for aluminum alloy (AA6063-T5) corrosion in ($1M H_3PO_4$ at pH of 4) at different temperatures.

| Temperature (°C) | $K_F$ ( mg/g ) | n" | $R^2$ |
|---|---|---|---|
| 30 | 3.5651 | 0.5149 | 0.9606 |
| 40 | 3.1578 | 0.5471 | 0.9858 |
| 50 | 2.3261 | 0.3217 | 0.971 |
| 60 | 1.8887 | 0.3053 | 0.991 |

Table (4.17): Equilibrium constant ($K_F$), slope (n"), and correlation coefficient ($R^2$) for Freundlich type adsorption isotherm of the nanomaterial ($TiO_2$) inhibitor for aluminum corrosion in ($1M H_3PO_4$ at pH of 4) at different temperatures.

| Temperature (°C) | $K_F$ ( mg/g ) | n" | $R^2$ |
|---|---|---|---|
| 30 | 3.6396 | 0.4565 | 0.9543 |
| 40 | 2.9793 | 0.4064 | 0.9902 |
| 50 | 2.4773 | 0.3875 | 0.9793 |
| 60 | 2.0525 | 0.3713 | 0.9673 |

Table (4.18): Equilibrium constant ($K_F$), slope (n"), and correlation coefficient ($R^2$) for Freundlich type adsorption isotherm of the nanomaterial ($TiO_2$) inhibitor for aluminum alloy (AA6063-T5) corrosion ($1MH_3PO_4$ at pH of 4) at different temperatures.

| Temperature (℃) | $K_F$ ( mg/g ) | n" | $R^2$ |
|---|---|---|---|
| 30 | 4.7469 | 0.6169 | 0.914 |
| 40 | 3.8412 | 0.5788 | 0.992 |
| 50 | 2.6847 | 0.3385 | 0.9942 |
| 60 | 2.4088 | 0.3907 | 0.993 |

## 4.3.3-Temkin adsorption isotherm

The adsorption of inhibitors on aluminum and aluminum alloy (AA6063-T5) surface was also defined using the equation.(2.25) temkin adsorption isotherm of the leaves extracts and nanomaterial on aluminum metal and aluminum alloy (AA6063 – T5) surface in figures (4.43) to (4.48), The values of (a) and ($K_T$) respectively and the data given in tables (4.19-4.24) were created by plotting surface coverage (Ɵ) versus ($lnC_i$) with slope and intercept yield that Temkin isotherm .Since correlation coefficient values are lower, it does not apply well to this method. The coefficient values for correlation are higher, hence the Langmuir adsorption isotherm is the best [75].

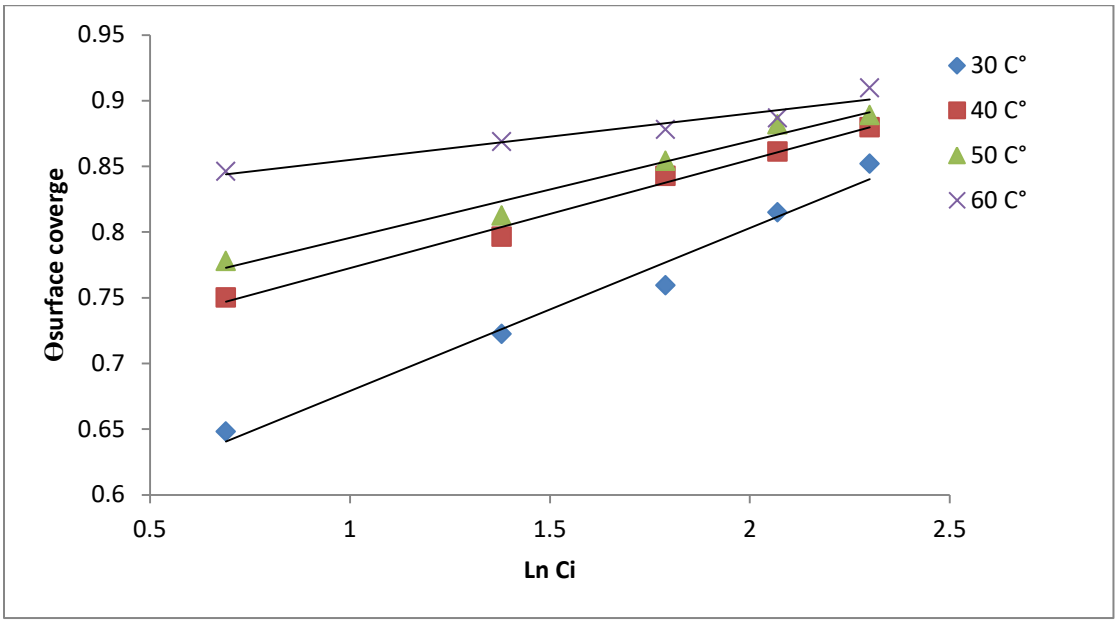


Figure (4.43): Temkin adsorption isotherm of Cordia myxa plant leaves (CML) extract inhibitor for aluminum corrosion in $(1\ M\ H_3PO_4)$.

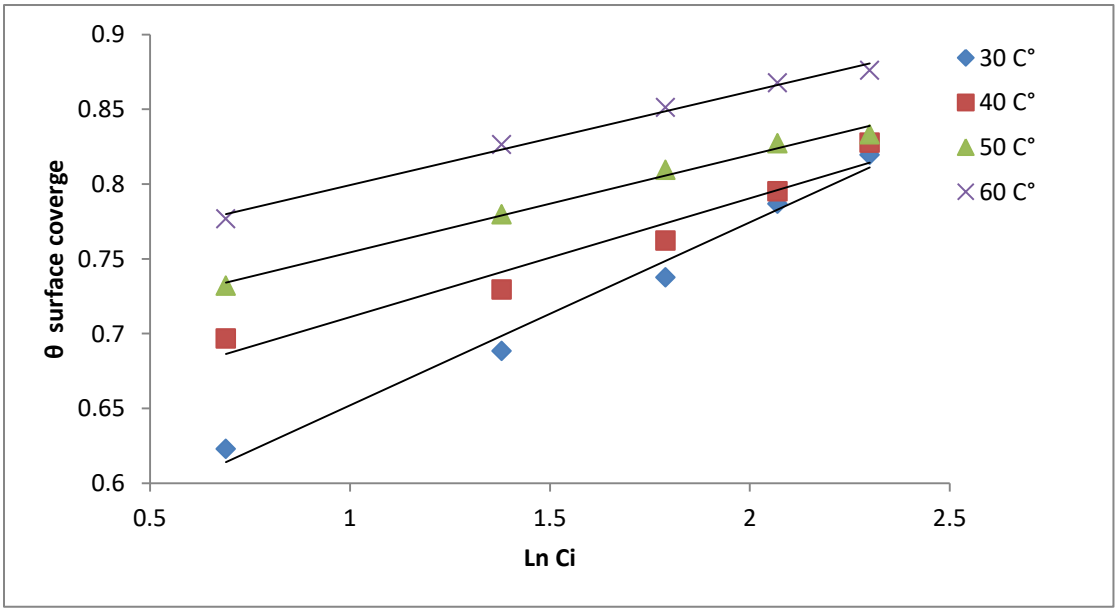


Figure (4.44): Temkin adsorption isotherm of Cordia myxa plant leaves(CML) extract inhibitor for aluminum alloy (AA6063-T5) corrosion in $(1MH_3PO_4)$.

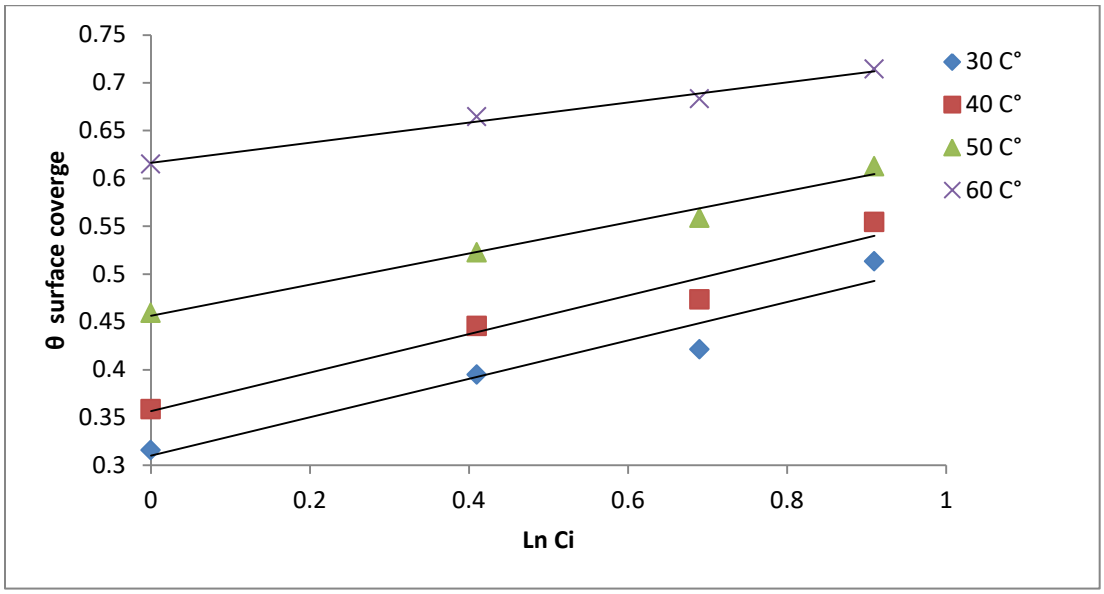


Figure (4.45): Temkin adsorption isotherm of nanomaterial ($Fe_2O_3$) inhibitor for aluminum corrosion in (1M $H_3PO_4$ at pH of 4).

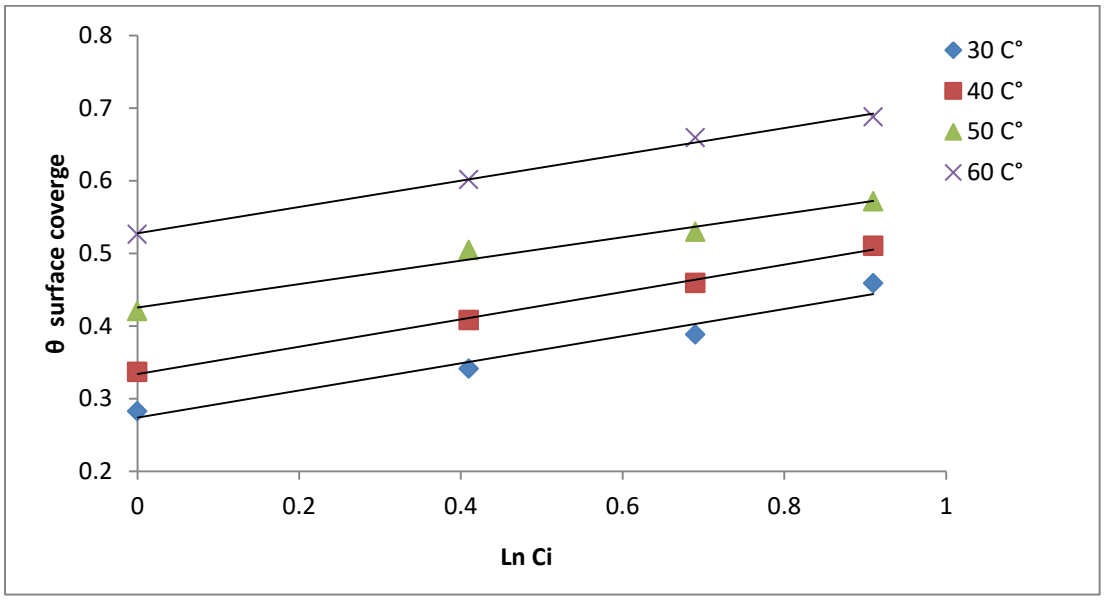


Figure (4.46): Temkin adsorption isotherm of nanomaterial ($Fe_2O_3$) for aluminum alloy (AA6063 T5) corrosion in (1M $H_3PO_4$ at pH of 4).

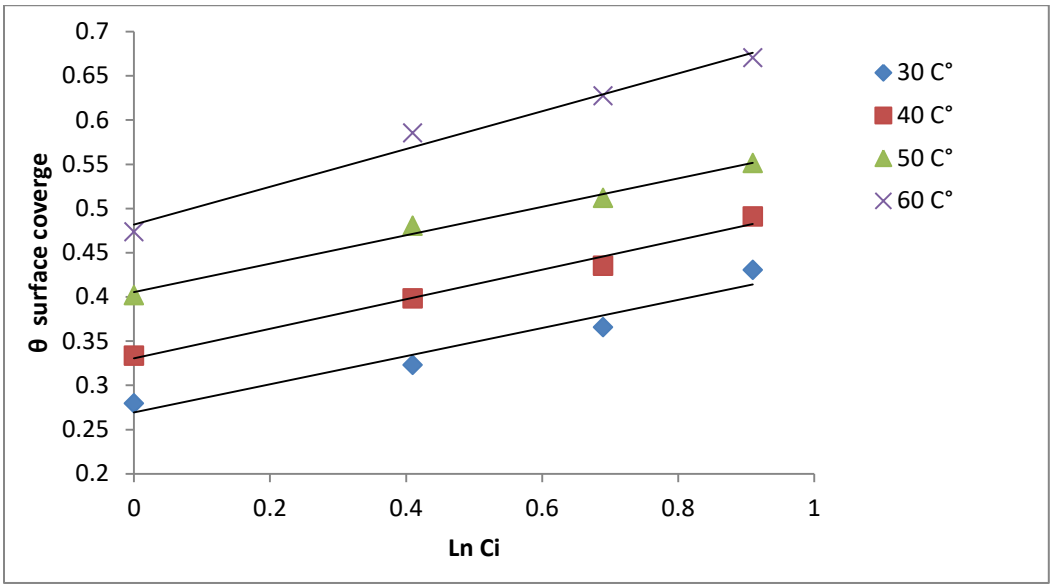


Figure (4.47): Temkin adsorption isotherm of nanomaterial ($TiO_2$) inhibitor for aluminum corrosion in (1M $H_3PO_4$ at pH of 4).

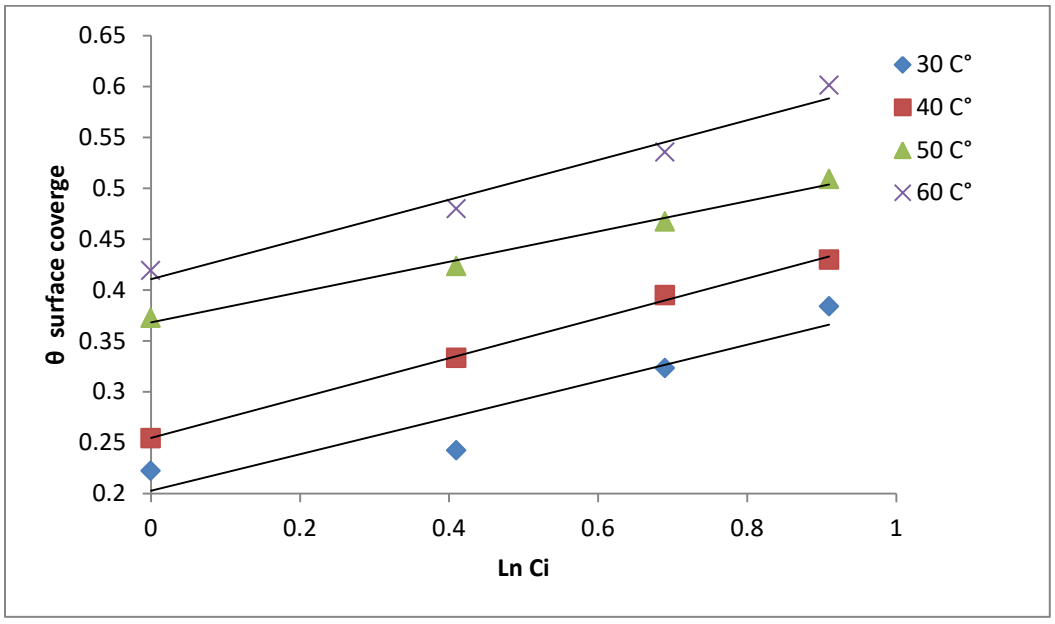


Figure (4.48): Temkin adsorption isotherm of nanomaterial ($TiO_2$) inhibitor for aluminum alloy (AA6063-T5) corrosion in (1M $H_3PO_4$ at pH of 4).

Table (4.19): Equilibrium constant ($K_T$), slope (a), and correlation coefficient ($R^2$) for Temkin type adsorption isotherm of the (CML) extract inhibitor for aluminum corrosion in ($1\ M\ H_3PO_4$) at different temperatures.

| Temperatures(K) | a | $K_T$(L/gm) | $R^2$ |
|---|---|---|---|
| 303 | 0.1241 | 1.7417 | 0.979 |
| 313 | 0.0824 | 1.9943 | 0.9917 |
| 323 | 0.0735 | 2.0585 | 0.9765 |
| 333 | 0.0355 | 2.2689 | 0.9357 |

Table (4.20): Equilibrium constant ($K_T$), slope (a), and correlation coefficient ($R^2$) for Temkin type adsorption isotherm of the (CML) extract inhibitor for aluminum alloy ($AA6063-T5$) corrosion in ($1\ M\ H_3PO_4$) at different temperatures.

| Temperatures(K) | $a$ | $K_T$(L/gm) | $R^2$ |
|---|---|---|---|
| 303 | 0.1223 | 1.6986 | 0.9842 |
| 313 | 0.0795 | 1.8804 | 0.948 |
| 323 | 0.0651 | 1.9921 | 0.9911 |
| 333 | 0.0626 | 2.0888 | 0.9921 |

Table (4.21): Equilibrium constant ($K_T$), slope (a), and correlation coefficient ($R^2$) for Temkin type adsorption isotherm of the nanomaterial ($Fe_2O_3$) inhibitor for aluminum corrosion in ($1MH_3PO_4$ at pH of 4) at different temperatures.

| Temperatures(K) | a | $K_T$(L/gm) | $R^2$ |
|---|---|---|---|
| 303 | 0.201 | 1.3637 | 0.9393 |
| 313 | 0.2016 | 1.4284 | 0.9617 |
| 323 | 0.1626 | 1.5785 | 0.9856 |
| 333 | 0.1054 | 1.8521 | 0.9875 |

Table (4.22): Equilibrium constant ($K_T$), slope (a), and correlation coefficient ($R^2$) for Temkin type adsorption isotherm of the nanomaterial ($Fe_2O_3$) inhibitor for aluminum alloy (AA6063-T5) corrosion in($1MH_3PO_4$ at pH of 4) at different temperatures.

| Temperatures(K) | a | $K_T$(L/gm) | $R^2$ |
|---|---|---|---|
| 303 | 0.1866 | 1.3151 | 0.9644 |
| 313 | 0.1883 | 1.3964 | 0.9961 |
| 323 | 0.1609 | 1.5302 | 0.9802 |
| 333 | 0.1814 | 1.6945 | 0.9958 |

Table (4.23): Equilibrium constant ($K_T$), slope (a), and correlation coefficient ($R^2$) for Temkin type adsorption isotherm of the nanomaterial ($TiO_2$) inhibitor for aluminum corrosion in ($1MH_3PO_4$ at pH of 4) at different temperatures.

| Temperatures(K) | a | $K_T$(L/gm) | $R^2$ |
|---|---|---|---|
| 303 | 0.1591 | 1.3093 | 0.9447 |
| 313 | 0.1671 | 1.3915 | 0.9856 |
| 323 | 0.1607 | 1.4999 | 0.9904 |
| 333 | 0.1135 | 1.6188 | 0.9833 |

Table (4.24): Equilibrium constant ($K_T$), slope (a), and correlation coefficient ($R^2$) for Temkin type adsorption isotherm of the nanomaterial ($TiO_2$) inhibitor for aluminum alloy (AA6063-T5) corrosion in ($1MH_3PO_4$ at pH of 4) at different temperatures.

| Temperatures(K) | a | $K_T$(L/gm) | $R^2$ |
|---|---|---|---|
| 303 | 0.1794 | 1.2248 | 0.8891 |
| 313 | 0.1658 | 1.2899 | 0.9979 |
| 323 | 0.1488 | 1.4451 | 0.991 |
| 333 | 0.1254 | 1.5077 | 0.9749 |

## 4.4.Thermodynamic adsorption of corrosion inhibitor

Values of apparent corrosion activation energies ($E_a$) for the corrosion phase of aluminum and aluminum alloy (AA6063-T5) in (1 M $H_3PO_4$) and (1M$H_3PO_4$ at pH of 4) in the presence and absence of (CML) extract inhibitor and nanomaterial ($Fe_2O_3$ and $TiO_2$) inhibitor were calculated by using equation (2.11) and plotting the Arrhenius plots of ($\ln CR$) versus ($1/T$) from the data given in Tables (4.1-4.6) which give straight lines with slopes equal to ($-E_a/R$) as in Figures (4.49) to (4.54).The estimated values of ($E_a$) for aluminum and aluminum alloy ($AA6063-T5$) corrosion in the presence of (CML) extract inhibitor and nanomaterial($Fe_2O_3$ and $TiO_2$) are listed in the tables (4.25-4.30).The activation energy of aluminum corrosion was found to be ($21.8699$ kJ $mol^{-1}$) in the absence of the extract and decreased to ($14.3715$ kJ $mol^{-1}$) in the presence of (CML) extract, whereas the activation energy of aluminum alloy ($AA6063-T5$) was found to be ($21.5315$ kJ $mol^{-1}$) in the absence of the extract and decreased to (16.4874kJ$mol^{-1}$) with its presence. Also the activation energy of aluminum was found to be ($11.2588$ kJ $mol^{-1}$) in the absence of the ($Fe_2O_3$) and decreased to ($3.4383$ kJ $mol^{-1}$) in the presence ($Fe_2O_3$). The activation energy of aluminum alloy ($AA6063-T5$) ($10.7375$ kJ $mol^{-1}$) in the absence of the ($Fe_2O_3$) and decreased to ($2.6351$ kJ $mol^{-1}$) .The values of activation energy of aluminum were (10.4698kJ $mol^{-1}$) in the absence of the ($TiO_2$) and decreased to ($2.3814$ kJ $mol^{-1}$). In the presence of whereas The activation energy of aluminum alloy (AA6063-T5) was found to be ($10.4132$ kJ $mol^{-1}$) in the absence of the ($TiO_2$) and decreases then to ($3.6214$ kJ $mol^{-1}$) if inhibitor ($TiO_2$) used .It has been reported that when the values of Ea> 80 kJ/mol indicated a chemical adsorption type whereas Ea< 80 kJ/mol infers physical adsorption [101] .

It is clear that the concentration of the inhibitor plays a role in lowering the activation energy values, indicating the more inhibitory effect, so ($E_a$) is less in the presence of inhibitor in general [102].

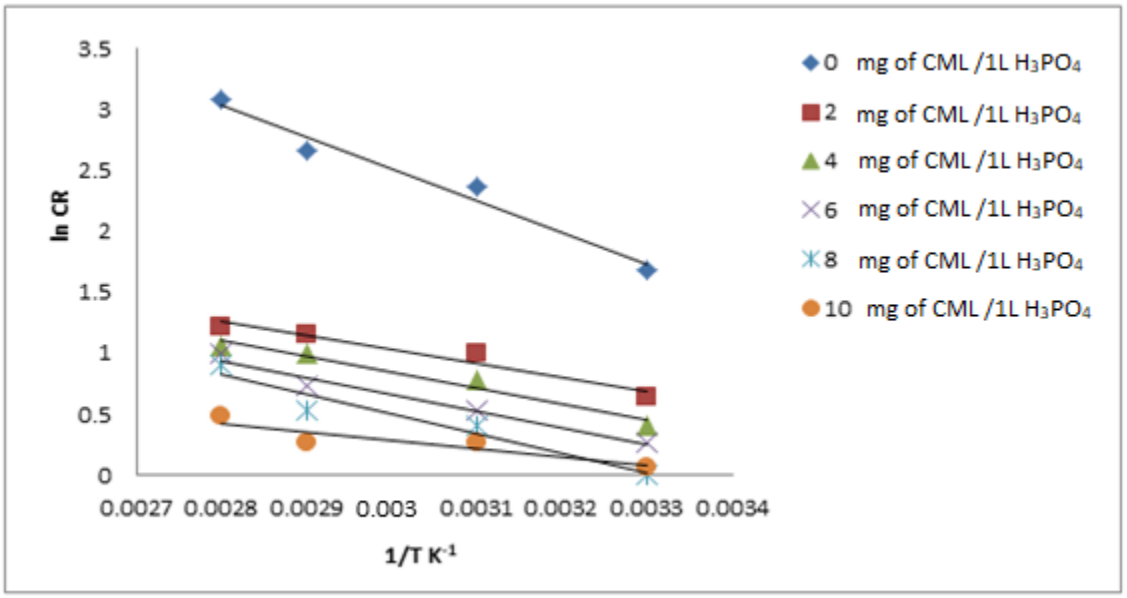


Figure (4.49): Arrhenius plot of aluminum corrosion in $(1\ M H_3PO_4)$ containing various concentrations Cordia myxa plant leaves (CML) extract as corrosion inhibitors.

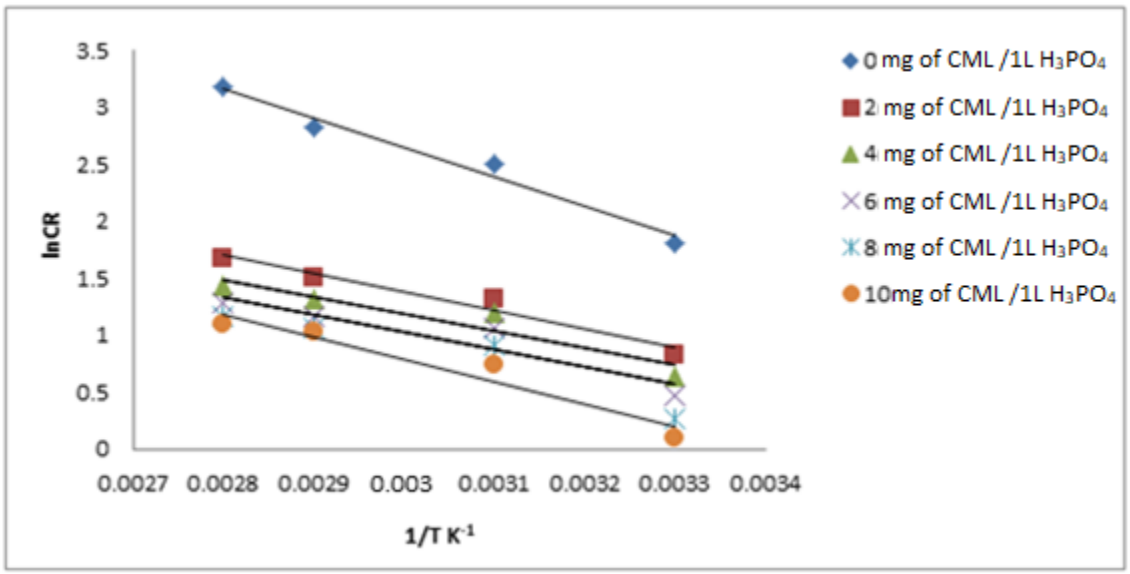


Figure (4.50):Arrhenius plot of aluminum alloy ( $AA6063-T5$) corrosion in $(1\ M\ H_3PO_4)$ containing various concentrations Cordia myxa plant leaves (CML) extract at different temperatures as corrosion inhibitors.

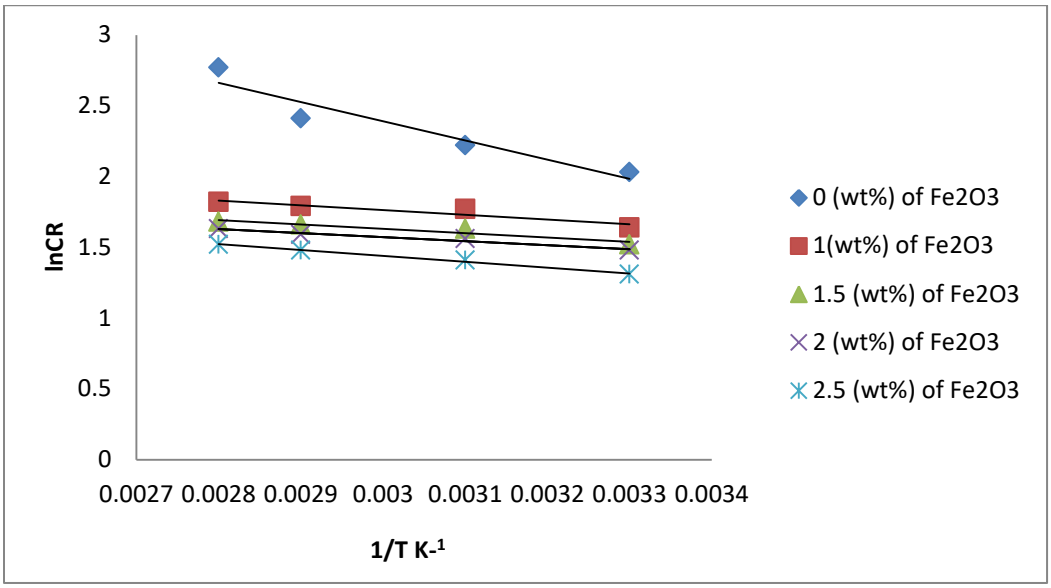


Figure (4.51): Arrhenius plot of aluminum corrosion in ($1MH_3PO_4$ at pH of 4) containing various concentrations ($Fe_2O_3$) corrosion inhibitor at different temperatures .

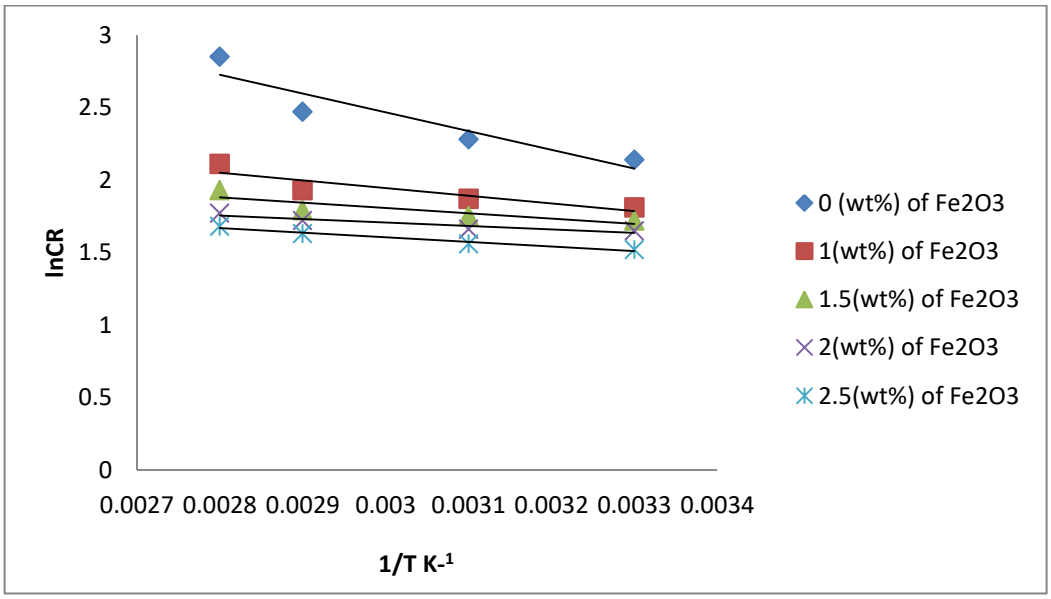


Figure (4.52): Arrhenius plot of aluminum alloy (AA6063 – T5) corrosion in ($1MH_3PO_4$ at pH of 4) containing various concentrations ($Fe_2O_3$) corrosion inhibitor at different temperatures.

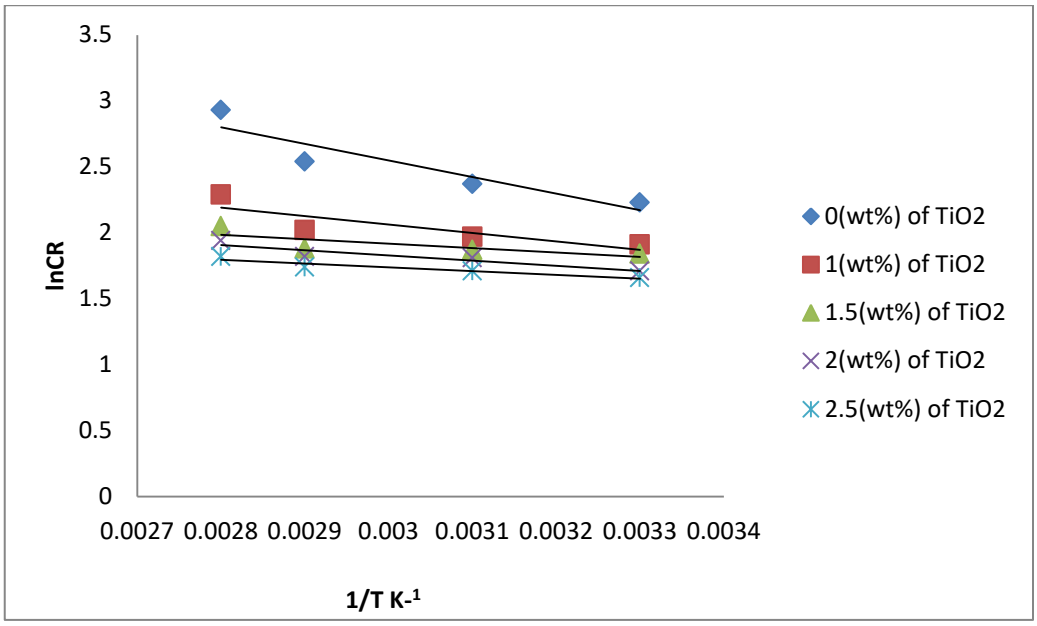


Figure (4.53): Arrhenius plot of aluminum corrosion in($1MH_3PO_4$ at pH of 4) containing various concentrations ($TiO_2$) corrosion inhibitor at different temperatures.

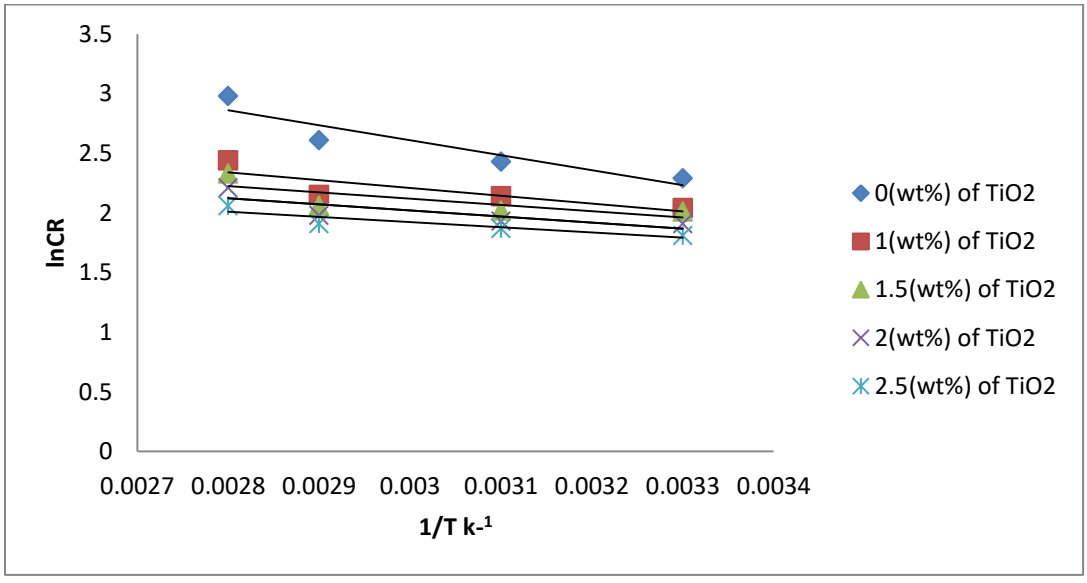


Figure (4.54): Arrhenius plot of aluminum alloy (AA6063 – T5) corrosion in ($1MH_3PO_4$ at pH of 4) containing various concentrations ($TiO_2$) corrosion inhibitor at different temperatures.

Table (4.25): Values of activation energies for the corrosion of aluminum ($1\ M\ H_3PO_4$) in presence and absence Cordia myxa leaves (CML) extract as the corrosion inhibitor.

| $C_i$ (mg /L) | $E_a$ (kJ $mol^{-1}$) |
|---|---|
| Blank | 21.8699 |
| 2 | 9.5412 |
| 4 | 10.7657 |
| 6 | 11.4991 |
| 8 | 13.5418 |
| 10 | 14.3715 |

Table (4.26): Values of activation energies for the corrosion of aluminum alloy ($AA6063-T5$) $1\ M\ H_3PO_4$ in presence and absence Cordia myxa leaves (CML) extract as the corrosion inhibitor.

| $C_i$ (mg /L) | $E_a$ (kJ $mol^{-1}$) |
|---|---|
| Blank | 21.5315 |
| 2 | 13.5418 |
| 4 | 12.4144 |
| 6 | 12.6397 |
| 8 | 14.3025 |
| 10 | 16.4874 |

Table (4.27): Values of activation energies for the corrosion of aluminum ($1MH_3PO_4$ at pH of 4) presence and absence of ($Fe_2O_3$) as the corrosion inhibitor.

| $C_i$ ( mg/L) | $E_a$ (kJ $mol^{-1}$) |
|---|---|
| Blank | 11.2588 |
| 1 | 2.7911 |
| 1.5 | 2.5505 |
| 2 | 2.3392 |
| 2.5 | 3.4383 |

Table (4.28): Values of activation energies for the corrosion of aluminum alloy (AA6063-T5) ($1MH_3PO_4$at pH of 4) presence and absence of ($Fe_2O_3$) as the corrosion inhibitor.

| $C_i$ ( mg/L) | $E_a$ (kJ $mol^{-1}$) |
|---|---|
| Blank | 10.7375 |
| 1 | 4.3965 |
| 1.5 | 3.0297 |
| 2 | 1.9728 |
| 2.5 | 2.6351 |

Table (4.29): Values of activation energies for the corrosion of aluminum ($1MH_3PO_4$at pH of 4) presence and absence of ($TiO_2$) as the corrosion inhibitor.

| $C_i$ ( mg/L) | $E_a$ (kJ $mol^{-1}$) |
|---|---|
| Blank | 10.4698 |
| 1 | 5.3406 |
| 1.5 | 2.8182 |
| 2 | 3.2692 |
| 2.5 | 2.3814 |

Table (4.30): Values of activation energies for the corrosion of aluminum alloy (AA6063-T5) ($1MH_3PO_4$at pH of 4) presence and absence of ($TiO_2$) as the corrosion inhibitor.

| $C_i$ ( mg/L) | $E_a$ (kJ $mol^{-1}$) |
|---|---|
| Blank | 10.4132 |
| 1 | 5.4252 |
| 1.5 | 4.3683 |
| 2 | 4.2133 |
| 2.5 | 3.6214 |

Experimental corrosion rates values determine from weight loss measurements for aluminum and aluminum alloy (AA6063-T5) corrosion in ($1MH_3PO_4$) and the absence and presence of (CML) extract and ($Fe_2O_3$ and $TiO_2$) were used to determine the enthalpy of activation, ($\Delta H^*$) and entropy of activation ($\Delta S^*$) for the formation of the activated complex from the transition state equation. The enthalpy of activation ($\Delta H^*$) and entropy of activation ($\Delta S^*$) were calculated by using equation (2.16) and plotting ($\ln CR/T$) versus ($1/T$) as shown in figures

(4.55) to (4.60) where straight lines obtained with slopes of $(-\Delta H^*/R)$ and intercepts of $\{(\ln R/Nh) + (\Delta S^*/R)\}$ from which $(\Delta H^*)$ and $(\Delta S^*)$ were calculated and listed in Tables (4.31-4.36) There is a positive sign of change in activation enthalpy, which denotes an endothermic aluminum and aluminum alloy (AA6063-T5) corrosion activation phase [103].The large and negative values of $\Delta S^*$ means that the activated complex is the rate–determining phase and represents a phase of interaction rather than dissociation, which means that a continuous decrease in disorder from reactants to the activated complex takes place [104].

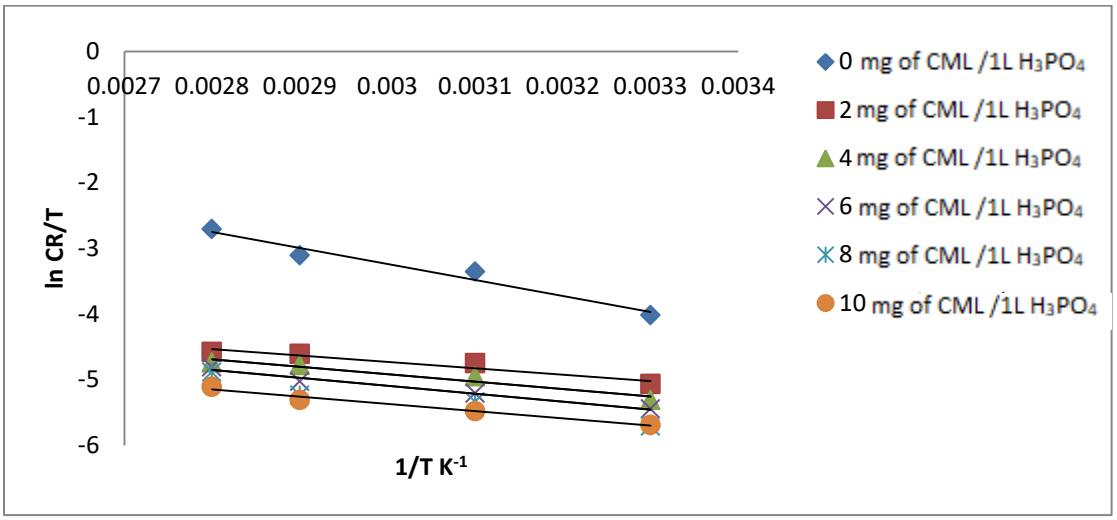


Figure (4.55): Transition state plot for aluminum corrosion in $(1\ M\ H_3PO_4)$ in absence and presence of different concentrations of (CML) extract.

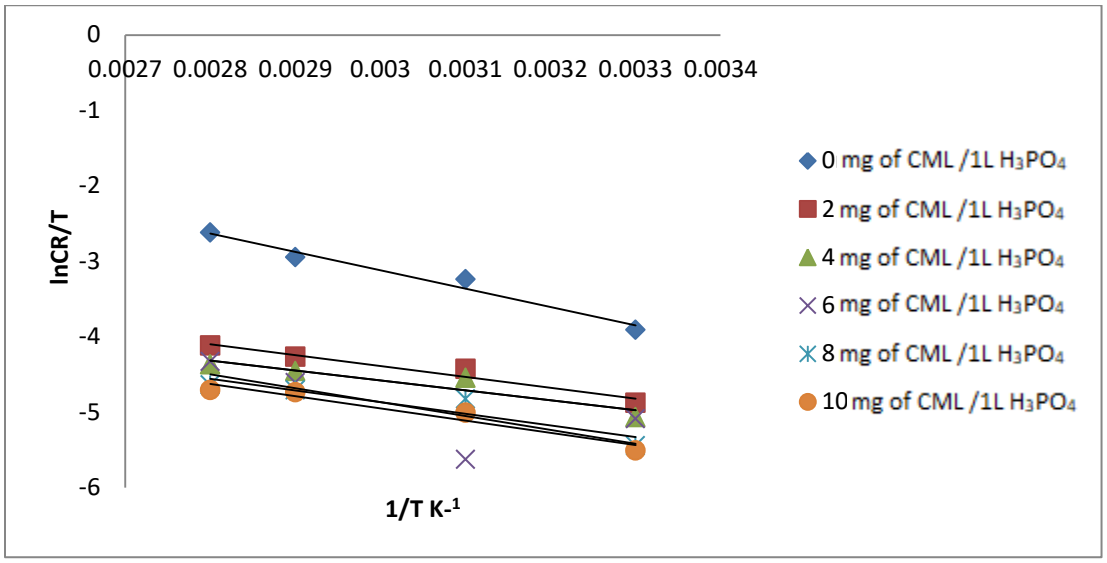


Figure (4.56): Transition state plot for aluminum alloy (AA6063 – T5) corrosion in (1 M $H_3PO_4$) in absence and presence of different concentrations of (CML) extract.

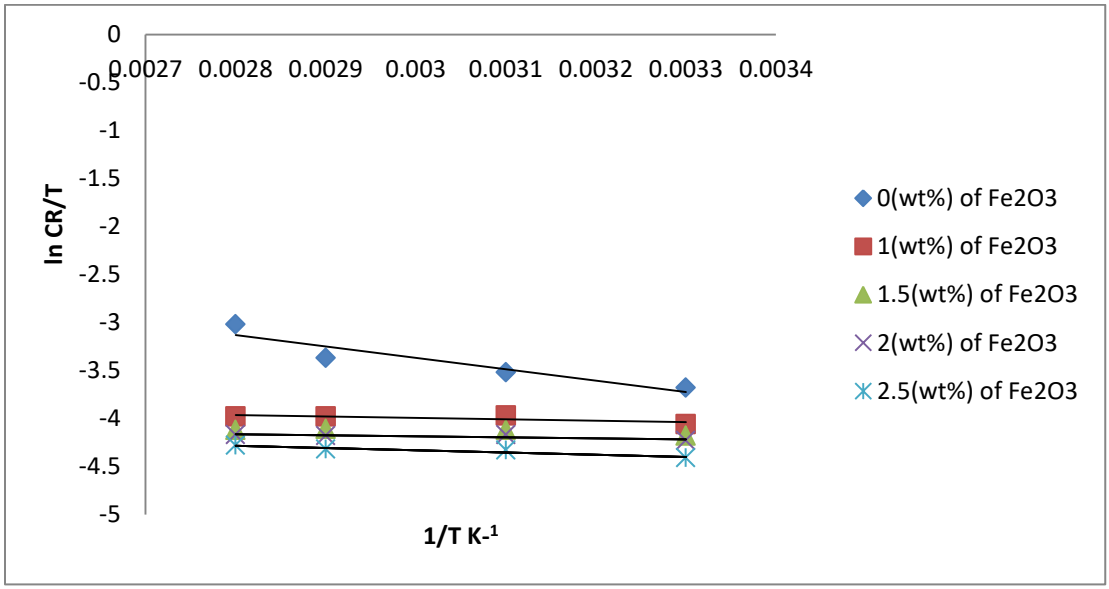


Figure (4.57): Transition state plot for aluminum corrosion in (1M$H_3PO_4$ at pH of 4) in absence and presence of different concentrations of nanomaterial ($Fe_2O_3$) inhibitor.

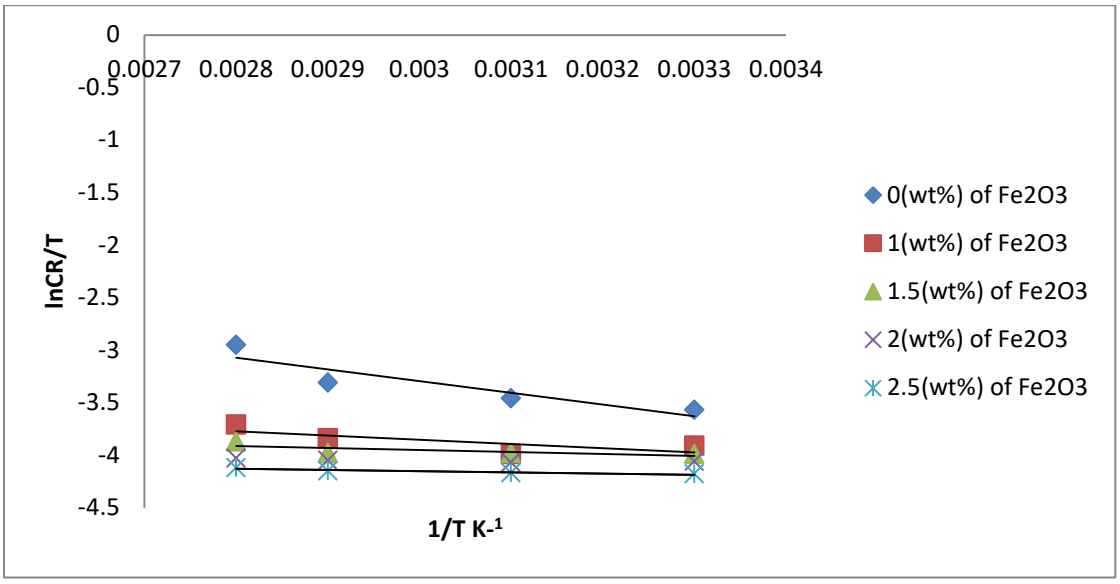


Figure (4.58): Transition state plot for aluminum alloy (AA6063-T5) corrosion in ($1MH_3PO_4$ at pH of 4) in absence and presence of different concentrations of nanomaterial ($Fe_2O_3$) inhibitor.

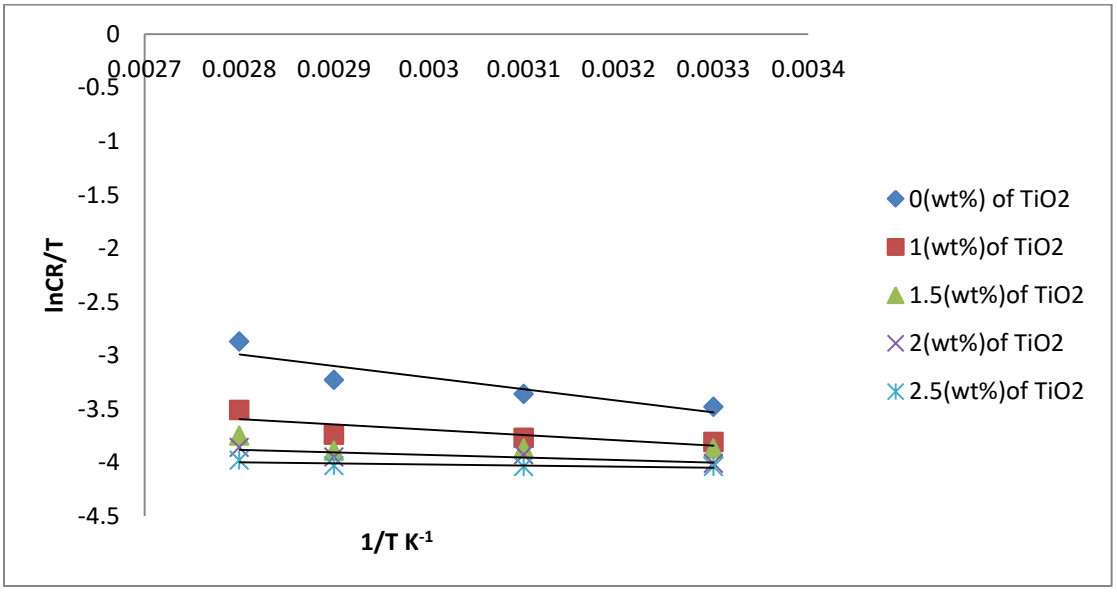


Figure (4.59): Transition state plot for aluminum corrosion in($1MH_3PO_4$ at pH of 4) in absence and presence of different concentrations of nanomaterial ($TiO_2$) inhibitor.

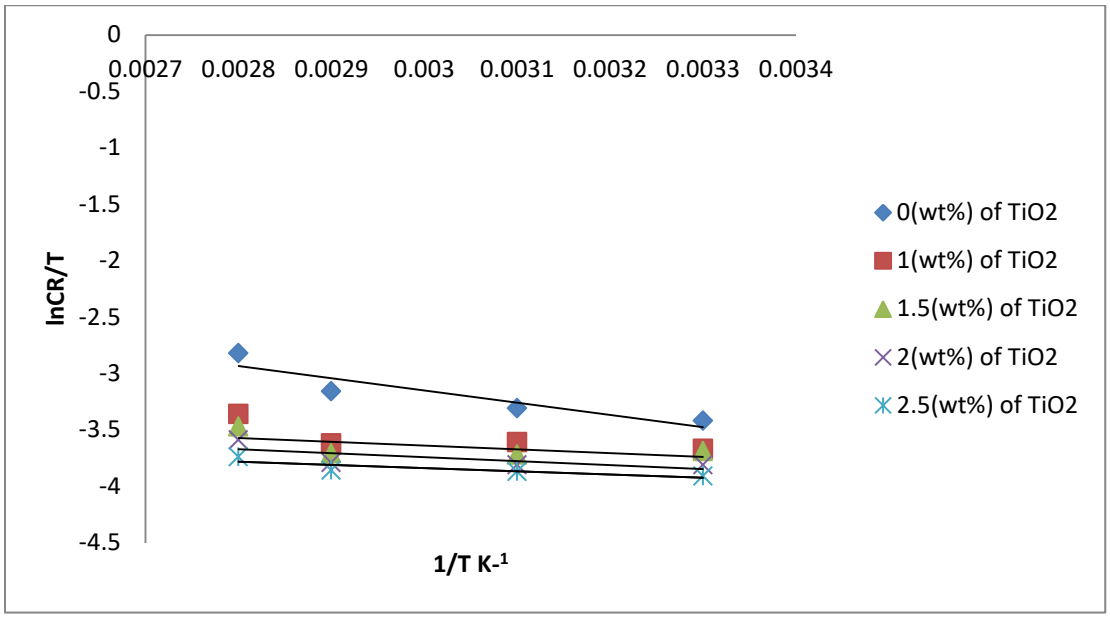


Figure (4.60): Transition state plot for aluminum alloy (AA6063-T5) corrosion in($1MH_3PO_4$ at pH of 4) in absence and presence of different concentrations of nanomaterial ($TiO_2$) inhibitor.

Table (4.31): Enthalpy and Entropy of activation values of the aluminum corrosion reaction with various concentrations of Cordia myxa plant leaves (CML) extract in ($1MH_3PO_4$).

| $C_i$ (mg /L) | $\Delta H^*(kJmol^{-1})$ | $\Delta S^*(kJmol^{-1}K^{-1})$ |
|---|---|---|
| Blank | 20.2354 | -0.1637 |
| 2 | 8.1026 | -0.1825 |
| 4 | 9.4413 | -0.1849 |
| 6 | 10.0616 | -0.1853 |
| 8 | 12.1467 | -0.1902 |
| 10 | 12.8093 | -0.1921 |

Table (4.32): Enthalpy and Entropy of activation values of the aluminum alloy (AA6063- T5) reaction with various concentrations of Cordia myxa plant leaves (CML) extract in (1 M $H_3PO_4$).

| $C_i$ (mg /L) | $\Delta H^*(kJmol^{-1})$ | $\Delta S^*(kJmol^{-1}K^{-1})$ |
|---|---|---|
| Blank | 20.2919 | -0.1625 |
| 2 | 12.0345 | -0.1971 |
| 4 | 10.9769 | -0.1923 |
| 6 | 11.2031 | -0.1918 |
| 8 | 12.8659 | -0.1956 |
| 10 | 15.0076 | -0.1938 |

Table (4.33): Enthalpy and Entropy of activation values of the aluminum corrosion reaction with various concentrations of ($Fe_2O_3$) inhibitor in ($1MH_3PO_4$ at pH of 4).

| $C_i$( mg/L) | $\Delta H^*(kJmol^{-1})$ | $\Delta S^*(kJmol^{-1}K^{-1})$ |
|---|---|---|
| Blank | 9.8778 | -0.1959 |
| 1 | 11.9779 | -0.1679 |
| 1.5 | 10.5280 | -0.1662 |
| 2 | 11.7385 | -0.1653 |
| 2.5 | 13.4878 | -0.1673 |

Table (4.34): Enthalpy and Entropy of activation values of the aluminum alloy (AA 6063-T5) corrosion reaction with various concentrations of ($Fe_2O_3$) inhibitor in ($1MH_3PO_4$ at pH of 4).

| $C_i$ (mg/L) | $\Delta H^*(kJmol^{-1})$ | $\Delta S^*(kJmol^{-1}K^{-1})$ |
|---|---|---|
| Blank | 9.12302 | -0.1972 |
| 1 | 3.3678 | -0.1756 |
| 1.5 | 1.5506 | -0.1693 |
| 2 | 4.9162 | -0.1653 |
| 2.5 | 6.5791 | -0.1658 |

Table (4.35): Enthalpy and Entropy of activation values of the aluminum corrosion reaction with various concentrations of ($TiO_2$) inhibitor in ($1MH_3PO_4$ at pH of 4).

| $C_i$ (mg/L) | $\Delta H^*(kJmol^{-1})$ | $\Delta S^*(kJmol^{-1}K^{-1})$ |
|---|---|---|
| Blank | 8.9907 | -0.1972 |
| 1 | 4.1288 | -0.1792 |
| 1.5 | 1.3809 | -0.1697 |
| 2 | 1.9868 | -0.1708 |
| 2.5 | 2.2362 | -0.1666 |

Table (4.36): Enthalpy and Entropy of activation values of the aluminum alloy (AA 6063-T5 ) corrosion reaction with various concentrations of ($TiO_2$) inhibitor in ($1MH_3PO_4$ at pH of 4).

| $C_i$ (mg/L) | $\Delta H^*(kJmol^{-1})$ | $\Delta S^*(kJmol^{-1}K^{-1})$ |
|---|---|---|
| Blank | 8.9766 | -0.1968 |
| 1 | 4.0302 | -0.1809 |
| 1.5 | 2.7761 | -0.1756 |
| 2 | 2.9310 | -0.1752 |
| 2.5 | 2.3392 | -0.1736 |

## 4.5 .FTIR Spectroscopy analysis

In order to gain some understanding of potential interactions between the adsorbed (CML) inhibitor and aluminum metal and aluminum alloy (AA6063-T5) surface in ($1MH_3PO_4$) solution at (10mg /L) inhibitor concentration and (333K). Fourier transform infrared analysis was used. The main component of the (CML) extract is (O-H) groups, depending on the molecular structure of the (CML) inhibition .The (FTIR) spectrum of (CML) extract is shown in figure (4.61a). Where alcohol ($O-H$) stretching vibration appeared at (3413) $cm^{-1}$. The peak at (2078) $cm^{-1}$ can be assigned to aliphatic (C-H) and the (C=C) stretching vibration frequency appeared at (1639) $cm^{-1}$.The (C-O) stretching vibration frequency appeared at (1250) $cm^{-1}$.So, it seem that the main constituent of Cordia myxa leaves extract is alcohol groups such as (Linalool, $C_{10}H_{18}O$). Table (4.37) describes the infrared absorption bands and their allocation. The (FTIR) spectrum of the protective film formed on the surface of the metal after immersion in ($1MH_3PO_4$) is shown in figure (4.61b) and undoubtedly shows that some of the peaks have fully disappeared while some have moved to the region of lower

frequencies, as shown for extract, aluminum immersed in (1 M $H_3PO_4$) containing (10 mg / L) of (CML) extract is also found as shown in Figure (4.61b). Alcohol $(O-H)$ stretching vibration has shifted from $(3413 \text{ to } 3408)\ cm^{-1}$. The aliphatic $(C-H)$ stretching shifted from $(2078 \text{ to } 2066)\ cm^{-1}$. The $(C=C)$ stretching vibration frequency has been shifted from $(1639 \text{ to } 1637)\ cm^{-1}$. The aliphatic $(C-O)$ stretching vibration frequency has been shifted from $(1250 \text{ to } 1211\ cm^{-1})$. Figure (4.61c) shows the (FTIR) spectrum of the protective film formed on the surface of the metal after immersion in (1 M $H_3\ PO_4$) and undoubtedly shows that some of the peaks have completely disappeared while some have moved to the region of lower frequencies, noted for extract is also noted for aluminum alloy (AA6063-T5) immersed in (1 M $H_3\ PO_4$) containing (10 mg /L) of (CML). Alcohol $(O-H)$ stretching vibration has shifted from (3413 to $3391\ cm^{-1}$). The aliphatic $(C-H)$ stretching shifted from $(2078 \text{ to} 2058\ cm^{-1})$. The $(C=C)$ stretching vibration frequency has been shifted from $(1639$ to $1631\ cm^{-1})$. The aliphatic $(C-O)$ stretching vibration frequency has been shifted from (1250 to 1167) $cm^{-1}$ This means an association occurs between the inhibitor molecules and the surface of the aluminum and aluminum alloy (AA6063-T5) for adsorption [105].

Table $(4.37)$: Important peaks in the FTIR spectra of ( CML) extract.

| CML extract | |
|---|---|
| Functional groups | Vibrational Frequency $/(cm^{-1})$ |
| $O-H$ stretching | 3413 to 3391 |
| $C-H$ stretching | 2078 to 2058 |
| C=C stretching | 1639 to 1631 |
| $C-O$ stretching | 1250 to1167 |

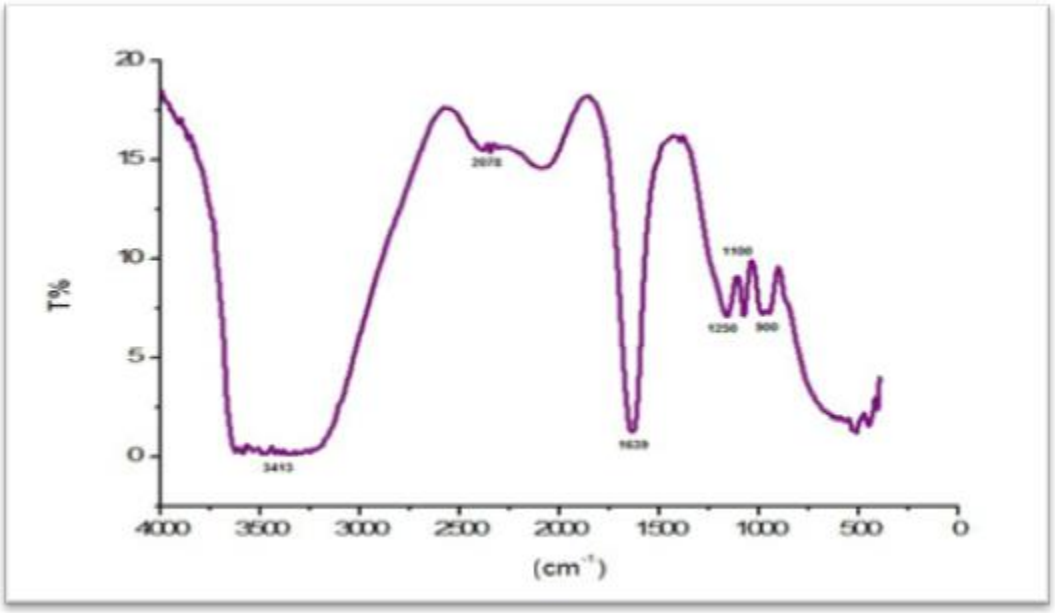


Figure (4.61.a):FTIR spectra of CML extract.

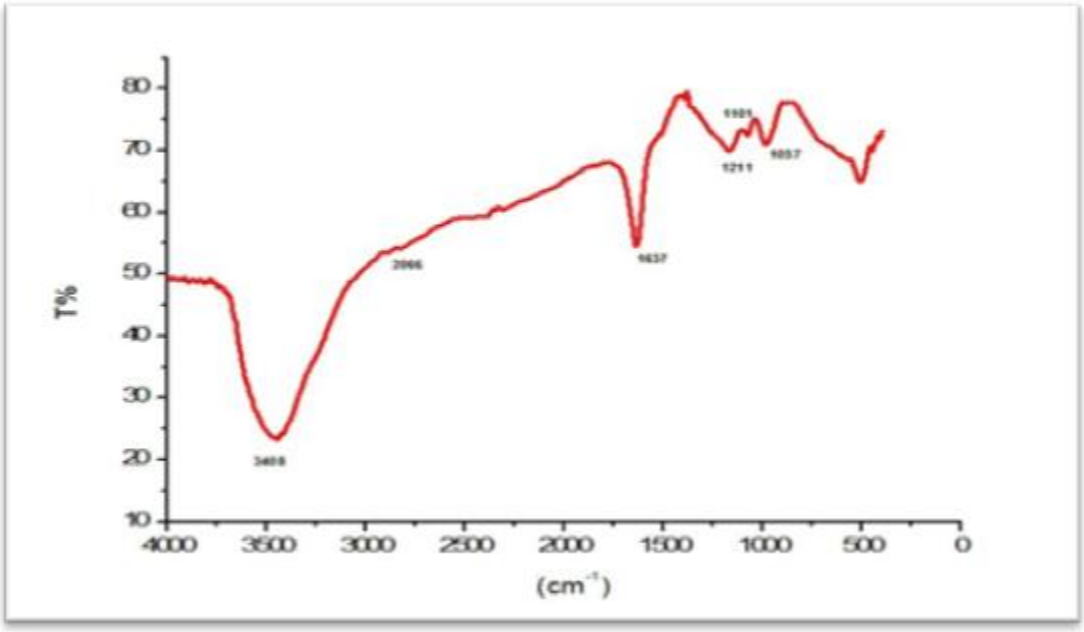


Figure (4.61.b):FTIR spectra of adsorbed film of CML extract on to aluminum surface after immersion (1M $H_3PO_4$).

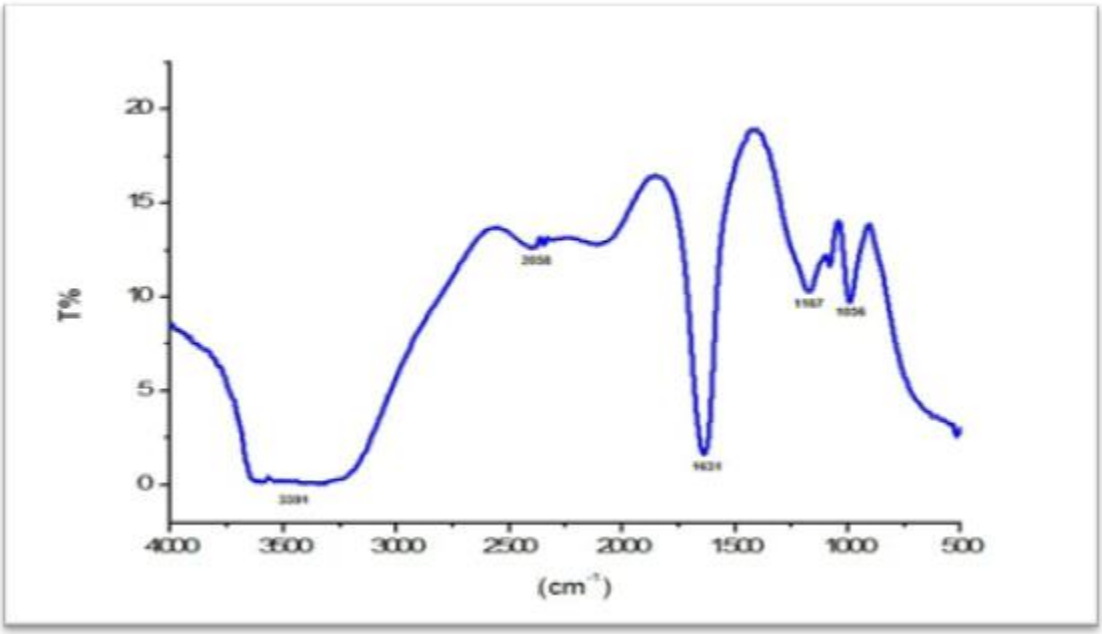


Figure (4.61.c):FTIR spectra of adsorbed film of CML extract on to aluminum alloy (AA6063-T5) surface after immersion (1M $H_3PO_4$).

## 4.6. X-ray diffraction

The X-Ray diffraction was employed to check and determine the crystalline structure of materials.

### 4.6.1 - ray diffraction of aluminum surface.

The data of strongest three peaks and the X-ray diffraction pattern for aluminum surface are shown in Table (4.38) and figures (4.62) respectively.

Table ( 4.38 ): The strongest three peaks in the XRD pattern of aluminum surface.

| No. | 2θ (deg) | d (Å) | FWHM (deg) | Intensity (counts) |
|---|---|---|---|---|
| **1** | 29.5137 | 3.02664 | 0.2460 | 100 |
| **2** | 35.6597 | 2.51783 | 0.3444 | 30.01 |
| **3** | 47.7771 | 1.90374 | 0.2952 | 23.09 |

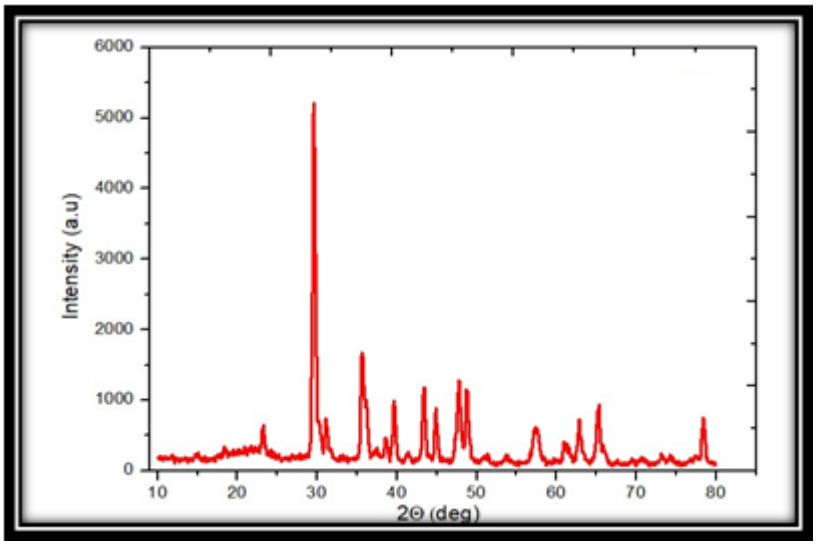


Figure (4.62) :X-ray diffraction of aluminum surface**.**

### 4.6.2- X-ray diffraction of aluminum surface immersed in ($1MH_3PO_4$ at PH of 4) in presence of ($2.5wt\%Fe_2O_3$) as nanomaterial inhibitor.

The data for the strongest three peaks of aluminum surface immersed in ($1MH_3PO_4$ at PH of 4) in presence of ($2.5wt\%Fe_2O_3$) are shown in table (4.39) respectively. The X-ray diffraction pattern of surface are shown in figures (4.63) for aluminum surface immersed in ($1MH_3PO_4$ at PH of 4) in presence ($2.5wt\%Fe_2O_3$) . The particle sizes were calculated from Deby-Sherrer formula given below [106].

$$D = \frac{0.9\,\lambda}{\beta \cos\theta} \qquad \text{.....(4.3)}$$

In which :

**D**: is the crystallite size.

**λ**: is the wave length of radiation.

**θ**: is the Bragg's angle.

**β**: is the full width at half maximum (FWHM).

The estimated particle size of the ($Fe_2O_3$) was (28.2857) nm .The presence of sharp peaks in XRD pattern and particle size being less than (100) nm refers to the nano-crystalline nature.

Table (4.39 ): The strongest three peaks in the XRD pattern of aluminum surface immersed in ($1MH_3PO_4$ at PH of 4) in presence of ($2.5wt\%Fe_2O_3$).

| No. | 2θ (deg) | d (Å) | FWHM (deg) | Intensity (counts) |
|---|---|---|---|---|
| 1 | 29.4091 | 3.03716 | 0.2952 | 100 |
| 2 | 35.3919 | 2.53626 | 0.2460 | 28.13 |
| 3 | 47.5191 | 1.91347 | 0.2460 | 27.26 |

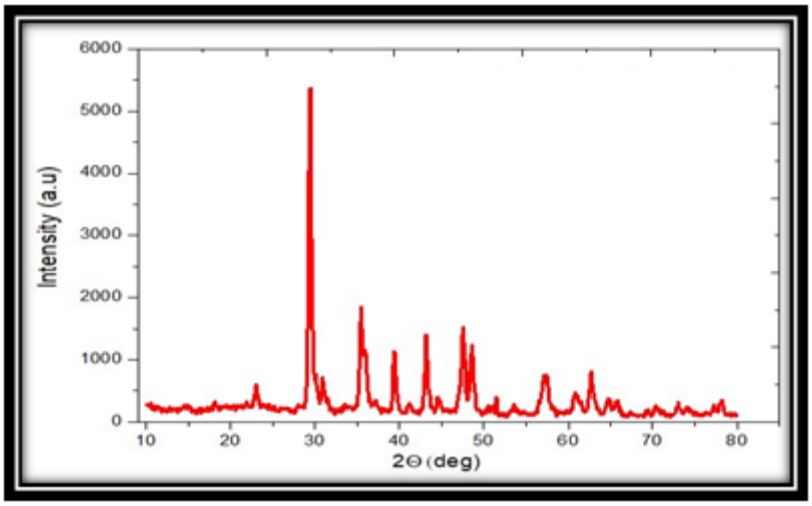


Figure (4.63) :X-ray diffraction of aluminum surface immersed in ($1MH_3PO_4$ at PH of 4) in Presence of ($2.5wt\%Fe_2O_3$).

### 4.6.3-X-ray diffraction of aluminum alloy (AA6063-T5) surface.

The data of strongest three peaks and The X-ray diffraction pattern for Aluminum alloy (AA6063-T5) surface are shown in table (4.40 ) and Figures (4.64) respectively.

Table ( 4.40 ): The strongest three peaks in the XRD pattern of aluminum alloy (AA6063-T5) surface.

| No. | 2θ (deg) | d (Å) | FWHM (deg) | Intensity (counts) |
|---|---|---|---|---|
| 1 | 29.4383 | 3.03422 | 0.3444 | 100 |
| 2 | 35.6115 | 2.52112 | 0.2952 | 26.43 |
| 3 | 47.7060 | 1.90641 | 0.2952 | 23.87 |

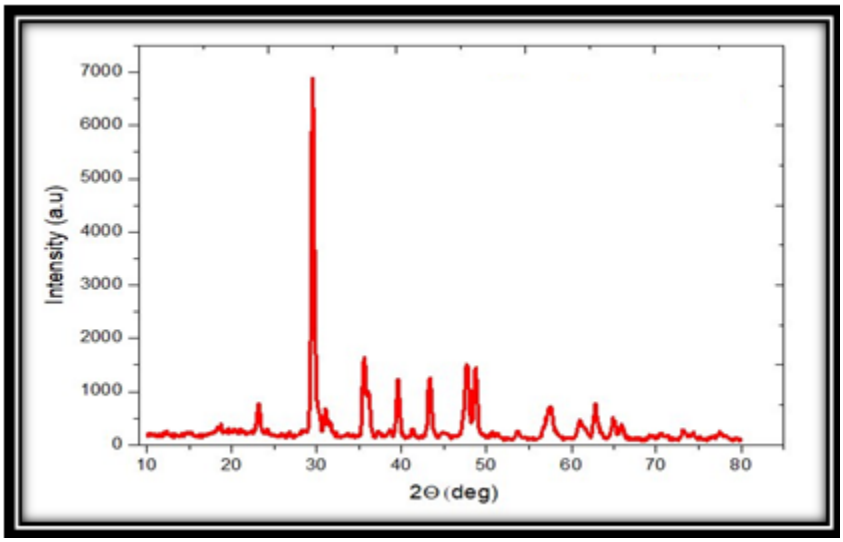


Figure ( 4.64 ) :X-ray diffraction of aluminum alloy (AA6063-T5) surface.

### 4.6.4- X-ray diffraction of aluminum alloy (AA6063-T5) surface immersed in ($1MH_3PO_4$ at pH of 4) in presence of ($2.5wt\%Fe_2O_3$) as nanomaterial inhibitor.

The data of the strongest three peaks of aluminum alloy (AA6063-T5) surface immersed in ($1MH_3PO_4$ at pH of 4) in Presence ($2.5wt\%Fe_2O_3$) are shown in table (4.41). The X-ray diffraction pattern of surface are shown in figures (4.65) for aluminum alloy (AA6063-T5) surface immersed in ($1MH_3PO_4$ at pH of 4) in presence of ($2.5wt\%Fe_2O_3$) . The estimated particle size of the ($Fe_2O_3$) was (28.2857) nm .The presence of sharp peaks in XRD pattern and particle size being less than (100) nm refers to the nano-crystalline nature.

Table (4.41): The strongest three peaks in the XRD pattern of aluminum alloy (AA6063-T5) surface immersed in ($1MH_3PO_4$ at pH of 4) in presence of ($2.5wt\%Fe_2O_3$).

| No. | 2θ (deg) | d (Å) | FWHM (deg) | Intensity (counts) |
|---|---|---|---|---|
| **1** | 29.4028 | 3.03780 | 0.2952 | 100 |
| **2** | 35.3819 | 2.53696 | 0.2952 | 38.90 |
| **3** | 47.5134 | 1.91369 | 0.3936 | 24.84 |

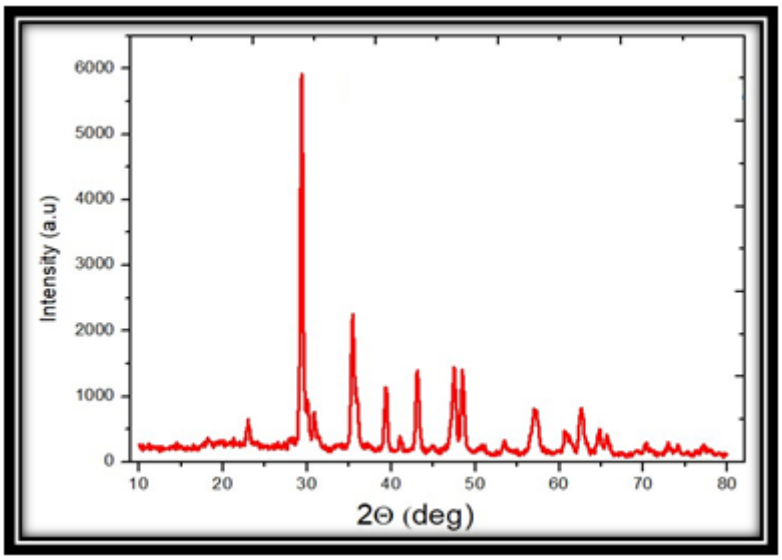


Figure (4.65) :X-ray diffraction of aluminum alloy (AA6063-T5) surface immersed in ($1MH_3PO_4$ at pH of 4) in presence of ($2.5wt\%Fe_2O_3$).

### 4.6.5- X-ray diffraction of aluminum surface immersed in ($1MH_3PO_4$ at pH of 4) in presence of (2.5 wt%$TiO_2$) as nanomaterial inhibitor.

The data of strongest three peaks for aluminum surface immersed in ($1MH_3PO_4$ at pH of 4) in Presence of (2.5wt%$TiO_2$) are shown in table (4.42). The X-ray diffraction pattern of surface are shown in figures (4.66) for aluminum surface immersed in ($1MH_3PO_4$ at PH of 4) in presence of (2.5wt%$TiO_2$). The estimated particle size of the ($TiO_2$) was (23.8965) nm .The presence of sharp peaks in XRD pattern and particle size being less than (100) nm refers to the nano-crystalline nature.

Table (4.42): The strongest three peaks in the XRD pattern of aluminum surface immersed in ($1MH_3PO_4$ at pH of 4) in presence of (2.5wt%$TiO_2$).

| No. | 2θ (deg) | d (Å) | FWHM (deg) | Intensity (counts) |
|---|---|---|---|---|
| 1 | 29.3168 | 3.04651 | 0.3444 | 100 |
| 2 | 35.4647 | 2.53122 | 0.3444 | 30.89 |
| 3 | 47.5670 | 1.91166 | 0.2952 | 27.79 |

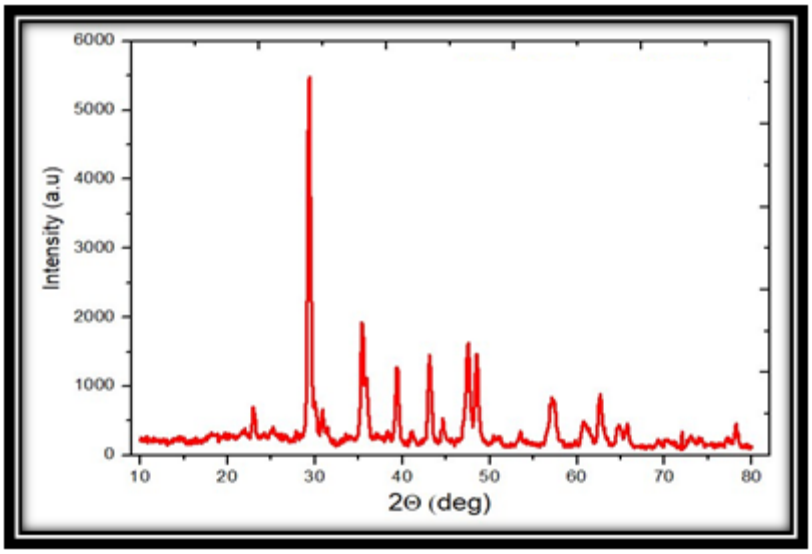


Figure (4.66) :X-ray diffraction of aluminum surface immersed in ($1MH_3PO_4$ at pH of 4) in presence of ($2.5wt\%TiO_2$).

**4.6.6- X-ray diffraction of aluminum alloy (AA6063-T5) surface immersed in ($1MH_3PO_4$ at pH of 4) in presence of ($2.5\ wt\%TiO_2$) as nanomaterial inhibitor.**

The data of the strongest three peaks of aluminum alloy (AA6063-T5) surface immersed in ($1MH_3PO_4$ at PH of 4) in presence ($2.5wt\%TiO_2$) are shown in table (4.43). The X-ray diffraction pattern of surface are shown in figures (4.67) for aluminum alloy (AA6063-T5) surface immersed in ($1MH_3PO_4$ at pH of 4) in presence ($2.5wt\%TiO_2$). The estimated particle size of the ($TiO_2$) was (23.8965) nm The presence of sharp peaks in XRD pattern and particle size being less than (100) nm refers to the nano-crystalline nature.

Table (4.43): The strongest three peaks in the XRD pattern of aluminum alloy (AA6063-T5) surface immersed in ($1MH_3PO_4$ at pH of 4) in presence of ($2.5wt\%TiO_2$).

| No. | 2θ (deg) | d (Å) | FWHM (deg) | Intensity (counts) |
|---|---|---|---|---|
| 1 | 29.3081 | 3.04739 | 0.3444 | 100 |
| 2 | 35.2868 | 2.54357 | 0.2952 | 33.56 |
| 3 | 47.4252 | 1.91704 | 0.2952 | 29.99 |

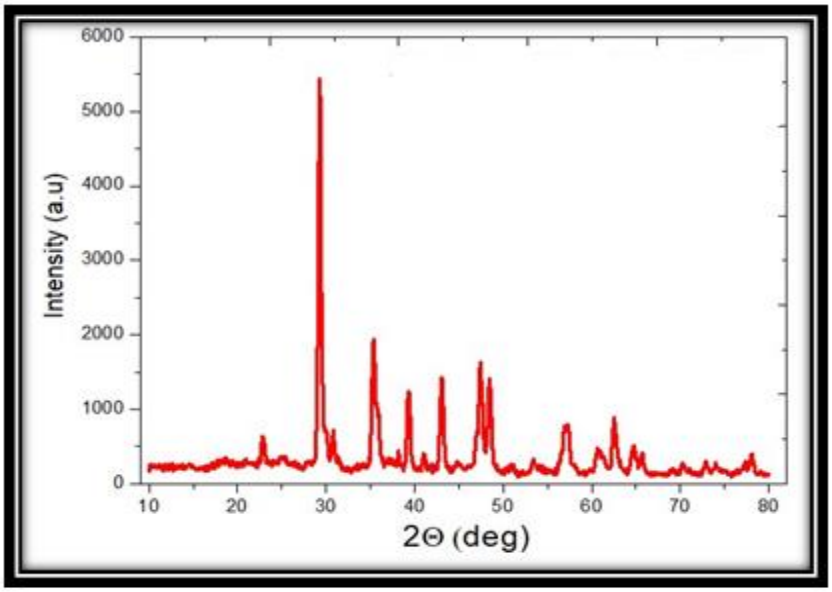


Figure (4.67) :X-ray diffraction of aluminum alloy (AA6063-T5) surface immersed in ($1MH_3PO_4$ at pH of 4) in presence of ($2.5wt\%TiO_2$).

## 4.7. Surface analysis using (AFM)

Atomic Force Microscopy Characterization (AFM) is a powerful technique used to investigate the surface morphology at nano –to micro– scale and has become a new choice to study the influence of inhibitor on the generation and the progress of the corrosion at the metal solution interface [107,108]. Atomic Force Microscopy (AFM) analysis is provides a measure of average roughness (Ra) the average deviation of all points roughness profile from a mean line over the evaluation length, root–mean–square roughness (Rq) the average of the measured height deviations taken within the evaluation length and measured from the mean line) [107]. In figure (4.68),(4.69) and (4.70), (A) is the (AFM) image in three dimension (3D),it explain structure shape of grain and (B) is AFM image in two dimension (2D) for polished aluminum immersed in 1M $H_3PO_4$ (blank sample) and aluminum surfaces immersed in 1M $H_3PO_4$ in presence of 10 mL of (CML) extract as inhibitor respectively. Also table (4.44) show AFM data for aluminum surface corrosion .

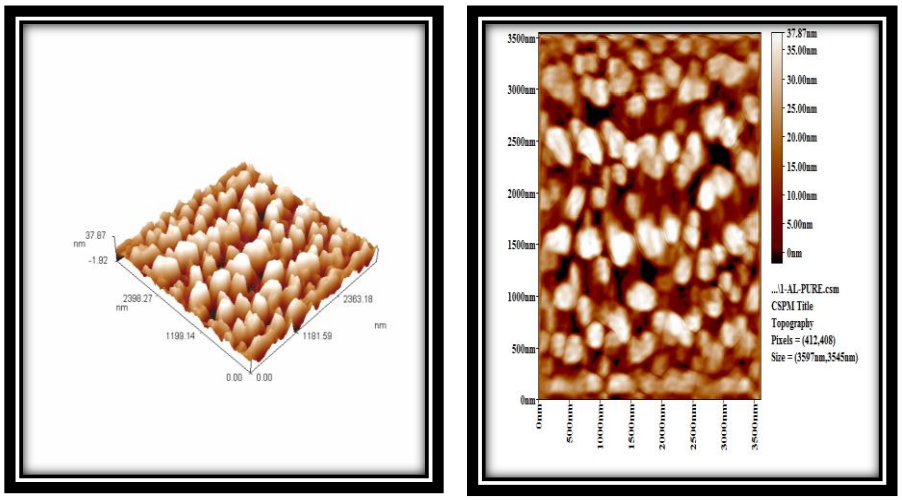


**A** B

Figure (4.68) : AFM images of polished aluminum surface.

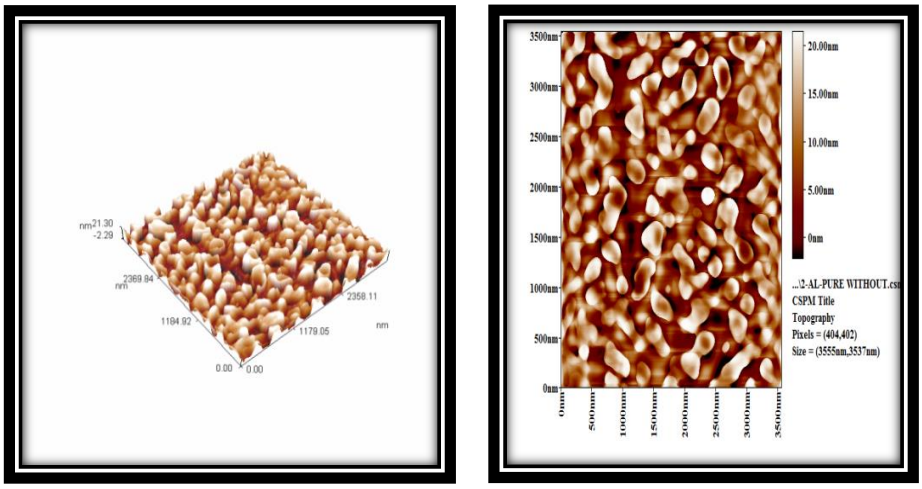


**A** **B**

Figure (4.69 ): AFM images of aluminum surface immersed in (1M $H_3PO_4$).

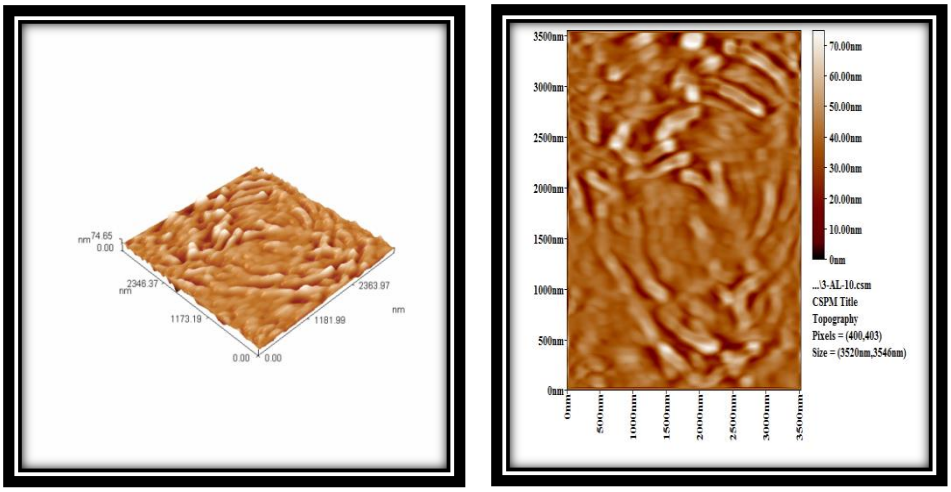


**A** **B**

Figure (4.70) : AFM images of aluminum immersion in (1M $H_3PO_4$) presence (10ml) of CML extract.

Table (4.44): AFM data for aluminum surface immersed in inhibited and uninhibited media.

| Sample | Average Roughness (Ra) (nm) | RMS (Rq) Roughness (nm) |
|---|---|---|
| 1- Polished aluminum pure | 9.53nm | 11.2 nm |
| 2- Aluminum immersed in 1M $H_3PO_4$ (blank) | 5.9 nm | 6.81 nm |
| 3.Aluminum immersed in 1M $H_3PO_4$ with10 ml of (CML) inhibitor | 6.74 nm | 9.09 nm |

Tables (4.45), (4.46) and (4.47) and figures (4.71), (4.72) and (4.73), show the granularity cumulating distribution and average diameter data of the polished aluminum surface, aluminum surface immersed in (1M $H_3PO_4$), aluminum immersion in (1M $H_3PO_4$) presence (10ml) of CML extract.

The average diameter of Polished aluminum surface (174.18**)** nm ,and the particle size of less than 10 % of the total particles is (110) nm, less than 50 % was (150) nm and less than 90% was ( 240) nm and the average diameter of regenerated Aluminum surface immersed in (1M $H_3PO_4$) is (136.41) nm ,and the particle size of less than 10 % of the total particles was (80) nm, less than 50 % was (130) nm and less than 90% was (190) nm and finally the average diameter of the aluminum immersed in(1M $H_3PO_4$) in presence (10ml) of CML extract was (191.96) nm and the particle size of less than 10 % of the total particles was 140 nm, less than 50 % was (180) nm and less than 90% was ( 250) nm.

Table (4.45): Granularity cumulating distribution and average diameter of polished aluminum surface.

| Diameter(nm)< | Volume(%) | Cumulation(%) | Diameter(nm)< | Volume(%) | Cumulation(%) | Diameter(nm)< | Volume(%) | Cumulation(%) |
|---|---|---|---|---|---|---|---|---|
| 110.00 | 4.15 | 4.15 | 200.00 | 4.15 | 74.09 | 300.00 | 1.04 | 94.30 |
| 120.00 | 7.77 | 11.92 | 210.00 | 4.15 | 78.24 | 310.00 | 1.04 | 95.34 |
| 130.00 | 11.40 | 23.32 | 220.00 | 6.22 | 84.46 | 320.00 | 1.04 | 96.37 |
| 140.00 | 11.92 | 35.23 | 230.00 | 2.07 | 86.53 | 330.00 | 1.04 | 97.41 |
| 150.00 | 6.22 | 41.45 | 240.00 | 3.11 | 89.64 | 360.00 | 0.52 | 97.93 |
| 160.00 | 10.36 | 51.81 | 250.00 | 1.55 | 91.19 | 370.00 | 0.52 | 98.45 |
| 170.00 | 6.22 | 58.03 | 260.00 | 1.04 | 92.23 | 380.00 | 1.04 | 99.48 |
| 180.00 | 6.74 | 64.77 | 280.00 | 0.52 | 92.75 | 420.00 | 0.52 | 100.00 |
| 190.00 | 5.18 | 69.95 | 290.00 | 0.52 | 93.26 | | | |

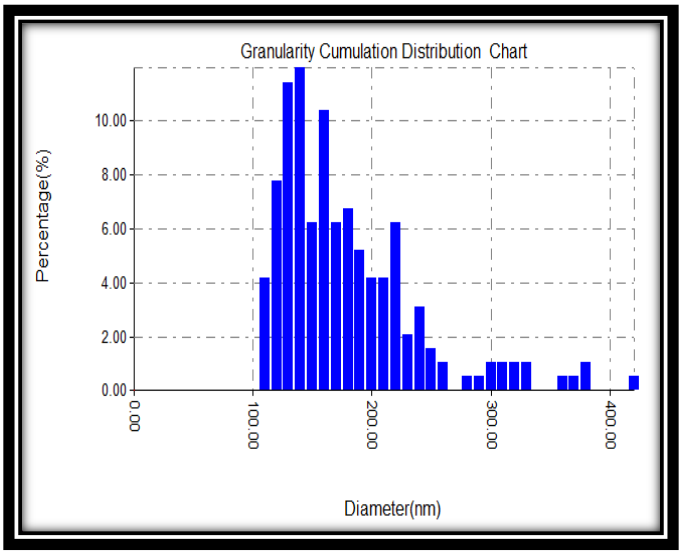


Figure (4.71): Granularity cumulating distribution of polished aluminum surface.

Table (4.46): Granularity cumulating distribution and average diameter of aluminum surface immersed in (1M $H_3PO_4$).

| Diameter(nm)< | Volume(%) | Cumulation(%) | Diameter(nm)< | Volume(%) | Cumulation(%) | Diameter(nm)< | Volume(%) | Cumulation(%) |
|---|---|---|---|---|---|---|---|---|
| 80.00 | 6.77 | 6.77 | 150.00 | 7.10 | 63.55 | 220.00 | 1.61 | 95.81 |
| 90.00 | 10.65 | 17.42 | 160.00 | 6.45 | 70.00 | 230.00 | 0.32 | 96.13 |
| 100.00 | 7.42 | 24.84 | 170.00 | 8.71 | 78.71 | 240.00 | 1.29 | 97.42 |
| 110.00 | 8.06 | 32.90 | 180.00 | 5.48 | 84.19 | 250.00 | 0.97 | 98.39 |
| 120.00 | 7.42 | 40.32 | 190.00 | 5.48 | 89.68 | 270.00 | 0.97 | 99.35 |
| 130.00 | 9.03 | 49.35 | 200.00 | 2.90 | 92.58 | 280.00 | 0.65 | 100.00 |
| 140.00 | 7.10 | 56.45 | 210.00 | 1.61 | 94.19 | | | |

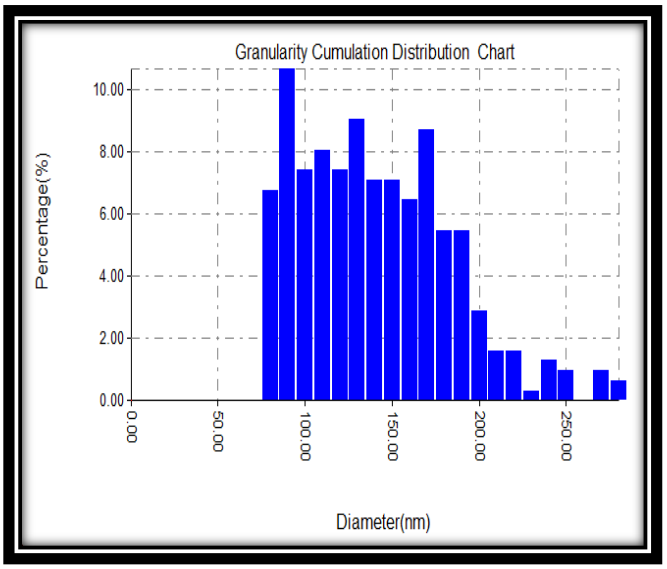


Figure (4.72): Granularity cumulating distribution of aluminum surface immersed in (1M $H_3PO_4$).

Table (4.47): Granularity cumulating distribution and average diameter of aluminum immersed in (1M $H_3PO_4$) in presence of (10ml) of CML extract.

| Diameter(nm)< | Volume(%) | Cumulation(%) | Diameter(nm)< | Volume(%) | Cumulation(%) | Diameter(nm)< | Volume(%) | Cumulation(%) |
|---|---|---|---|---|---|---|---|---|
| 140.00 | 6.82 | 6.82 | 210.00 | 6.82 | 68.18 | 280.00 | 2.27 | 96.59 |
| 150.00 | 11.93 | 18.75 | 220.00 | 6.82 | 75.00 | 290.00 | 0.57 | 97.16 |
| 160.00 | 9.66 | 28.41 | 230.00 | 6.25 | 81.25 | 300.00 | 0.57 | 97.73 |
| 170.00 | 11.36 | 39.77 | 240.00 | 3.41 | 84.66 | 310.00 | 1.14 | 98.86 |
| 180.00 | 8.52 | 48.30 | 250.00 | 5.11 | 89.77 | 320.00 | 0.57 | 99.43 |
| 190.00 | 6.82 | 55.11 | 260.00 | 3.41 | 93.18 | 360.00 | 0.57 | 100.00 |
| 200.00 | 6.25 | 61.36 | 270.00 | 1.14 | 94.32 | | | |

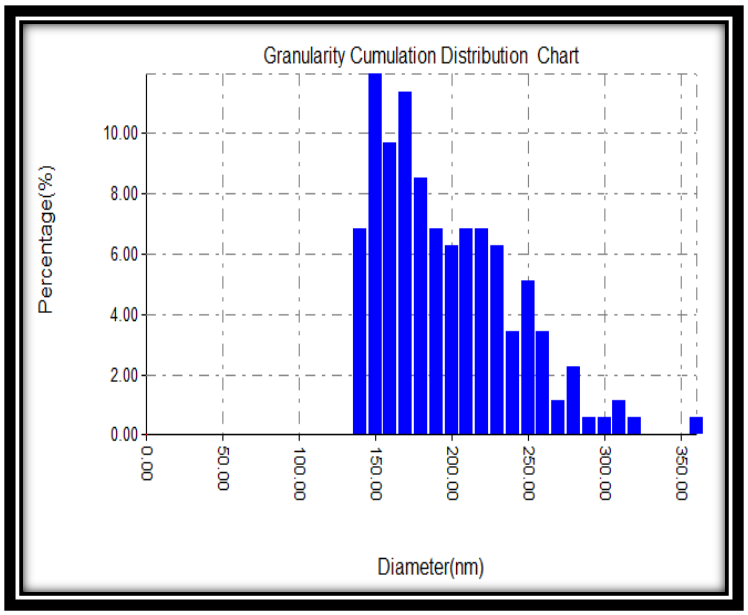


Figure (4.73): Granularity cumulating distribution and average diameter of aluminum immersed in (1M $H_3PO_4$) presence of (10ml) of CML extract.

In figure (4.74),(4.75) and (4.76) ,the AFM image for polished aluminum alloy (AA6063-T5), aluminum alloy (AA6063-T5) immersed in $1MH_3PO_4$ (blank sample) and aluminum alloy (AA6063-T5) immersed in $1MH_3PO_4$ in presence of 10mL 0f (CML) extract as corrosion inhibitor respectively. Table (4.48) show AFM data for aluminum alloy (AA6063-T5) surface.

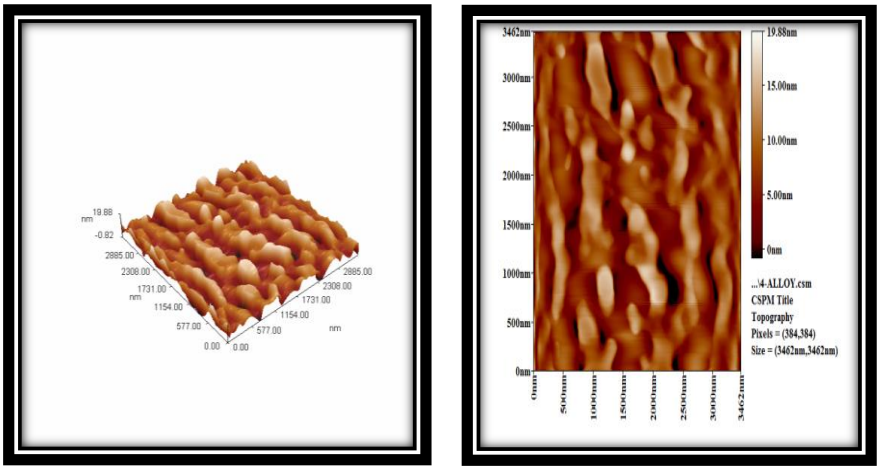


**A** **B**

Figure (4.74) : AFM images of polished aluminum alloy (AA6063-T5) surface.

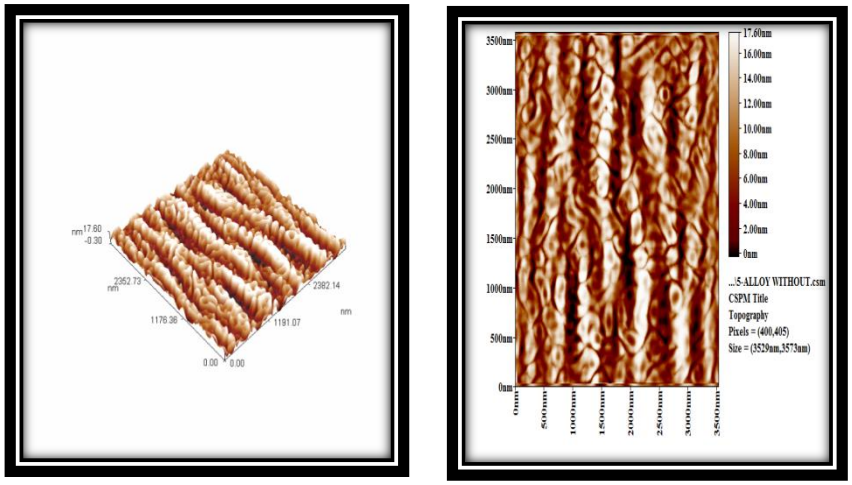


**A** **B**

Figure (4.75 ): AFM images of aluminum alloy (AA6063-T5) surface immersed in (1M $H_3PO_4$).

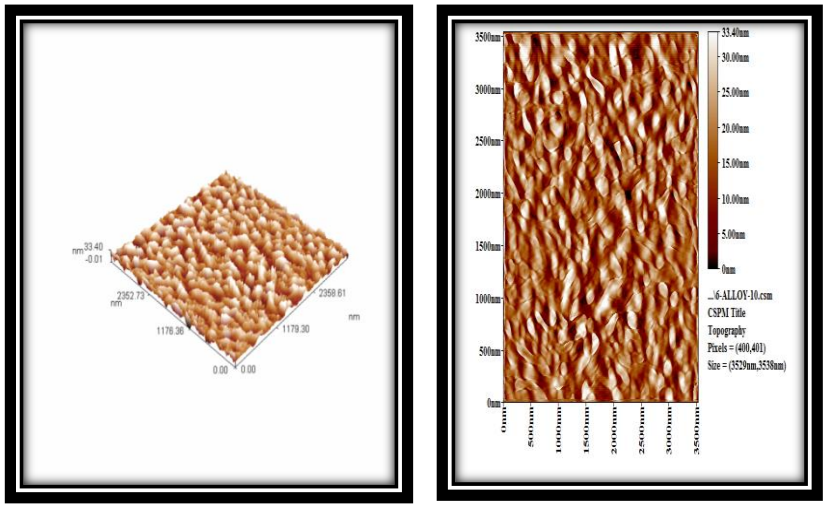


**A** **B**

Figure (4.76) : AFM images of aluminum alloy (AA6063-T5) immersed in ($1MH_3PO_4$) in presence of (10ml) of CML extract.

Table (4.48) AFM data for aluminum alloy (AA6063-T5) surface immersed in inhibited and uninhibited media.

| Sample | Average Roughness (Ra) (nm) | RMS (Rq) Roughness (nm) |
|---|---|---|
| 1-Polished aluminum alloy (AA6063-T5) | 3.02 nm | 3.68 nm |
| 2-Aluminum alloy (AA6063-T5) immersed in 1M $H_3PO_4$ (blank) | 4.47 nm | 5.17 nm |
| 3-Aluminum alloy (AA6063-T5) immersed in 1M $H_3PO_4$ with10ml of (CML) inhibitor | 6.69 nm | 7.99 nm |

Tables (4.49), (4.50) and (4.51) and figures (4.77), (4.78) and (4.79), show the granularity cumulating distribution and average diameter data of the Polished aluminum alloy (AA6063-T5 surface, aluminum alloy (AA6063-T5) surface immersed in (1M $H_3PO_4$), Aluminum alloy (AA6063-T5) immersed in (1M$H_3PO_4$) with presence of (10ml) of CML extract.

The average diameter of polished aluminum alloy (AA6063-T5) surface (179.56) nm ,and the particle size of less than 10 % was ( 0 nm) , less than 50 % was (170) nm and less than 90% was (230) nm and the average diameter of aluminum Alloy (AA6063-T5) surface immersed in (1M $H_3PO_4$) was (147.03) nm ,and the particle size of less than 10 % of the total particles was (110 ) nm, less than 50 % was (140) nm and less than 90% was (190) nm and the average diameter of the aluminum alloy (AA6063-T5) immersed in (1M $H_3PO_4$) in presence (10 ml) of CML extract was (110.12) nm ,and the particle size of less than10 % was ( 0 nm), less than 50 %(100) was nm and less than 90% was (140) nm.

Table (4.49): Granularity cumulating distribution and average diameter of polished aluminum alloy (AA6063-T5) surface.

| Diameter(nm)< | Volume(%) | Cumulation(%) | Diameter(nm)< | Volume(%) | Cumulation(%) | Diameter(nm)< | Volume(%) | Cumulation(%) |
|---|---|---|---|---|---|---|---|---|
| 140.00 | 13.01 | 13.01 | 210.00 | 8.22 | 81.51 | 280.00 | 0.68 | 97.26 |
| 150.00 | 17.81 | 30.82 | 220.00 | 4.79 | 86.30 | 300.00 | 0.68 | 97.95 |
| 160.00 | 8.90 | 39.73 | 230.00 | 1.37 | 87.67 | 310.00 | 0.68 | 98.63 |
| 170.00 | 9.59 | 49.32 | 240.00 | 4.79 | 92.47 | 320.00 | 0.68 | 99.32 |
| 180.00 | 8.90 | 58.22 | 250.00 | 1.37 | 93.84 | 340.00 | 0.68 | 100.00 |
| 190.00 | 5.48 | 63.70 | 260.00 | 2.05 | 95.89 | | | |
| 200.00 | 9.59 | 73.29 | 270.00 | 0.68 | 96.58 | | | |

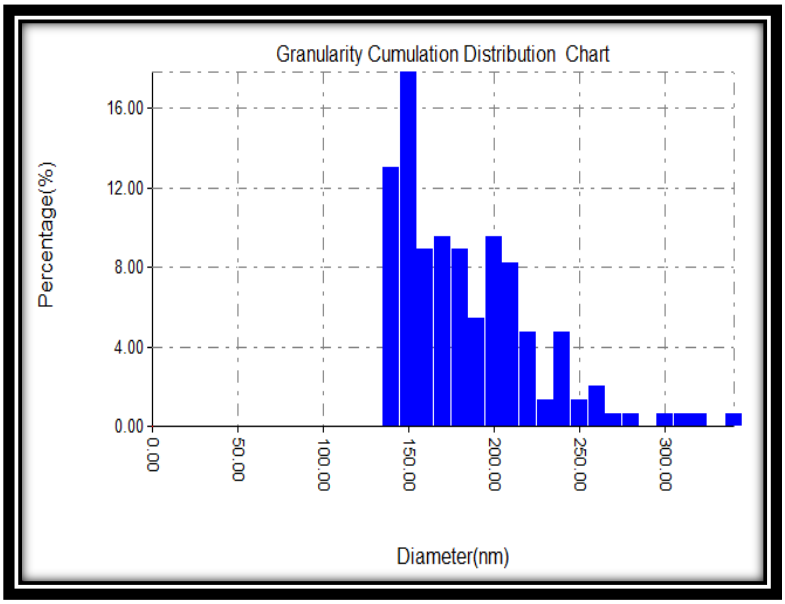


Figure (4.77): Granularity cumulating distribution and average diameter of polished aluminum alloy (AA6063-T5) surface.

Table (4.50): Granularity cumulating distribution and average diameter of aluminum alloy (AA6063-T5) surface immersed in (1M $H_3PO_4$).

| Diameter(nm)< | Volume(%) | Cumulation(%) | Diameter(nm)< | Volume(%) | Cumulation(%) | Diameter(nm)< | Volume(%) | Cumulation(%) |
|---|---|---|---|---|---|---|---|---|
| 110.00 | 9.41 | 9.41 | 170.00 | 9.02 | 79.61 | 230.00 | 1.57 | 98.04 |
| 120.00 | 16.08 | 25.49 | 180.00 | 4.31 | 83.92 | 250.00 | 1.18 | 99.22 |
| 130.00 | 11.76 | 37.25 | 190.00 | 5.49 | 89.41 | 320.00 | 0.39 | 99.61 |
| 140.00 | 11.76 | 49.02 | 200.00 | 2.35 | 91.76 | 340.00 | 0.39 | 100.00 |
| 150.00 | 11.76 | 60.78 | 210.00 | 2.35 | 94.12 | | | |
| 160.00 | 9.80 | 70.59 | 220.00 | 2.35 | 96.47 | | | |

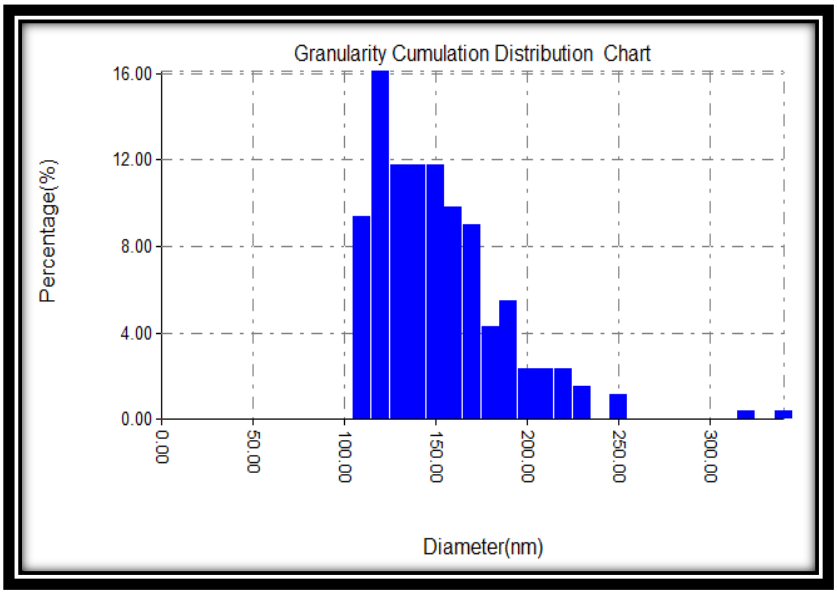


Figure (4.78): Granularity cumulating distribution and average diameter of aluminum alloy (AA6063-T5) surface immersed in (1M $H_3PO_4$).

Table (4.51): Granularity cumulating distribution and average diameter of aluminum alloy (AA6063-T5) immersed in (1M$H_3PO_4$) in presence of (10ml) of CML extract.

| Diameter(nm)< | Volume(%) | Cumulation(%) | Diameter(nm)< | Volume(%) | Cumulation(%) | Diameter(nm)< | Volume(%) | Cumulation(%) |
|---|---|---|---|---|---|---|---|---|
| 90.00 | 19.31 | 19.31 | 130.00 | 7.79 | 81.00 | 170.00 | 2.18 | 98.44 |
| 100.00 | 25.55 | 44.86 | 140.00 | 4.98 | 85.98 | 180.00 | 0.31 | 98.75 |
| 110.00 | 17.45 | 62.31 | 150.00 | 5.30 | 91.28 | 210.00 | 0.93 | 99.69 |
| 120.00 | 10.90 | 73.21 | 160.00 | 4.98 | 96.26 | 230.00 | 0.31 | 100.00 |

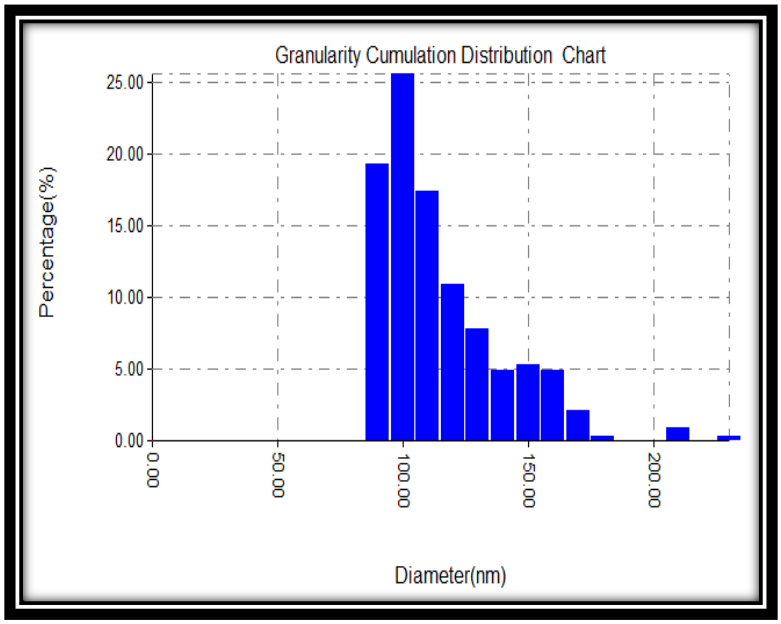


Figure (4.79): Granularity cumulating distribution and average diameter of aluminum alloy (AA6063-T5) immersed in ($1MH_3PO_4$) in presence of (10ml) of CML extract.

In figure (4.80),(4.81) and (4.82) are the AFM image for aluminum surface immersed in( $1MH_3PO_4$ at pH of 4) ,aluminum surface immersed in ($1MH_3PO_4$ at pH of 4) in presence of 2.5wt% 0f ($Fe_2O_3$) as corrosion inhibitor. Aluminum surface immersed in ($1MH_3PO_4$ at PH of 4) in presence of 2.5wt% of ($TiO_2$) as corrosion inhibitor as well.

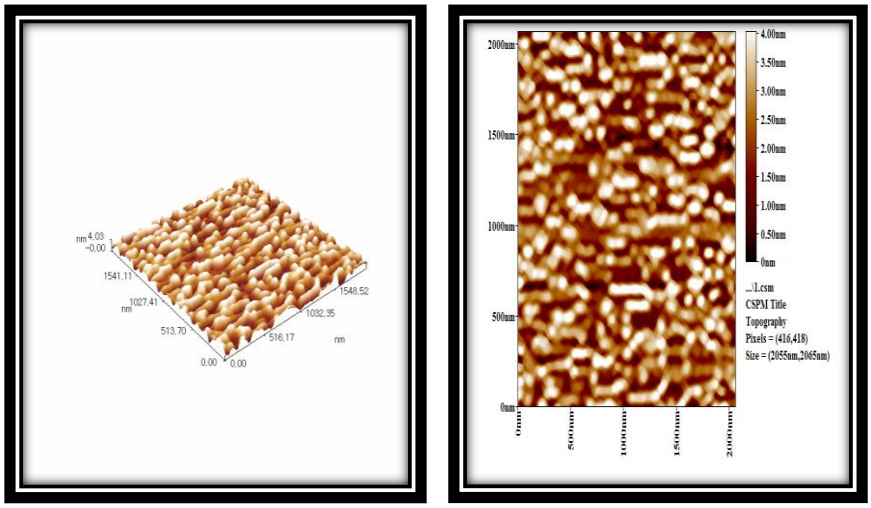


**A** **B**

Figure (4.80 ): AFM images of aluminum surface immersed in (1M $H_3PO_4$ at pH of 4).

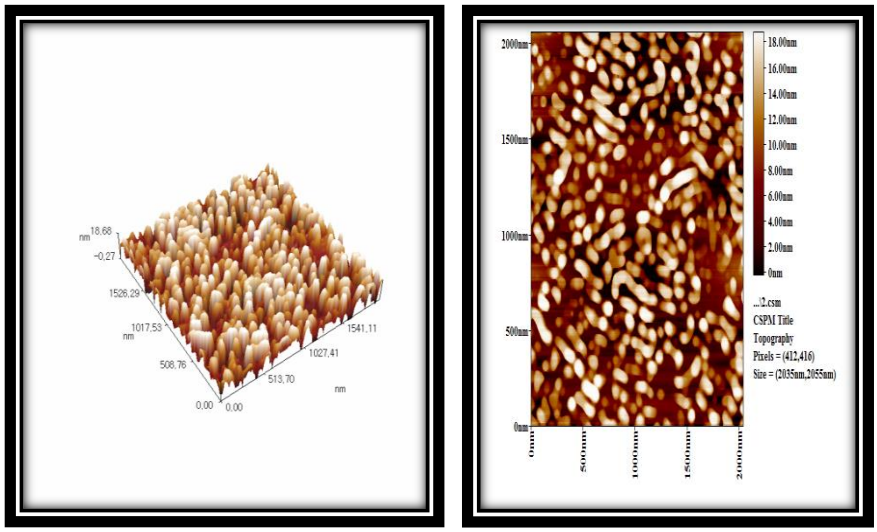


**A** **B**

Figure (4.81): AFM images of aluminum surface immersed in (1M $H_3PO_4$ at pH of 4) in presence of (2.5wt%$Fe_2O_3$) as nanomaterial inhibitor.

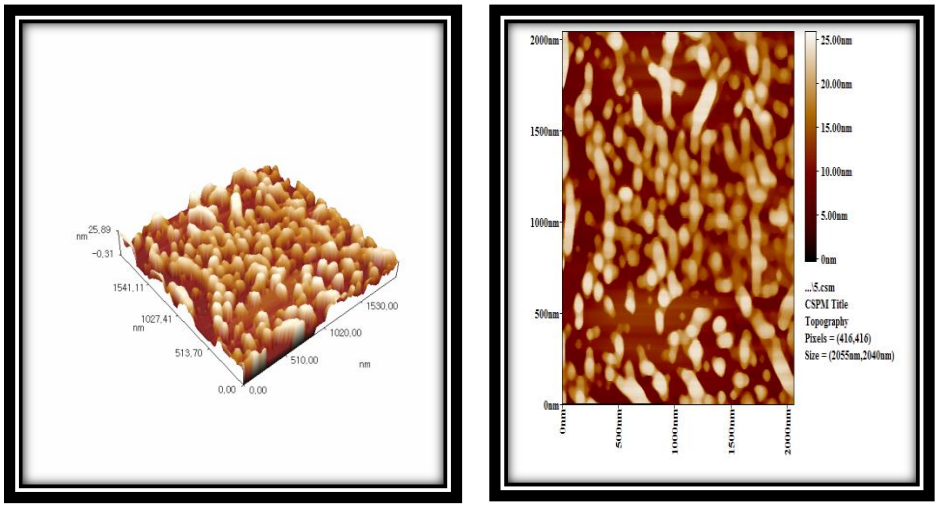


**A** **B**

Figure (4.82): AFM images of aluminum surface immersed in (1M $H_3PO_4$ at pH of 4) in presence of (2.5wt%$TiO_2$) as nanomaterial inhibitor.

Table (4.52): show AFM data for aluminum surface corrosion using immersed in (1M$H_3PO_4$ at pH of 4) in presence of (2.5 wt%$Fe_2O_3$ and $TiO_2$) the nanomaterials inhibitors.

| Sample | Average Roughness (Ra) (nm) | RMS (Rq) Roughness (nm) |
|---|---|---|
| 1- aluminum (blank) immersed in (1M$H_3PO_4$ at pH of 4) | 0.773 nm | 0.924 nm |
| 2- aluminum immersed (1M$H_3PO_4$ at pH of 4) presence (2.5wt%$Fe_2O_3$) | 4.74 nm | 5.47 nm |
| 3- aluminum immersed (1M$H_3PO_4$ at pH of 4) presence (2.5wt%$TiO_2$) | 4.51 nm | 5.17 nm |

Tables (4.53), (4.54) and (4.55), and figures (4.83), (4.84) and (4.85), show the granularity cumulating distribution and average diameter data of the aluminum surface immersed in (1M$H_3PO_4$ at pH of 4), aluminum surface immersed in (1M$H_3PO_4$ at pH of 4) in presence (2.5wt%$Fe_2O_3$), aluminum surface immersed in (1M$H_3PO_4$ at pH of 4) in presence (2.5wt%$TiO_2$) .

The average diameter of aluminum surface immersed in (1M$H_3PO_4$ at pH of 4) (88.71) nm ,and the particle size of less than 10 % of the total particles was (60) nm, less than 50 % was (90) nm and less than 90% was (110) nm and the average diameter of aluminum surface immersed in (1M$H_3PO_4$ at pH of 4) was (67.54) nm ,and the particle size of less than 10 % of the total particles was (40) nm, less than 50 % was (65nm) and less than 90% was (95) nm and the average diameter of the surface immersed in (1M$H_3PO_4$ at pH of 4) with (2.5wt%$TiO_2$) was (97.28) nm and the particle size of 10 % was less than (0 nm), less than 50 % was ( 90) nm and less than 90% was ( 130) nm.

Table (4.53): Granularity cumulating distribution and average diameter of aluminum surface immersed in (1M$H_3PO_4$ at pH of 4).

| Diameter(nm)< | Volume(%) | Cumulation(%) | Diameter(nm)< | Volume(%) | Cumulation(%) | Diameter(nm)< | Volume(%) | Cumulation(%) |
|---|---|---|---|---|---|---|---|---|
| 40.00 | 0.46 | 0.46 | 75.00 | 6.91 | 25.35 | 110.00 | 9.22 | 87.10 |
| 45.00 | 0.46 | 0.92 | 80.00 | 8.76 | 34.10 | 115.00 | 4.15 | 91.24 |
| 50.00 | 2.30 | 3.23 | 85.00 | 6.91 | 41.01 | 120.00 | 4.61 | 95.85 |
| 55.00 | 1.38 | 4.61 | 90.00 | 7.83 | 48.85 | 125.00 | 3.23 | 99.08 |
| 60.00 | 5.07 | 9.68 | 95.00 | 6.91 | 55.76 | 130.00 | 0.92 | 100.00 |
| 65.00 | 2.76 | 12.44 | 100.00 | 11.98 | 67.74 | | | |
| 70.00 | 5.99 | 18.43 | 105.00 | 10.14 | 77.88 | | | |

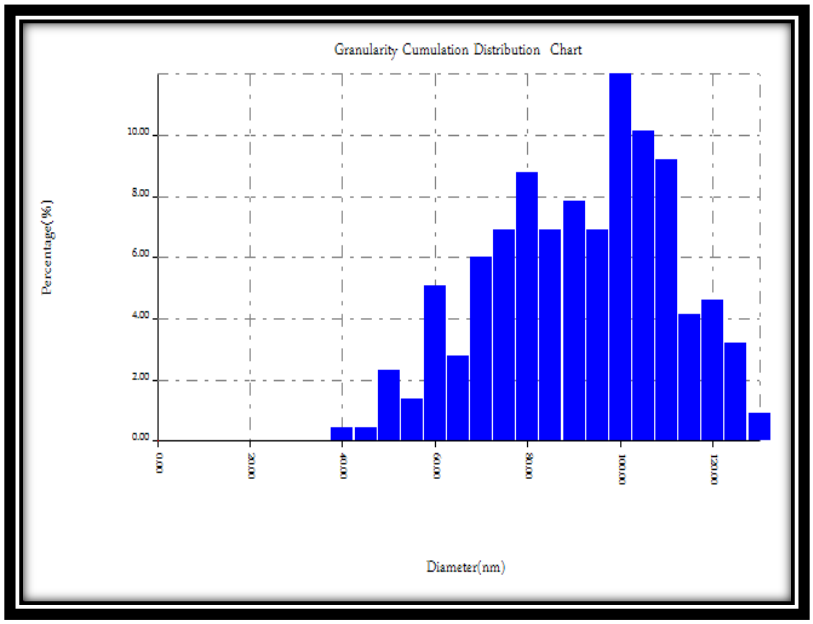


Figure (4.83): Granularity cumulating distribution and average diameter of aluminum surface immersed in (1M $H_3PO_4$ at pH of 4).

Table (4.54): Granularity cumulating distribution and average diameter of aluminum surface immersed in (1M $H_3PO_4$ at pH of 4) in presence of (2.5wt%$Fe_2O_3$) .

| Diameter(nm)< | Volume(%) | Cumulation(%) | Diameter(nm)< | Volume(%) | Cumulation(%) | Diameter(nm)< | Volume(%) | Cumulation(%) |
|---|---|---|---|---|---|---|---|---|
| 40.00 | 7.61 | 7.61 | 75.00 | 9.97 | 68.24 | 110.00 | 1.05 | 97.11 |
| 45.00 | 4.99 | 12.60 | 80.00 | 4.99 | 73.23 | 115.00 | 1.57 | 98.69 |
| 50.00 | 7.61 | 20.21 | 85.00 | 6.56 | 79.79 | 120.00 | 0.52 | 99.21 |
| 55.00 | 11.29 | 31.50 | 90.00 | 4.46 | 84.25 | 125.00 | 0.52 | 99.74 |
| 60.00 | 8.14 | 39.63 | 95.00 | 4.99 | 89.24 | 140.00 | 0.26 | 100.00 |
| 65.00 | 9.97 | 49.61 | 100.00 | 3.41 | 92.65 | | | |
| 70.00 | 8.66 | 58.27 | 105.00 | 3.41 | 96.06 | | | |

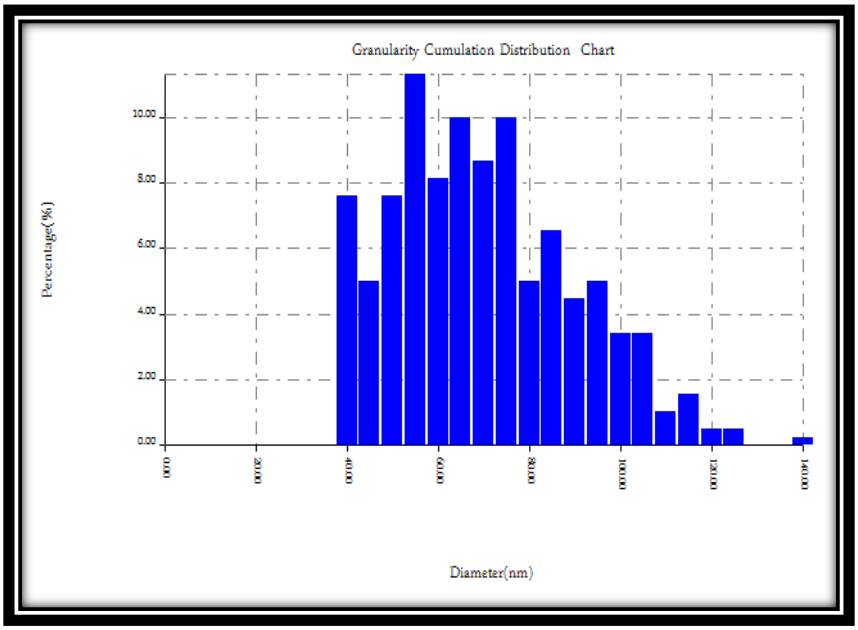


Figure (4.84): Granularity cumulating distribution and average diameter of aluminum surface immersed in ($1MH_3PO_4$ at pH of 4) in presence of ($2.5wt\%Fe_2O_3$) .

Table (4.55): Granularity cumulating distribution and average diameter of aluminum surface immersed in ($1MH_3PO_4$ at pH of 4) in presence of ($2.5wt\%TiO_2$).

| Diameter(nm)< | Volume(%) | Cumulation(%) | Diameter(nm)< | Volume(%) | Cumulation(%) | Diameter(nm)< | Volume(%) | Cumulation(%) |
|---|---|---|---|---|---|---|---|---|
| 70.00 | 10.24 | 10.24 | 110.00 | 14.15 | 74.63 | 150.00 | 1.95 | 95.61 |
| 80.00 | 19.02 | 29.27 | 120.00 | 7.80 | 82.44 | 160.00 | 2.44 | 98.05 |
| 90.00 | 14.63 | 43.90 | 130.00 | 7.32 | 89.76 | 170.00 | 0.98 | 99.02 |
| 100.00 | 16.59 | 60.49 | 140.00 | 3.90 | 93.66 | 180.00 | 0.98 | 100.00 |

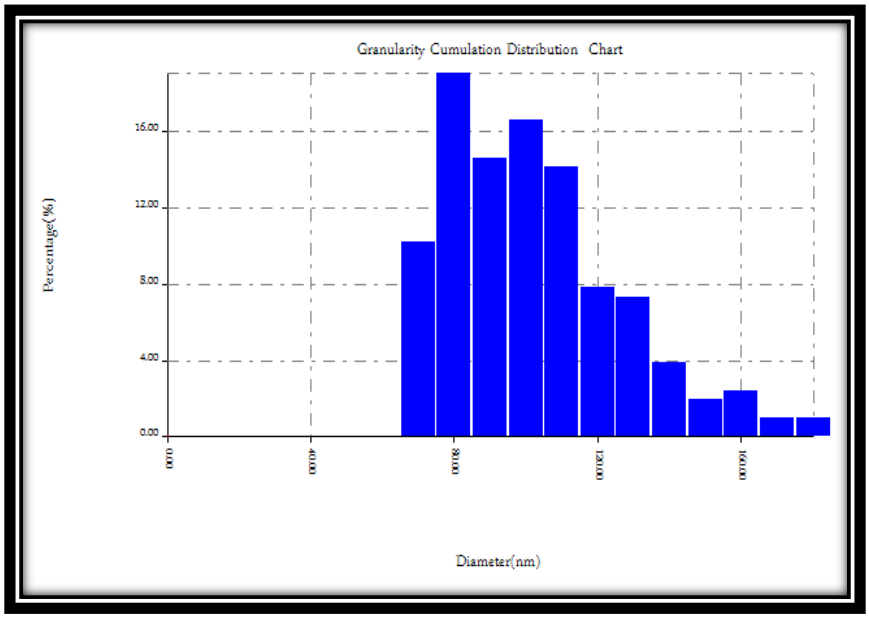


Figure (4.85): Granularity cumulating distribution and average diameter of aluminum surface immersed in ($1MH_3PO_4$ at pH of 4) in presence of ($2.5wt\%TiO_2$).

In figure (4.86),(4.87 ) and (4.88) , the AFM image for aluminum alloy (AA6063-T5) surface immersed in( $1MH_3PO_4$ at pH of 4) ,aluminum alloy (AA6063-T5) surface immersed in ($1MH_3PO_4$ at pH of 4) in presence of 2.5wt% 0f ($Fe_2O_3$) as corrosion inhibitor. aluminum alloy (AA6063-T5) surface immersed in ($1MH_3PO_4$ at pH of 4) in presence of 2.5wt% 0f ($TiO_2$) as corrosion inhibitor as well.

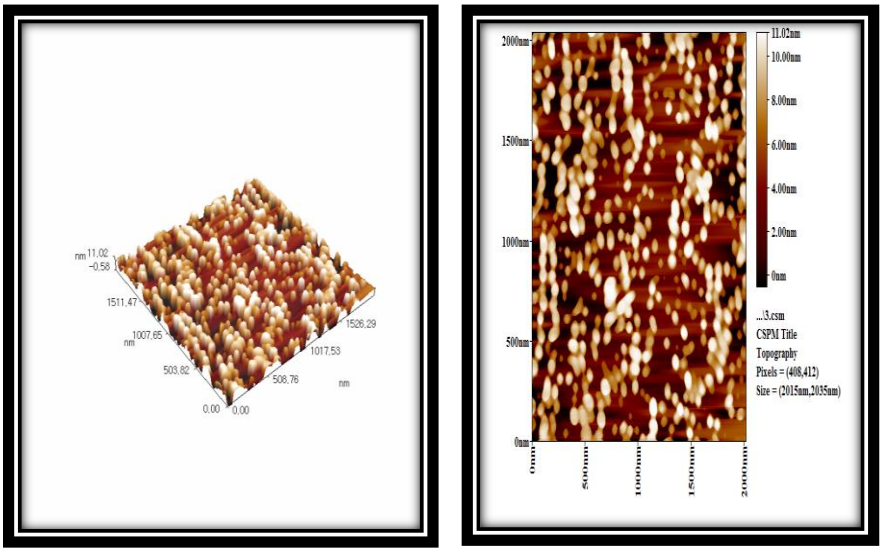


**A** **B**

Figure (4.86): AFM images of aluminum alloy (AA6063-T5) surface immersed in (1M$H_3PO_4$ at pH of 4).

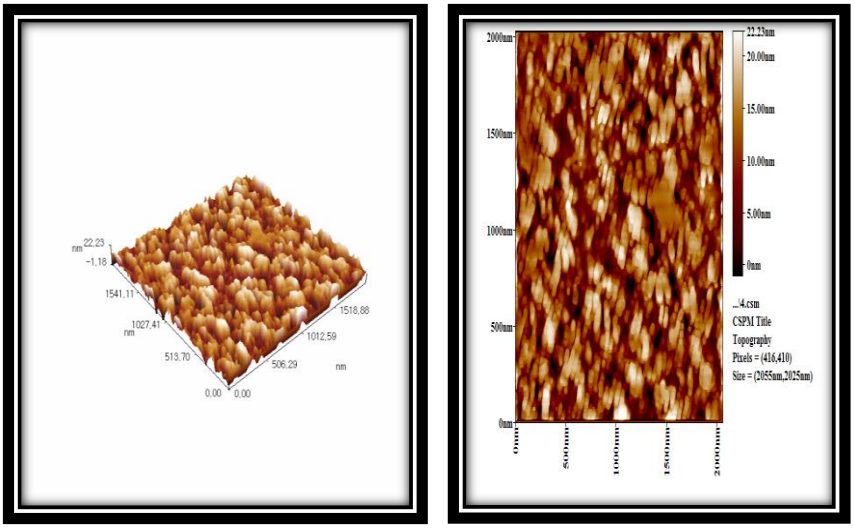


**A** **B**

Figure (4.87): AFM images of aluminum alloy (AA6063-T5) surface immersed in (1M $H_3PO_4$ at pH of 4) in presence of (2.5wt%$Fe_2O_3$) as nanomaterial inhibitor.

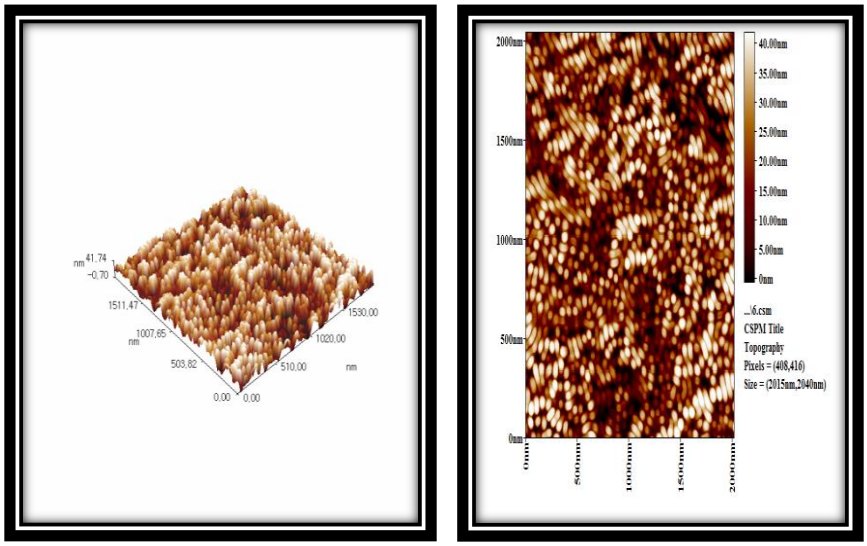


**A** **B**

Figure (4.88): AFM images of aluminum alloy (AA6063-T5) surface immersed in ($1MH_3PO_4$ at pH of 4) in presence of ($2.5wt\%TiO_2$) as nanomaterial inhibitor.

Table (4.56):show AFM data for aluminum alloy (AA6063-T5) Surface corrosion using immersed in ($1MH_3PO_4$ at pH of 4) and in Presence of ($2.5wt\%Fe_2O_3$ and $TiO_2$) the nanomaterials inhibitors.

| Sample | Average Roughness (Ra) (nm) | RMS (Rq) Roughness (nm) |
|---|---|---|
| 1- aluminum alloy (blank) immersed in ($1MH_3PO_4$ at pH of 4) | 2.9 nm | 3.35 nm |
| 2- aluminum immersed ($1MH_3PO_4$ at pH of 4) presence ($2.5wt\%Fe_2O_3$) | 4.31 nm | 5.22 nm |
| 3- aluminum immersed ($1MH_3PO_4$ at pH of 4) presence ($2.5wt\%TiO_2$) | 10.4 nm | 12 nm |

Tables (4.57), (4.58) and (4.59), and figures (4.89), (4.90) and (4.91), show the granularity cumulating distribution and average diameter data of the aluminum alloy (AA6063-T5) surface immersed in ($1MH_3PO_4$ at pH of 4), aluminum alloy (AA6063-T5) surface immersed in ($1MH_3PO_4$ at pH of 4) in Presence ($2.5wt\%Fe_2O_3$), aluminum alloy (AA6063-T5) surface immersed in ($1MH_3PO_4$ at pH of 4) in presence ($2.5wt\%TiO_2$) . The average diameter of aluminum alloy (AA6063-T5) surface immersed in ($1MH_3PO_4$ at pH of 4) (66.73) nm and the particle size of less than 10 % of the total particles was (40) nm, less than 50 % was (65) nm and less than 90% was (85) nm and the average diameter of aluminum alloy (AA6063-T5) surface immersed in ($1MH_3PO_4$ at pH of 4) was (83.18) nm and the particle size of less than 10 % was (0 nm) and less than 50 % was ( 75) nm and less than 90% was (100) nm and the average diameter of the aluminum alloy (AA6063-T5) surface immersed in ($1MH_3PO_4$ at pH of 4) in the presence ($2.5wt\%TiO_2$) was (63.15) nm and the particle size of less than 10 % of the total particles was (50) nm, less than 50 % was (60) nm and less than 90% was (70) nm.

Table (4.57): Granularity cumulating distribution and average diameter of aluminum alloy (AA6063-T5) surface immersed in ($1MH_3PO_4$ at pH of 4).

| Diameter(nm)< | Volume(%) | Cumulation(%) | Diameter(nm)< | Volume(%) | Cumulation(%) | Diameter(nm)< | Volume(%) | Cumulation(%) |
|---|---|---|---|---|---|---|---|---|
| 35.00 | 0.58 | 0.58 | 60.00 | 9.28 | 33.62 | 85.00 | 7.83 | 86.09 |
| 40.00 | 4.64 | 5.22 | 65.00 | 10.14 | 43.77 | 90.00 | 9.28 | 95.36 |
| 45.00 | 6.09 | 11.30 | 70.00 | 9.57 | 53.33 | 95.00 | 4.64 | 100.00 |
| 50.00 | 6.38 | 17.68 | 75.00 | 12.75 | 66.09 | | | |
| 55.00 | 6.67 | 24.35 | 80.00 | 12.17 | 78.26 | | | |

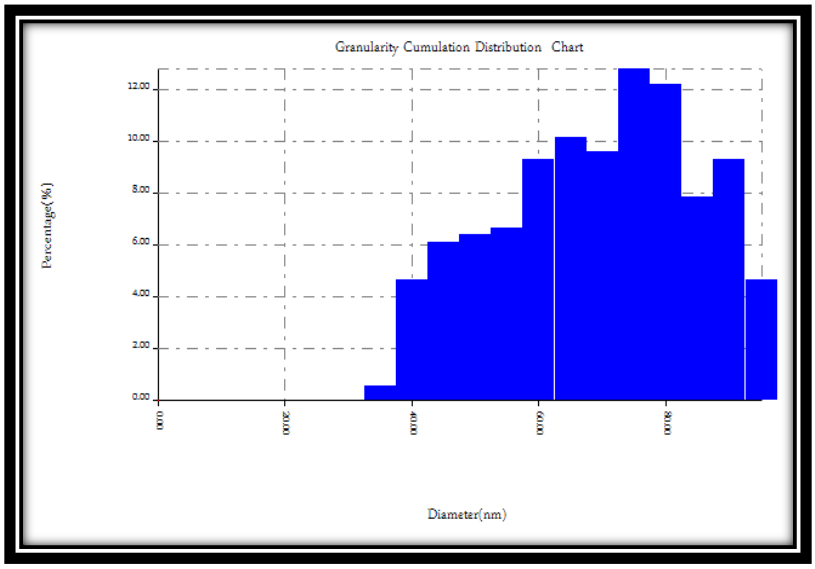


Figure (4.89): Granularity cumulating distribution and average diameter of aluminum alloy (AA6063-T5) surface immersed in ($1MH_3PO_4$ at pH of 4).

Table (4.58): Granularity cumulating distribution and average diameter of aluminum alloy (AA6063-T5) surface immersed in ($1MH_3PO_4$ at pH of 4) in presence of ($2.5wt\%Fe_2O_3$).

| Diameter(nm)< | Volume(%) | Cumulation(%) | Diameter(nm)< | Volume(%) | Cumulation(%) | Diameter(nm)< | Volume(%) | Cumulation(%) |
|---|---|---|---|---|---|---|---|---|
| 70.00 | 16.98 | 16.98 | 90.00 | 8.18 | 72.96 | 110.00 | 3.14 | 93.71 |
| 75.00 | 20.13 | 37.11 | 95.00 | 10.69 | 83.65 | 115.00 | 3.14 | 96.86 |
| 80.00 | 16.98 | 54.09 | 100.00 | 3.14 | 86.79 | 125.00 | 1.89 | 98.74 |
| 85.00 | 10.69 | 64.78 | 105.00 | 3.77 | 90.57 | 145.00 | 1.26 | 100.00 |

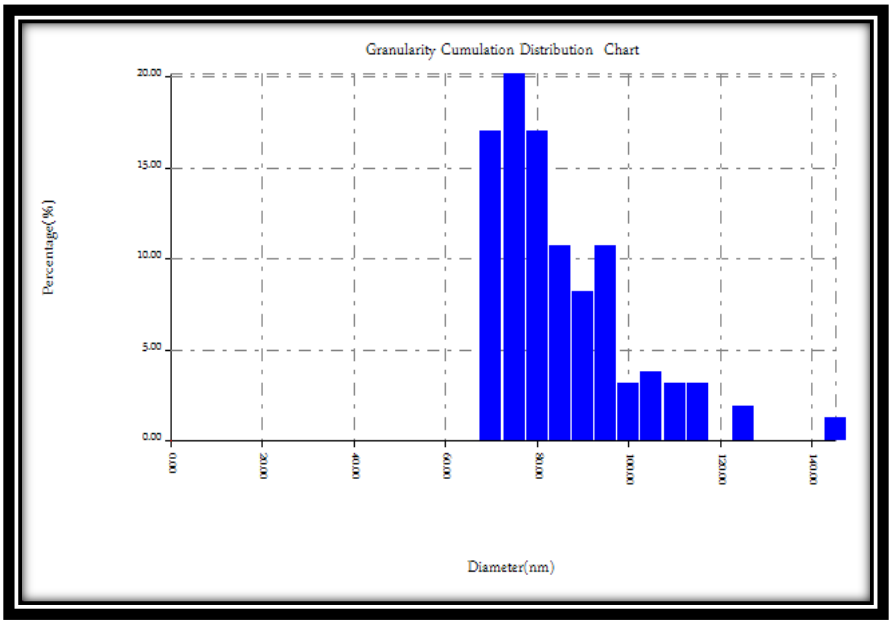


Figure (4.90): Granularity cumulating distribution and average diameter of aluminum alloy (AA6063-T5) surface immersed in (1M$H_3PO_4$ at pH of 4) in presence of (2.5wt%$Fe_2O_3$).

Table (4.59): Granularity cumulating distribution and average diameter of aluminum alloy (AA6063-T5) surface immersed in (1M$H_3PO_4$ at pH of 4) in presence of (2.5wt%$TiO_2$).

| Diameter(nm)< | Volume(%) | Cumulation(%) | Diameter(nm)< | Volume(%) | Cumulation(%) | Diameter(nm)< | Volume(%) | Cumulation(%) |
|---|---|---|---|---|---|---|---|---|
| 50.00 | 3.69 | 3.69 | 70.00 | 14.29 | 77.59 | 90.00 | 0.99 | 98.03 |
| 55.00 | 19.46 | 23.15 | 75.00 | 12.81 | 90.39 | 95.00 | 0.99 | 99.01 |
| 60.00 | 16.01 | 39.16 | 80.00 | 4.19 | 94.58 | 100.00 | 0.74 | 99.75 |
| 65.00 | 24.14 | 63.30 | 85.00 | 2.46 | 97.04 | 105.00 | 0.25 | 100.00 |

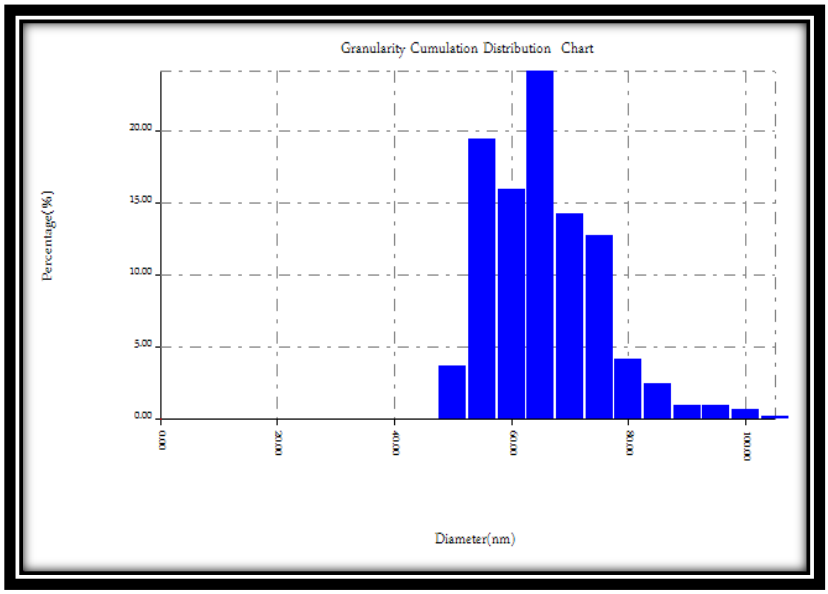


Figure (4.91): Granularity cumulating distribution and average diameter of aluminum alloy (AA6063-T5) surface immersed in ($1M H_3PO_4$ at pH of 4) in presence of ($2.5wt\% TiO_2$).

## 4.8. Scanning electron microscope (SEM)

Scanning electron microscope (SEM) was used to study the morphology of aluminum and aluminum alloy ($AA6063-T5$). The aluminum and aluminum alloy ($AA6063-T5$) surface and The aluminum and aluminum alloy ($AA6063-T5$) surface in presence of ($Fe_2O_3\ TiO_2$) immersed in ($1M H_3PO_4$ at PH of 4) the nanomaterials inhibitors for a period of (3 h) at (333K) were taken out. The SEM micrographs of the studied surfaces are shown in figures (4.92 A, B, and C ) and (4.93 A, B, and C ) for aluminum and aluminum alloy ($AA6063-T3$) coupons respectively. The (SEM) micrograph of the aluminum and aluminum alloy (AA6063-T5) surface given in figure (4.92A) and (4. 93A) as we notice a slight difference in the surface morphology, with some deformations as a result exposure to a corrosion medium. This indicates the process of reducing the corrosion rates due to the presence of the coating which result of isolating the metal surface from the corrosive medium, meaning that the coating acts as a protective layer that prevents access ions of the corrosion medium to the metal surface. On addition of the inhibitors there was an improvement in the metal surface as shown in figures (4.92B), (4.93B) , (4.92C )and (4.93 C) for

aluminum and aluminum alloy (AA6063 – T5) coupons respectively. We noticed a slight difference in surface morphology with some deformations due to exposure to it corrosion medium, which is indicative the corrosion rates are significantly reduced as a result of isolating the metal surface from the corrosion medium by the nano structured coating acts as a protective layer that prevents corrosion ions from reaching the metal surface.

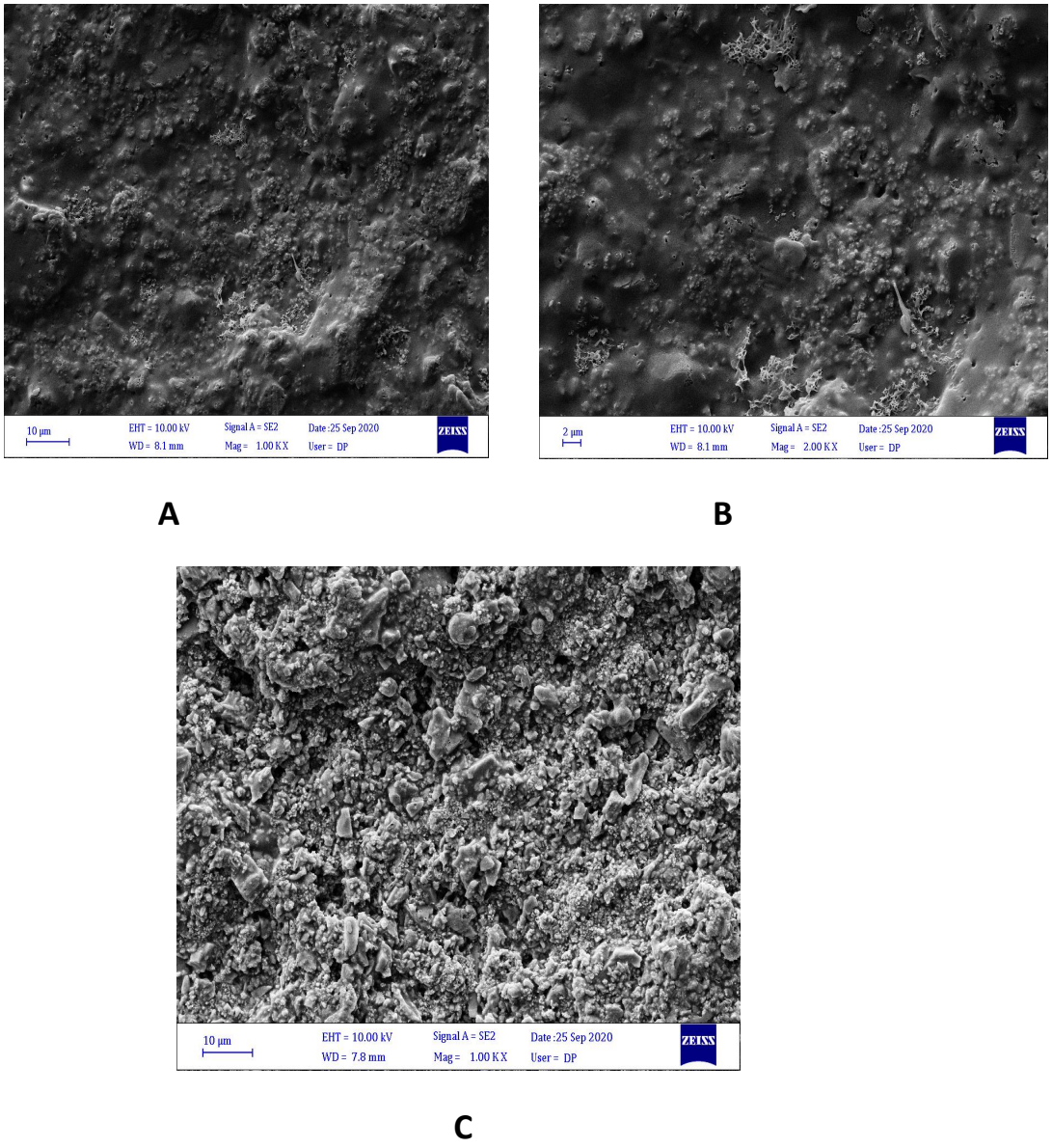


Figure (4.92): SEM images of aluminum surface corroded at (333 K) for (3 h): (A) aluminum surface only immersed in ($1MH_3PO_4$ at pH of 4).(B) aluminum surface immersed in ($1MH_3PO_4$ at pH of 4) in presence of ($Fe_2O_3$).(C) aluminum surface immersed in ($1MH_3PO_4$ at pH of 4) in presence of ($TiO_2$).

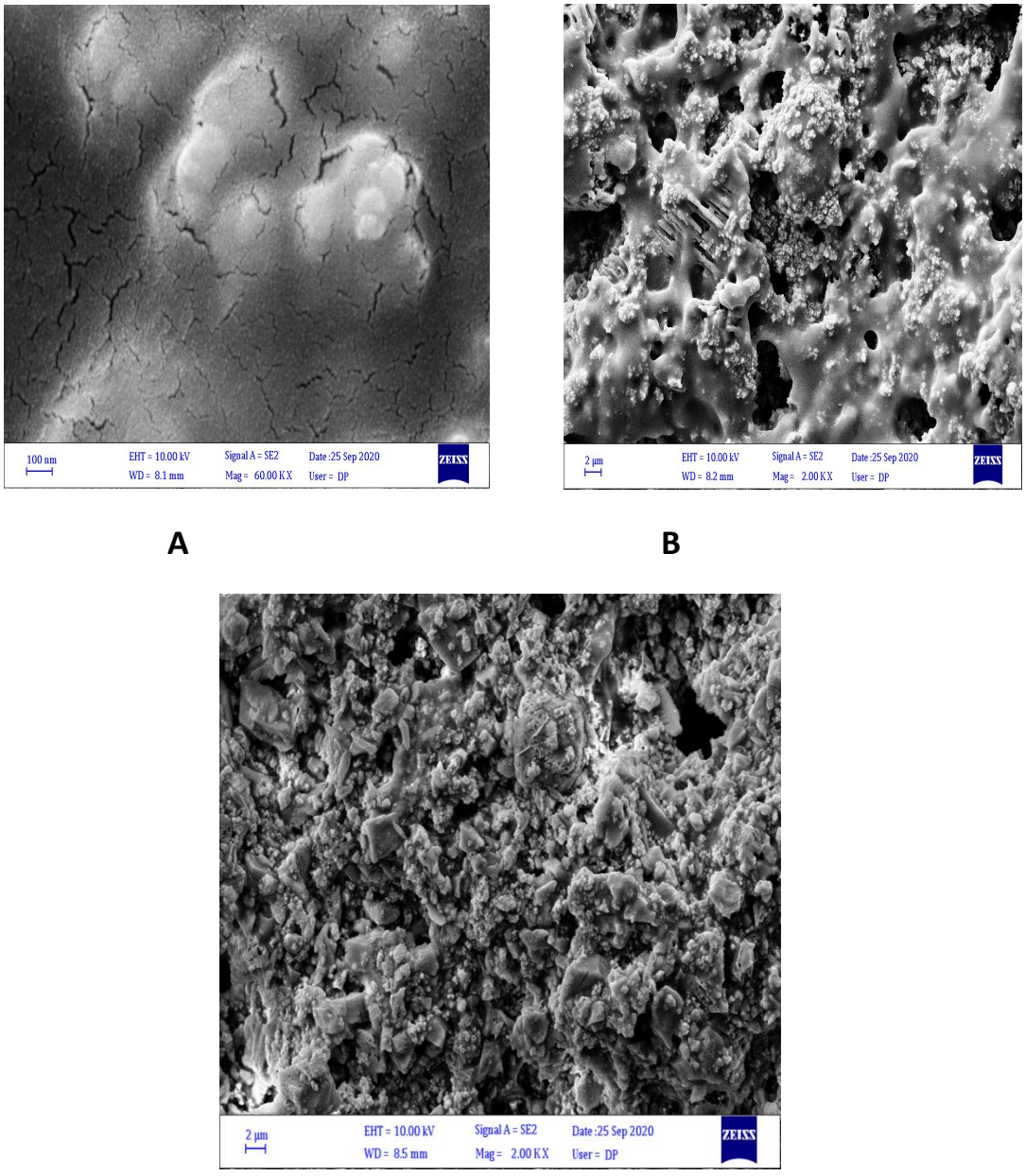


Figure (4.93): SEM images of aluminum alloy (AA6063-T5) surface corroded at (333 K) for (3 h): (A) aluminum alloy (AA6063-T5) surface only immersed in ($1MH_3PO_4$ at pH of 4).(B) aluminum alloy (AA6063-T5) surface immersed in ($1MH_3PO_4$ at pH of 4) in presence of ($Fe_2O_3$).(C) aluminum alloy (AA6063-T5) surface immersed in ($1MH_3PO_4$ at pH of 4) in Presence of ($TiO_2$).

## 4.9. Conclusions

A number of conclusions have been drawn via the current analysis, the most important of which are

1. The extract of Cordia myxa leaves has been shown to be an effective 1 M ($H_3PO_4$) solution inhibitor for aluminum and aluminum alloy (AA6063-T5) corrosion (90.95 %) and (87.60 %) with inhibitor concentration of (10 mg / L) is the highest inhibition efficiency.
2. Standard coating was increased by adding titanium and iron oxides to nanoparticles to increase the coating efficiency..
3. The adsorption on aluminum and aluminum alloy (AA6063-T5) of inhibitor molecules and nanomaterials on the surface was due to physical adsorption.
4. Testing adsorption isotherms as a way of learning the adsorption model agreed with Langmuir isotherm adsorption
5. The negative value of free energy adsorption indicated that the adsorption on the metal surface of (CML) and ($Fe_2O_3$ and $TiO_2$) was a spontaneous in nature.
6. A thermodynamic data of the coefficients (activation enthalpy, activation entropy) were in good agreement with the literature .
7. In the presence of the leaves extract and nanomaterial, , the activation energy was reduced.
8. Analysis of FTIR shows that (CML) plant extract contains compound mixtures, and mainly i.e. (Linalool, $C_{10}H_{18}O$).

**9.** X-ray confirms the corrosion of aluminum and aluminum alloy (AA6063-T5) in ($1MH_3PO_4$ at pH of 4) is also inhibited by nanomaterials ($Fe_2O_3$and$TiO_2$).

**10.** AFM confirms that the corrosion of aluminum and aluminum alloy (AA6063-T5) in (1M $H_3PO_4$) and ($1MH_3PO_4$at pH of 4) inhibited by Cordia myxa leaves extract and nanomaterial ($Fe_2O_3$and$TiO_2$).

**11.** SEM confirms the corrosion of aluminum and aluminum alloy (AA6063-T5) in ($1MH_3PO_4$ at pH of 4) also inhibited by nanomaterials ($Fe_2O_3$and$TiO_2$).

## 4.10.Suggestion for further research

Study on aluminum and aluminum alloys, which can be summarized as: (Several suggestions can be forwarded for further work:

1. Other acids such as ($H_2SO_4$) and (HCL) in the absence and the presence of (CML) and ($Fe_2O_3$and $TiO_2$) can also be applied to the corrosion medium.
2. Similar work can be repeated for other metals such as (Fe ,Cu) and alloys such as aluminum alloy (AA5054 – T3) and aluminum alloy (AA6061-T6).
3. Other types of coating can also be used .
4. Adopting other types of nanomaterials can be added to coating.

# *References*

## References


**[1] Dariva, C.G; Galio, A.F.( 2014).** Corrosion inhibitors–principles, mechanisms and applications. In Development sin Corrosion Protection; Aliofkhazraei, M., Ed.; INTECH: Winchester, UK; pp. 365–379.

**[2] Sathishkumar ,P., Kumaravelan, V. and Priya, D. D. (2015).** Comparative study of mild steel corrosion using hydrochloric acid and phosphoric acid medium with osmium tenuiflorum (l) plant extract. International Journal of Advanced Research, 3(4): 643-651.

**[3] Wazarkar, K. Patil, D. Rane, A. Balgude, D. Kathalewar, M. Sabnis. (2016).** Microencapsulation: An emerging technique in the modern coating industry. RSC Adv. 6, 106964–106979.

**[4] Ahmed , Z.W. (2015).** Corrosion of aluminum and some of Its alloys and inhibition in acidic and basic media by environmentally friendly inhibitors at different temperatures. $PhD$. Thesis, College of Education for Pure Sciences Ibn Al-Haitham , University of Baghdad.

**[5] L. Popoola, A. Grema, G. Latinwo, B. Gutti, A. Balogun.(2013).** Corrosion problems during oil and gas production and its mitigation, Int. J. Ind. Chem. 4 (1) 35.

**[6] Bataineh , T.T., Al-Qudah , M.A., Nawafleh , E. and Ajlouni , A.M. (2013).** Corrosion control of aluminum alloy in alkaline solution using leave extract of Plumb ago european. 8 (3), pp. 169-178.

**[7] Yaro ,A.S., Khadom, A.A. and Wael, R.K. (2013).** Apricot juice as green corrosion inhibitor of mild steel in phosphoric acid. Alexandria Engineering Journal, 52:129-135.

**[8] Al-Ajaj, I A., Abd M M., and Jaffer, H. I. (2013).** Mechanical Properties of Micro and Nano TiO2/Epoxy Composites, International Journal of Mining, Metallurgy & Mechanical Engineering (IJMMME) , 1 (2) . pp. 93-97.

**[9] Panaite, V. and Mușat, V. (2014).** Effect of ZnO Nanoparticles on The Anticorrosion Properties Of Epoxy Coating, Metallurgy and Materials Science , 2, pp. 24-28.

**[10] Kumar, S S.(2015).** Applications of Nano Pigment Particles for the Development in Corrosion and Scratch Resistance of Epoxy-Zeolite Coatings, International Journal of Engineering and Applied Sciences 2(11). pp. 103-109.

**[11] Vasudha, K.S. and Therese, V. G. (2015).** Thermodynamic and adsorption studies for corrosion inhibition of mild steel using Millingtonia Hortensis. International Journal of Information Research and Review, 2(1): 261-266.

**[12] Noor ,E.A., Aisha, Al-M., Aqlah, H. Al-Z. and Hubani, M.H. (2016).** Testing and the inhibitory action of red Onion seeds and peels extracts on the corrosion of steel in phosphoric acid. International Journal of Electrochemical Science, 11:6523 - 6539.

**[13] Khorram, M. , Shishesaz, M. , Danaee, I. and Zaarel, D. (2016).** Synthesis and corrosion protection behavior of epoxy – TiO2-Micaceous iron oxide Nano composite coating St-37, Iranian Journal of Material Science and Engineering, 13(1). pp. 11-20.

**[14] Kwolek,P.,Dychton,K.,Szydełko,J.,Gradzik,A.,Drajewicz,M.,Sieniawski,J.(2016).** The Influence of Sodium Moly date on the Rate of Corrosion of Aluminum in Phosphoric (V) Acid. In Materials Science Forum (Vol. 844, pp. 31-37).

**[15] Ajeel ,S.A.(2017).** Green Corrosion Inhibitor for Protection of Mild Steel. Engineering and Technology Journal, 35(9) Part (A) Engineering), 914-921.

**[16] Chaubey , N., Singh , V.K. and Quraishi , M.A. (2017).** Corrosion inhibition performance of different bark extracts on aluminum in alkaline solution. Journal of the Association of Arab Universities for Basic and Applied Sciences, 22, pp. 38-44.

**[17] Xhanari , K., Finsgar , M., Hrncic , M.K., Maver , U., Knez , Z. and Seiti, B. (2017).** Green corrosion inhibitors for aluminum and its alloys: a review. RSC Advances, 7(44), pp. 27299-27330.

**[18] Awad,Z.M.,Abd, A.N. and Hassan,K.H.(2018).** Corrosion Prevention of Aluminum in Acidic Media Using Cydonia Vulgaris Leaves Extract as Environmentally Friendly Corrosion Inhibitor. Journal of Biochemical Technology, 9(3), 10.

**[19] Khadom, A.A., Abd, A.N. and Ahmed, N.A.(2018).**Potassium Iodide as a Corrosion Inhibitor of Mild Steel in Hydrochloric Acid : Kinetics and Mathematical studies. Journal of Bio-and Tribo -Corrosion, 4(2), 17.

**[20] Desai , P.S. (2018).** Calotropis gigantean leaves ark used as corrosion inhibitor for aluminum in hydrochloric acid. Der Pharma Chemical, 10(1), pp. 7-12.

**[21] BinYehmed , F.M., Abdullah , A.M., Zainal , Z. and Zawawi , R.M. (2018).** Green Coffee bean extract as a green corrosion inhibitor for aluminum in artificial acid rain medium. International Journal of Applied Environmental Sciences, 13(2), pp. 171-183.

**[22] Wisdom , J., Kelechi , D. and Ugochukwu , J. (2018).** Green inhibitor for corrosion of aluminum alloy AA8011A in acidic environment. International Research Journal of Engineering and Technology (IRJET), 2(2), p. 121-124.

**[23] Coelho , L.B., Cossement , D. and Olivier , M.G. (2018).** Benzotriazole and cerium chloride as corrosion inhibitors for AA2024-T3: An EIS investigation supported by SVET and ToF-SIMS analysis. Corrosion Science, 130, pp. 177-189.

**[24] Hassan , R.M. and Zaafarany , I.A. (2013).** Kinetics of corrosion inhibition of aluminum in acidic media by water-soluble natural polymeric pectates as anionic polyelectrolyte inhibitors. Materials, 6(6), pp. 2436-2451.

**[25] Yaro, A.S. ,Abdul- Masih, N.S. and Kadhim, A.A.(2000).** The Influence of Temperature on Corrosion Inhibition of Carbon Steel in Air-Saturated 7NH3PO4 by Potassium Iodide. Iraqi Journal of Chemical and Petroleum Engineering, 1(1), 83-87.

**[26] Khadom ,A.A. (2000).** The influence of temperature on corrosion inhibition of carbon steel in phosphoric acid. University of Baghdad, Chemical Engineering Department (M.Sc.).

**[27] Jassim , R.A. (2013).** Corrosion protection of some metals and alloys in saline water by Appling nano materials coating. M.Sc. Thesis, College of Science For Women , University of Baghdad , Department of Chemistry.

**[28] Ismaeel ,H.K. (2014).** The effect of laser surface melting corrosion protection on alloys. University of Technology, Chemical Engineering Department (M.Sc.).

**[29] Schweitzer, P.A. (2010).** Fundamentals of metallic corrosion. 1ed. Taylor and Francis Group, LLC, United States of America**.**

**[30] P. E. Philip A. Schweitzer.( 2009).** Fundamentals of Corrosion: Mechanisms, Causes, and Preventative Methods: Taylor & Francis.

**[31] Muthukrishnan , P., Prakash , P., Jeyaprabha , B. and Shankar , K. (2015).** Stigmasterol extracted from Ficus hispida leaves as a green inhibitor for the mild steel corrosion in 1 M HCl solution. Arabian Journal of Chemistry.

**[32] Khorsheed , H.N. (2016).** Inhibition of carbon steel corrosion in acid medium using plant extracts. M.Sc. Thesis, College of Science , University of Diyala.

**[33] Umoren , S.A., Eduok, U.M., Solomon , M.M. and Udoh , A.P.(2016).** Corrosion inhibition by leaves and stem extracts of Sida acuta for mild steel in 1 M H2SO4 solutions investigated by chemical and spectroscopic techniques. Arabian journal of chemistry. 9, pp. S209-S224.

**[34] Ahmed , A.B. (2014).** Corrosion inhibition of low carbon steel in sulfuric acid by PVA and Piper longum extracts. PhD. Thesis, University of Baghdad, Chemical Engineering Department.

**[35] Revie, R. W.( 2008).** Corrosion and corrosion control, An introduction to corrosion science and engineering. 4th addition.

**[36] Yaro, A. S. , Hameed, K. W. , and Khadom, A. A. (2013).** Study for Prevention of Steel Corrosion by Sacrificial Anode Cathodic Protection, Theoretical Foundations of Chemical Engineering, 47( 3), pp. 266 – 273.

**[37] Hameed, K. W. and Khadom, A. A. (2012).** Prevention of Steel Corrosion by Cathodic Protection Techniques, International Journal of Chemical Technology, 4(1), pp. 17 – 30.

**[38] Kumar, S. Hari and Karthikeyan, S. (2012).** Inhibition of mild steel corrosion in hydrochloric acid solution by cloxacillin drug, J. Mater. Environ. Sci. 3 (5), pp. 925-934.

**[39] Kumar, A.( 2008).** Corrosion Inhibition of Mild Steel in Hydrochloric Acid by Sodium Lauryl Sulfate (SLS), E-Journal of Chemistry, 5(2), pp.275-280.

**[40] Kareem Mohammed ,S.(2018).**Effect Use of Two Chemical Compounds Sodium Nitrate and Sodium Silicate as Corrosion Inhibitor to Steel Reinforcement. Al-Khwarizmi Engineering Journal, 14(2), 123-128.

**[41] Popoola ,A. Olorunniwo, OE and Ige, OO. (2014).** Corrosion Resistance Through the Application of Anti-Corrosion Coatings, Chapter in book, Developments in Corrosion Protection.

**[42] Thirumalairaj,B. Jaganathan, M. (2016).** Corrosion protection of mild steel by a new binary inhibitor system in hydrochloric acid solution, Egyptian Journal of Petroleum, 25( 3), pp. 423–432.

**[43] Verma,C. Singh, P. Quraishi, M.A. (2016).** A Thermo dynamical, electrochemical and surface investigation of Bis (indolyl) methanes as Green corrosion inhibitors for mild steel in 1 M hydrochloric acid solution, Journal of the Association of Arab Universities for Basic and Applied Sciences 21, pp. 24–30.

**[44] Al-Saeed ISI, AL-Senani GM, Almufarij R. (2016).** Electrochemical investigations on the corrosion inhibition of aluminum by Green Leafy Vegetables in 1M HCl. Life Science Journal 13: 100-105.

**[45] Ennouri , A., Lamiri , A. and Essahli , M. (2017).** Corrosion inhibition of aluminum in acidic media by different extracts of Trigonellafoenum-graecum L seeds. Portugaliae Electrochimica Acta, 35(5), pp. 279-295.

**[46] G. Pereira, A. Lachenwitzer, M. Kasrai, P.R. Norton , T.W. Capehart, T.A. Perryb, Y.T. Cheng, B. Frazer ,P.U. Gilbert.(2007).** Tribology Letters.26, 103.

**[47] Nasim ziaifer, Jila talatmehrabad and farzad arjomendirad .(2011).** Aluminum corrosion inhibitors in Acidic Media", J.Basic Appl. Sci. Res, 1(12) 2886-2888.

**[48] J. R. Davis.(2001).** in alloying understanding the Basics, J. R. Davis, editor, p. 351, ASM International, Ohio.

**[49] Fouda AS, Abdallah M, Eissa M.(2013).** Corrosion inhibition of Aluminum in 1 M phosphoric acid solutions using some Chalcones derivatives and synergistic action with halide ions. African Journal of Pure and Applied Chemistry.;7(12):394-404. DOI: 10.5897/ AJPAC2013. 0534.

**[50] Fayomi , O.S.I., Anawe , P.A.L. and Daniyan , A. (2018).** The impact of drugs as corrosion inhibitors on aluminum alloy in coastal-acidified medium. In Corrosion Inhibitors, Principles and Recent Applications. In Tech.

**[51] Prabhu , D. (2013).** Studies of corrosion of aluminum and 6063 aluminum alloy in phosphoric acid medium. International Journal of Chem Tech Research, 5(6), pp. 2690-2705.

**[52] B.E.A. Rani , B.B.J. Basu. (2012).** Green inhibitors for corrosion protection of metals and alloys: An overview, International Journal of Corrosion, 1-15.

**[53] M. Chigondo M., F. Chigondo. (2016).** Recent Natural Corrosion Inhibitors for Mild Steel: An Overview, J. Chem Article ID 6208937, 1-7.

**[54] Kumar S. H, Karthikeyan r.S; Jeeves P. A; Sundaramali G. (2012).** A review on corrosion inhibition of aluminum with special reference to green inhibitors ,Int. J. of Recent Sci. Res., 3(2), 61 -67.

**[55] Iloamaeke, I. M; Onuegbu, T. U. (2012).**Corrosion Inhibition of Mild Steel by Pterocarpus Soyauxi Leaves Extract in HCl Medium. International Journal of Plant, Animal and Environmental Sciences, 2, 22-28.

**[56] Nnanna, L.A, Obasi V. U; Nwadiuko O. C; Mejeh K. I; Ekekwe N. D. ; S. C. Udensi S. C.( 2012).**Inhibition by Newbouldia leavis Leaf Extract of the Corrosion of Aluminum in HCl and H2SO4 Solutions, Arch .Appl. Sci. Res., 4(1), 207-217.

**[57] Raymond, P. P; Pascal Regis A. P. Rajendran S; Manivannan M. (2013).** Investigation of Corrosion Inhibition of Stainless steel by Sodium tungstate, Res. J. Chem. Sci., 3(2), 54–58.

**[58] Afia L, Rezki N; Aouad M. R; Zarrouk; A., Zarrok H. ; Salghi R; Hammouti B; Messali; M ; Al-Deyab S. S.(2013**).Investigation of the Inhibitive Effect of 2-(Ethylthio)-1,4,5-Triphenyl-1H-Imidazole on Corrosion of Steel in 1 M HCl Int. J. Electrochemical. Sci., 8, 4346 – 4360.

**[59] Ahamad I, Quraishi M. A.(2009).** Bis (benzimidazol-2-yl) disulphide: An efficient water soluble inhibitor for corrosion of mild steel in acid media ,Corros. Sci. 51.

**[60] Gopiraman M, Sakunthala P, Kanmani R, Alex Ramani V, Sulochana N. (2011).** Inhibitive action of Clematis gouriana extract on the corrosion of mild steel in acidic medium. Ionics DOI:10.1007/s11581-011-5480584-9.

**[61] Ahmed , N.A. (2017).** Synergistic effect of natural inhibitors and iodide Ion for corrosion control of steel in acidic medium. M.SC. Thesis, College of Science , University of Diyala.

**[62] Al – Jeilawi , H.O. (2013).** Synthesis of some organic compounds as corrosion inhibitors in petroleum industry. M.SC. Thesis, College of Science, University of Baghdad , Department of Chemistry.

**[63] Jadhav RS, Hundiwale DG, Mahulikar PP .(2010).** Synthesis of nano polyaniline and poly-o-anisidine and applications in alkyd paint formulation to enhance the corrosion resistivity of mild steel. J Coat Technol Res 7:449-454.

**[64] Martinez S, Stern I. (2001).** Inhibitory mechanism of low-carbon steel corrosion by mimosa tannin in sulphur acid solutions. J Appl Electrochemistry 31:973-978.

**[65] Mobin, M, Khan MA, Parveen M. (2011).** Inhibition of mild steel corrosion in acidic medium using starch and surfactants additives. J Appl Poly Sci 121:1558-1565.

**[66] Raja PB, Sethuraman MG. (2008).** Natural products as corrosion inhibitor for metals in corrosive media-A review. Mater Letts 62:113-116.

**[67] Yurt A, Balaban A, Kandemir SU, Bereket G, Erk B. (2004).** Investigation on some Schiff bases as HCl corrosion inhibitors for carbon steel. Materials Chemistry and Physics.85: 420-426.

**[68] Eddy ,N.O. and Odoemelam, S.A. (2009).** Inhibition of corrosion of mild steel in acidic medium using ethanol extract of Aloe vera. Pigment and Resin Technology, 38( 2): 111-115.

**[69] Peme ,T., Olasunkanmi, L.O., Bahadur, I., Adekunle, A. S., Kabanda, M.M. and Ebenso, E.E. (2015).** Adsorption and corrosion inhibition studies of some selected dyes as corrosion inhibitors for mild steel in acidic medium: gravimetric, electrochemical, quantum chemical studies and synergistic effect with iodide ions. Molecules, 20:16004-16029.

**[70] AL-Ati, T.(2011).Assyrian plum (Cordia myxa L).**Postharvest Biology and Technology of Tropical and Subtropical Fruits,116-126e.

**[71] Chauban, L.R,Gunasekaran, G. (2007).** Corrosion inhibition of mild steel by plant extract in dilute HCl medium. Corr. Sci. 49, 1143-1161.

**[72] M. G. Tsoeunyane, M. E. Makhatha, O. A.(2019 ).** Arotiba Corrosion Inhibition of Mild Steel by Poly(butylene succinate)-L-histidine Extended with 1,6-diisocynatohexane Polymer Composite in 1 M HCl Int. J. Corr.,)., Article ID 7406409, 12 pages, https://doi.org/10.1155/2019/7406409.

**[73] Adejoro , I.A., Ojo , F.K. and Obafemi , S.K. (2015).** Corrosion inhibition potentials of ampicillin for mild steel in hydrochloric acid solution. Journal of Taibah University for Science, 9(2), pp. 196-202**.**

**[74] Hassan , K.H., Khadom , A.A. and Kurshed , N.H. (2016).** Citrus aurantium leaves extracts as a sustainable corrosion inhibitor of mild steel in sulfuric acid. South African Journal of Chemical Engineering, 22, pp.1-5.

**[75] Ejikeme , P.M., Umana , S.G., Menkiti , M.C. and Onukwuli , O.D. (2015).** Inhibition of mild Steel and aluminum corrosion in 1M H2SO4 by leaves extract of African bread fruit. International Journal of Materials and Chemistry, 5(1), pp. 14-23.

**[76] Rubaye , A.Y.I., Abdul sahib , H.T. and Abdul Wahid , A.A. (2015).** Corrosion inhibition properties of norepinephrine molecules on mild steel in acidic media. Journal of Encapsulation and Adsorption Sciences, 5(03), p. 155.

**[77] Patel , N.S., Jauhariand , S., Mehta, G.N., Al-Deyab , S.S., Warad , I. and Hammouti , B. (2013).** Mild steel corrosion inhibition by various plant extracts in 0.5M sulphuric acid. Int. J. electrochemical. Sci, 8, pp. 2635-26551664.

**[78] Jarullah, A.A. (2013).** Removal of Ni (II) ions from aqueous solutions by adsorption technique using activated carbon as adsorbent. Ph.D. thesis, College of Science for Women, University of Baghdad, Iraq.

**[79] Stephenson, C, Hubler, A. (2015).** Stability and conductivity of self-assembled wires in a transverse electric field. Sci. Rep. 5: 15044. Bibcode:2015NatSR...515044S. doi:10.1038/srep15044. PMC 4604515. PMID 26463476.

**[80] Hubler, A, Lyon, D. (2013).** Gap size dependence of the dielectric strength in nano vacuum gaps. IEEE Transactions on Dielectrics and Electrical Insulation20 (4): 1467–1471. doi:10.1109/TDEI.2013.6571470.

**[81] Valenti G, Rampazzo R, Bonacchi S, Petrizza L, Marcaccio M, Montalti M, Prodi L, Paolucci F. (2016).** Variable Doping Induces Mechanism Swapping in Electrogenerated Chemiluminescence of Ru(bpy)32+ Core−Shell Silica Nanoparticles. J. Am. Chem. Soc. 138 (49): 15935−15942. doi:10.1021/jacs.6b08239. PMID 27960352.

**[82] Kerativitayanan, P; Carrow, JK; Gaharwar, AK .(2015).** Nanomaterials for Engineering Stem Cell Responses. Advanced Healthcare Materials. 4 (11): 1600–27. doi:10.1002/adhm.201500272. PMID 26010739.

**[83] Wei, Hui; Wang, Erkang .(2013).** Nanomaterials with enzyme-like characteristics (nanoezymes): next-generation artificial enzymes". Chemical Society Reviews. 42 (14): 6060–93. doi:10.1039/C3CS35486E. PMID 23740388.

**[84] Juzgado, A; Solda, A.; Ostric, A.; Criado, A; Valenti, G; Rapino, S; Conti, G; Fracasso, G; Paolucci, F; Prato, M. (2017).** Highly sensitive electro Chemiluminescence detection of a prostate cancer biomarker. J. Mater. Chem. B. 5 (32): 6681–6687. doi:10.1039/c7tb01557g.

**[85] Anis, Mohab; AlTaher, Ghada; Sarhan, Wesam; Elsemary, Mona. (2017).** Nan ovate. Springer. p. 105. ISBN 9783319448619.

**[86] Wang, Shujun .(2019).** Laser-driven nanomaterials and laser-enabled nanofabrication for industrial applications (1st ed.). Elsevier. pp. 181–203. ISBN 978-0-12-815749-7**.**

**[87] Isa , W.A. and Ahmed , Z.W. (2015).** Corrosion inhibition of aluminum in acidic medium using amino acid (methionine). Ibn AL-Haitham Journal For Pure and Applied Science, 28(3), pp. 86-102.

**[88] Kadhom.F.A ,Abd,A.N.and Hassan,K.H.(2018).** Corrosion Inhibition of Iron of the crude Oil pipelines using commercial Red Oxide Doped with Nan oxides. M.SC. Thesis, College of Science , University of Diyala.

**[89] J. T. Nwabanne, V. N. Okafor.(2012).** Adsorption and thermodynamics study of the inhibition of corrosion of mild steel in H2SO4 medium using Vernonia amygdalina, J. Minerals Mater. Characteri. Eng., 11, 885-890.

**[90] Vashi , R.T. and Prajapati , N.I. (2017).** Corrosion inhibition of aluminum in hydrochloric acid using Bacopa monnieri leaves extract as green inhibitor. International Journal of Chem Tech Research, 10(15), PP. 221-231.

**[91] Nnabuk , E.O. and Awe , F. (2018).** Experimental and quantum chemical studies on ethanol extract of Phyllanthus amarus (EEPA) as a green corrosion inhibitor for aluminum in 1 M HCl. Portugaliae Electrochimica Acta, 36(4), pp. 231-247.

**[92] Urkovic L C, Helena Otmac ic C urkovic , Sara Salopek, Marijana Majic´ Renjo a , Suzana Segota. (2013).** Enhancement of corrosion protection of AISI 304 stainless steel by nanostructured sol–gel TiO2 films, Corrosion Science , 77, pp. 176–184.

**[93] Paulo S. G. da Silva, Alberto N. C. Costa, Oscar R. Mattos, Adriana N. Correia, P. de Lima-Neto.( 2006).** Evaluation of the corrosion behavior of gal annealed steel in chloride aqueous solution and in tropical marine environment, Journal of Applied Electrochemistry. 36(3), pp. 375– 38.

**[94] Chaubey , N., Quraishi , M.A. and Ebenso , E.E. (2015).** Corrosion inhibition of aluminum alloy in alkaline media by Neolamarkia cadamba bark extract as a green inhibitor. Int. J. electrochemical. Sci , 10, pp. 504 – 518.

**[95] Khadom, A. A. , Aprael S. Yaro, Abdul Amir H. Kadum, Ahmed S. AlTaie and Ahmed Y. Musa.( 2009).** The Effect of Temperature and Acid Concentration on Corrosion of Low Carbon Steel in Hydrochloric Acid Media, American Journal of Applied Sciences, 6 (7): pp. 1403-1409.

**[96] ABAKEDI , O.U. (2017).** Aluminum Corrosion inhibition by Microdesmis puberula leaf extract in 2 M hydrochloric acid solution. International Journal of Innovative Scientific & Engineering Technologies Research 5(3), pp. 6-14**.**

**[97] Beda , R.H.B., Niamien , P.M., Avo Bilé , E.B. and Trokourey , A. (2017).** Inhibition of aluminum corrosion in 1.0 M HCl by caffeine: experimental and DFT studies. Advances in Chemistry, 2017.

**[98] Raghavendra , N. and Bhat, J.I. (2018).** Anti-corrosion properties of Areca palm leaf extract on aluminum in 0.5 M HCl environment. South African Journal of Chemistry, 71(1), pp. 30-38.

**[99] Fouda ,A.S., Elewady, G.Y., Shalabi, K. and Habouba, S. (2014).** Anise extract as green corrosion inhibitor for carbon steel in hydrochloric acid solutions. International Journal of Innovative Research in Science, Engineering and Technology. 3(4): 2319-8753.

**[100] Fouda , A.S., Abdallah, M., Ahmed , I.S. and Eissa , M. (2012).** Corrosion inhibition of aluminum in 1M H3PO4 solutions by ethanol amines. Arabian Journal of Chemistry, 5(3), pp. 297-307.

**[101] Olasehinde ,E.F., Adesina, A.S., Fehintola, E.O., Badmus, B.M. and Aderibigbe, A.D. (2012).** Corrosion inhibition behaviour for mild steel by extracts of Musa sapientum peels in HCl solution: Kinetics and Thermodynamics Study. IOSR Journal of Applied Chemistry, 2(6): 15-23.

**[102] Al-Jeilawi , U.H.R ; Al-Majidi , S.M.H. and Al- Saadie , K.A.S. (2013).** Corrosion inhibition effects of some new synthesized N-Aroyl-NAryl thiourea derivatives for carbon steel in sulfuric acid media . Journal of Al-Nahrain University , 16(4), pp. 80 – 93.

**[103] Silvère , D.J.Y; Valery , B.K; Guy-Richard , K.M; Augustin , O. and Albert , T. (2018).** Cefadroxil drug as corrosion inhibitor for aluminum in 1M HCl medium: Experimental and Theoretical Studies. IOSR Journal of Applied Chemistry (IOSR-JAC), 11(4), pp. 24-36.

**[104] Fouda , A.S., Elmorsi , M.A. and Elmekkawy , A. (2013).** Eco-friendly chalcones derivatives as corrosion inhibitors for carbon steel in hydrochloric acid solution. African Journal of Pure and Applied Chemistry, 7(10), pp. 337-349.

**[105] Hamdy,A. and El-Gendy, N.S. (2013).** Thermodynamic, adsorption and electrochemical studies for corrosion inhibition of carbon steel by henna extract in acid medium. Egyptian Journal of Petroleum, 22:17-25.

**[106] Ahamed, M., Alhadlaq, H. A., Khan, M. A., Karuppiah, P., and Al-Dhabi, N. A. (2014).** Synthesis, characterization, and antimicrobial activity of copper oxide nanoparticles. Journal of Nanomaterials, 2014. 17.

**[107] Anbarasi, C.M., Rajendran,S.(2014).**Surface Protection of Carbon Steel by Hexane sulphonic Acid-Zinc Ion System. ISRN Corrosion, 2014.

**[108] Wang,B.,Du, M.,Zhang, J.and Gao,C. J.(2011).** Electrochemical and Surface Analysis Studies on Corrosion Inhibition of Q235 Steel by Imidazole Derivative Against CO2 Corrosion. Corrosion Science, 53(1), 353-361.

# *Appendix*

# Appendix

Below is a picture of the results of examination of the mineral samples that were measured in the Ministry of Planning Central Organization for Standardization and Quality Control .

| | | |
|---|---|---|
| رقم الاصدار : ١<br>تاريخ الاصدار :٢٠١٦/٣/١٥<br>الصفحات : ١/١ | الجهاز المركزي للتقييس والسيطرة النوعية<br>مختبرات دائرة السيطرة النوعية<br>استمارة تقرير الاختبار<br>F/EG/AS/5.10/1 | C.O.S.Q.C IRAQ |

**تقرير الاختبار S/EG/2019/11/ 20/612**

القسم : الصناعات الهندسية الشعبة : مختبر الكيمياوي عنوان المختبر : بغداد /الجادرية / ص.ب ١٣٠٣٢

اسم النموذج : سبيكة المنيوم نقي رقم ( ١ )

وصف النموذج : سبيكة المنيوم نقي رقم ( ١ )

التأشير على النموذج :/

تاريخ استلام النموذج : ٢٠١٩/١١/٢٠

مواصفة المنتج /المتطلبات المعتمدة : /

اسم الجهة : وزارة التعليم العالي والبحث العلمي/ جامعة ديالى / كلية العلوم / شعبة الدراسات العليا

عنوان الجهة: ديالى – بعقوبة

النتائج :

| نوع الفحص | مواصفة الفحص | متطلبات المواصفة | النتائج | | | |
|---|---|---|---|---|---|---|
| تحليل كيمياوي | ASTM E 1251 | / | Si% | 0.0666 | Na% | اقل من 0.0005 |
| | | | Fe % | 0. 139 | Bi % | 0.0020 |
| | | | Cu % | 0.0039 | Zr% | اقل من 0.0005 |
| | | | Mn % | 0.0017 | B % | 0.0028 |
| | | | Mg % | اقل من 0.0001 | Ga% | 0.0078 |
| | | | Zn% | 0.0070 | Cd % | اقل من 0.0003 |
| | | | Cr % | اقل من 0.0001 | Co % | 0.0002 |
| | | | Ni % | 0.0008 | Ag% | 0.0011 |
| | | | Ti % | اقل من 0.0002 | Hg% | اقل من 0.0005 |
| | | | Be % | اقل من 0.0001 | In % | اقل من 0.0005 |
| | | | Ca % | اقل من 0.0001 | P% | اقل من 0.0020 |
| | | | Li % | اقل من 0.0001 | As% | اقل من 0.0030 |
| | | | Pb% | 0.0009 | Ce % | اقل من 0.0010 |
| | | | Sn % | 0.0597 | La % | اقل من 0.0002 |
| | | | Sr% | 0.0001من اقل | Sb% | اقل من 0.0050 |
| | | | V% | 0.0028 | Al% | المتبقي |

ملاحظة : - هذه النتائج تعود الى المفردات التي تم اختبارها فقط

- مدة حفظ النموذج اسبوعين من تاريخ اصدار الكتاب وبخلافه يسقط حقكم بالمطالبة بالنموذج

التفسيرات ان وجدت : /

نهاية التقرير

التوقيع :

الإسم : نهلة ناظر عبد المنعم

التاريخ : ٢٠١٩/١١/ ٢٥

الجهاز المركزي للتقييس والسيطرة النوعية ص.ب ١٣٠٣٢ Minist Of Planing Cosqc

نظام ادارة اعتماد مختبرات دائرة السيطرة النوعية ISO – IEC- 17025

| | | |
|---|---|---|
| رقم الاصدار: ١<br>تاريخ الاصدار :١٥/٣/ ٢٠١٦<br>الصفحات : ١/١ | الجهاز المركزي للتقييس والسيطرة النوعية<br>مختبرات دائرة السيطرة النوعية<br>استمارة تقرير الاختبار<br>F/EG/AS/5.10/1 | C.O.S.Q.C IRAQ |

## تقرير الاختبار S/EG/2019/11/ 20/648

القسم : الصناعات الهندسية الشعبة : مختبر الكيمياوي عنوان المختبر : بغداد /الجادرية / ص.ب ١٣٠٣٢

اسم النموذج : سبيكة المنيوم رقم ٣ (٦٠٦٣ )

وصف النموذج : سبيكة المنيوم رقم ٣ (٦٠٦٣ )

التاشير على النموذج :/

تاريخ استلام النموذج :٢٠١٩/١١/٢٠

مواصفة المنتج /المتطلبات المعتمدة : /

اسم الجهة : وزارة التعليم العالي والبحث العلمي/ جامعة ديالى / كلية العلوم/ شعبة الدراسات العليا

عنوان الجهة: ديالى – بعقوبة

النتائج :

| نوع الفحص | مواصفة الفحص | متطلبات المواصفة لسبيكة ٦٠٦٣ | | النتائج |
|---|---|---|---|---|
| تحليل كيمياوي | ASTM E 1251 | Si% = 0.2 – 0.6 | | 0.478 |
| | | Fe % = 0.35 max | | 0.177 |
| | | Cu % = 0.1 max | | 0.0266 |
| | | Mn % = 0.1 max | | 0. 0044 |
| | | Mg % = 0.45 – 0.9 | | 0.734 |
| | | Cr % = 0.1 max | | اقل من 0.0001 |
| | | Ni % = ---- | | --- |
| | | Zn% = 0.1max | | 0.0097 |
| | | Ti % = 0.1 max | | اقل من 0.0002 |
| | | Ga% = --- | | --- |
| | | V% = ----- | | -- |
| | | Each= 0.05 | other | 0.0454 |
| | | Total= 0.15 max | | 0.0707 |
| | | Aluminium% | | المتبقي |

ملاحظة : - هذه النتائج تعود الى المفردات التي تم اختبارها فقط

- مدة حفظ النموذج اسبوعين من تاريخ اصدار الكتاب وبخلافه يسقط حقكم بالمطالبة بالنموذج

التفسيرات ان وجدت : /

نهاية التقرير

التوقيع :

الإسم : نهلة ناظر عبد المنعم

التاريخ :٢٠١٩/١١/ ٢٠

الجهاز المركزي للتقييس والسيطرة النوعية الصادر س.ب ١٣٠٣٢ Minist Of Planing \ Cosqc

نظام ادارة اعتماد مختبرات دائرة السيطرة النوعية ISO – IEC- 17025

## الخلاصة

جرى في هذا البحث دراسة معدلات تأكل الألمنيوم وسبيكة الألمنيوم (AA6063-T5 ) في حامض الفسفوريك ($1M\ H_3PO_4$) و(at PH of 4) عند درجات حرارة مختلفة (303,313,323and 333K ) بوجود المواد المثبطة للتأكل المستخلصة من اوراق نبات البمبر ضمن الحدود ( 2-10 ملغرام /لتر ) والمواد النانوية ضمن الحدود (1- 2.5 نسب وزنية مئوية ) عند الزمن (3 ساعات) تم استخدام طريقة فقدان الوزن في هذا البحث ,وان النتائج بينت ان معدلات التأكل بوجود المواد المثبطة مستخلص اوراق نبات البمبر( CML) والمواد النانوية ($Fe_2O_3$and $TiO_2$) ومعدل التأكل يزداد بزيادة درجات الحرارة ويقل بزيادة تركيز المواد المثبطة وقد تبين ان الحد الأعلى لكفاءة المواد المثبطة كانت (90.95%) للألمنيوم و (87.60%) لسبيكة الألمنيوم (AA6063 T5) لمستخلص (CML ) و (71.43%) للألمنيوم و(68.785) لسبيكة الألمنيوم(AA6063-T5 ) للمادة النانوية ($Fe_2O_3$ ) و (67.02%) للألمنيوم و(60.01%) لسبيكة الألمنيوم (AA6063-T5) للمادة النانوية ($TiO_2$) عند درجة الحرارة (333K) والحد الاعلى للتركيز ولقد تم تطبيق موديلات ثلاث لتفسير عملية امتزاز مثبطات التأكل على سطح المعدن وقد وجد ان المواد المثبطة تتبع امتزاز ايزوثيرم لانكماير وتم استخدام معادلة ارينوس ومعادلة الحالة الانتقالية لإيجاد قيم طاقات التنشيط وتم ايجاد الطاقة المنشطة للتفاعل وانثالبية التنشيط وانتروبي التنشيط بوجود وعدم وجود المواد المثبطة للتأكل تم استخدام تقنية طيف الأشعة تحت الحمراء (FTIR) لمعرفة المجاميع الفعالة في المستخلص النباتي قبل عملية الغمر في محلول التأكل وبعد عملية الغمر ولقد وجد ان هناك اختلاف بين النتائج والازاحة في قمم طيف الاشعة تحت الحمراء وهذا يعزى الامتزاز المجاميع على سطح المعدن و ايضا تم استخدام تقنيات (XRD,SEM) لدراسة السطح المعدني المطلي بعد التأكل بوجود وغياب مثبطات المواد النانوية ($Fe_2O_3$and $TiO_2$) واستخدام تقنية الفحص المجهري للقوة الذرية (AFM) لدراسة سطح المعدن قبل وبعد التأكل بوجود وغياب المثبط من مستخلص اوراق نبات البمبر(CML) وايضا دراسة سطح المعدن المطلي بوجود وغياب المواد النانوية بعد التأكل ($Fe_2O_3$and $TiO_2$) لقد اظهرت الدراسات ان السطح يصبح املس بسبب تكوين طبقة مثبطة على سطح المعدن .

وزارة التعليم العالي والبحث العلمي

جامعـــــة ديـــــــالـى

كليـــــــة العلـــــــوم

قســـــــم الكيميـــــاء

# منع التآكل في الالمنيوم وسبيكة الالمنيوم(AA6063-T5 ) المستخدمة صناعيا باستخدام مستخلص اوراق البمبر والاكاسيد النانوية ($TiO_2$,$Fe_2O_3$ )

رســـالة مقدمـــة الى

مجلس كلية العلوم / جامعة ديالى

وهي جزء من متطلبات نيل درجة الماجستير في علوم الكيمياء

(كيمياء فيزيائية)

من قبل الطالبة

**هبه باسم ذياب**

**بكالوريوس في علوم الكيمياء 2009**

**كليـــــــة العلـــــوم – جامعـــــة ديالـــــى**

**بأشراف**

**أ.د. أحمد نجم عبد** **أ.د. كريم هنيكش حسن**

**1442هجرية** **العراق** **2020 ميلادية**